Dissertation
submitted to the
Combined Faculties for the Natural Sciences and for Mathematics
of the Ruperto-Carola University of Heidelberg, Germany
for the degree of
Doctor of Natural Sciences

presented by

Master of Science Philippe Golfier
Born in Ludwigshafen am Rhein
Oral examination: 2nd May 2018

Transcriptional regulation of secondary cell wall biosynthesis in *Miscanthus sinensis*

Referees: Professor Dr. Thomas Rausch
Dr. Sebastian Wolf

Contents

*Section is adapted from Golfier et al., 2017

*Section is adapted from Golfier et al., 2017

Summary

Cell wall recalcitrance is a major limitation hindering the exploitation of the enormous potential of lignocellulosic biomass as a renewable resource for energy and bio-based products. In the last decades, C4 grasses from the genus *Miscanthus* have emerged as a most promising energy crop for the production of lignocellulosic biomass in temperate climates. Secondary cell walls, which represent the largest proportion of lignocellulosic biomass are formed in specialised cells after cessation of growth. In higher plants, the formation of secondary cell walls is tightly regulated, both spatially and temporally, by a complex network of transcription factors. However, in *Miscanthus* only little is known about molecular players regulating secondary cell wall formation and lignin biosynthesis.

In this study, application of the herbicide isoxaben was shown to trigger ectopic lignification in *Miscanthus* seedling roots. The chemical treatment may be exploited in the future to identify regulators and biosynthetic genes involved in lignification in *Miscanthus*.

In addition, *Miscanthus sinensis* transcription factors related to SECONDARY WALL-ASSOCIATED NAC DOMAIN1 (SND1) and SECONDARY CELL WALL MYBs 1-4 (SCM1-4) were identified in the *Miscanthus* transcriptome, which act as regulators of secondary cell wall formation and lignin biosynthesis. During *Miscanthus* development, expression of Ms*SND1* and Ms*SCM*s coincided with the onset of secondary cell wall formation and lignification of vascular tissue and sclerenchyma fibers. MsSND1 and MsVND7 were capable to fully restore growth in a SCW-deficient *Arabidopsis thaliana* mutant, suggesting they are the *Miscanthus* orthologues of the well characterised *Arabidopsis* determinants of SCW formation in fibers and vessels. Ectopic expression of Ms*SND1* and Ms*VND7* in tobacco leaves prompted the formation of patterned deposition of lignin, cellulose, and hemicellulose reminiscent of xylem elements. This observation was in sharp contrast to uniform lignification after transient expression of various Ms*SCM*s. Expression of particular *Miscanthus* TFs led to specific cell wall compositions, providing attractive targets for biomass improvements. Transgenic *Arabidopsis* lines carrying an inducible system of MsSND1 revealed that MsSND1 regulates directly or indirectly the expression of a broad range of genes involved in secondary cell wall formation.

Zusammenfassung

Die energetische und stoffliche Nutzung von nachwachsender Lignozellulose wird größtenteils limitiert durch ihren schwierigen Aufschluss in ihre Bestandteile. Das aus Südostasien stammende C4-Gras Miscanthus vereint beeindruckende Wachstumsraten bei gleichzeitig geringem Bedarf an Wasser und Nährstoffen. Sekundäre Zellwände, welche den Hauptanteil der Lignozellulose ausmachen werden nur in speziellen Zellen gebildet, die einer präzisen Regulation durch ein komplexes Netzwerk aus einer Vielzahl an Transkriptionsfaktoren unterliegen. Jedoch sind in *Miscanthus* die molekularen Regulatoren weitgehend unerforscht.

Durch die vorliegende Arbeit konnte durch eine chemische Behandlung von *Miscanthus* Keimlinge mit dem Herbizid Isoxaben Lignifizierung herbeigeführt werden. Die Behandlung mit Isoxaben könnte in Zukunft dazu beitragen beteiligte Akteure der Lignifizierung schneller zu identifizieren.

Des Weiteren wurden SECONDARY WALL-ASSOCIATED NAC DOMAIN1 (SND1) und SECONDARY CELL WALL MYBs 1-4 (SCM1-4) als transkriptionelle Regulatoren der Zellwand- und Ligninbiosynthese in einem *Miscanthus* Transkriptom identifiziert. Entlang eines *Miscanthus*-Blattes, das einen Entwicklunggradienten widerspiegelt ging die höchste Expression von Ms*SND1* und Ms*SCM*s einher mit dem Beginn der Zellwandbildung in Fasern und Gefäßen. Die Fähigkeit von MsSND1 und MsVND7 das Wachstum einer zellwanddefekten *Arabidopsis thaliana* Mutante zu komplementieren weist auf eine Orthologie zu Zellwandregulatoren von Fasern und Gefäßen von *Arabidopsis* hin. Ektopische expression von Ms*SND1* und Ms*VND7* führte zu Xylem-ähnliche Strukturen und Bildung von Zellulose, Hemizellulose und Lignin. Im Gegensatz dazu resultierte transiente Expression von Ms*SCM*s in einheitlicher Lignifizierung von Zellwänden. Es zeigte sich zudem, dass die ektopische Expression verschiedener Transkriptionsfaktoren die Zellwandzusammensetzungen im unterschiedlichen Maßen beeinflusst, die dadurch besonders geeignet wären Biomass zu optimieren. Mit Hilfe von transgenen *Arabidopsis* Linien, welche ein induzierbares Ms*SND1*-Gen besitzen konnten direkte und indirekte Zielgene von MsSND1 gefunden werden.

Chapter 1

Introduction

1.1 Lignocellulosic biomass, the renewable energy source for the future?

In Europe's Renewable Energy Directive of the European parliament, targets were clearly defined for a successive transition from fossil energy towards 20 % renewable energy by 2020. Importantly, the directive also outlines extensive sustainability criteria to reduce greenhouse gas emissions, protect human health and environment while considering social and economic aspects.

The energy sector needs to be highly flexible because over- or undersupply cause blackouts. So far it remains unclear how to ensure a flexible energy system while expanding the share of renewable energy. Generation of energy from wind and solar are renewable but storability is still a major issue. In addition, the energy sector is highly competitive and generation of energy by renewable sources like biomass, wind, solar, or hydro can only compete against the low prices of coal, oil, and gas because of enormous subsidies. In Germany subsidies are allocated by the Renewable Energy Sources Act (EEG). The transition of the energy sector towards renewable resources has become the centre of attention and subsidies since 2000. In contrast, awareness for renewable materials especially biomass as basis for production of chemicals, cosmetics, pharmaceuticals, or detergents have been low. Only in 2012 the first federal program, namely BioEconomy Cluster, was lunched with a focus on material uses of biomass. Ever since national states like Baden-Wuerttemberg or North Rhine-Westphalia have developed individual programs promoting research on the production of energy and bio-based products from renewable resources.

In any case, lignocellulosic biomass has great potential as renewable resource for vari-

ous applications. Lignocellulosic biomass is storable and thus allows flexible and readily conversion into energy by well-establish systems such as gasification or combustion for heat and/or power. Moreover, lignocellulosic biomass can be thermochemically and biochemically converted into liquid fuels and platform chemicals. However, because of limited resources and a finite amount of arable land, the most suitable feedstocks need to be carefully selected for the best conversion technology. For example, bioethanol production from second generation feedstock such as lignocellulosic wheat straw saves more greenhouse gas emissions compared to bioethanol from first generation feedstock but is more expensive due to complex processing. Dual-purpose crops like wheat or maize can be converted to bioethanol or, if demanded, can be redirected into the food market contributing to food security and thereby contrasting with lignocellulosic feedstock (Dammer et al., 2017).
Many factors will have an influence on how lignocellulosic biomass will be utilised in the future such as policies, research, global and local prices of lignocellulosic biomass and other energy carriers, innovations, societal acceptance, and so on. The competition for biomass as raw material for bio-based products or for generation of energy has just begun but is expected to increase in the future.

1.2 Miscanthus, a promising energy crop

The genus *Miscanthus* harbours herbaceous and perennial C4 grasses, that originate from subtropical and tropical regions in East Asia. In the last two decades, *Miscanthus* has emerged as one of the most promising energy crops for the production of lignocellulosic biomass in temperate climates due to a unique combination of traits. C4 plants like *Miscanthus* combine high growth rates with low water requirements. This is due to unique leaf anatomy and high efficiency of photosynthetic C4 metabolism.
The rhizome of *Miscanthus* serves as storage compartment that allows translocation of nutrients, in particular nitrogen, during leaf senescence in autumn and mobilise them again to the shoot in spring, accounting for low fertiliser requirement of *Miscanthus* (Lewandowski et al., 2000). In addition, the rhizome functions as buffer to survive unfavourable periods of low water or nutrient availability, qualifying *Miscanthus* for marginal soils.
Despite these attractive characteristics, introduction of *Miscanthus* into agricultural systems has been slow because of four reasons. i) High establishment costs because the high-yielding hybrid *Miscanthus x giganteus* is sterile and can only be clonally propagated by rhizomes, ii) uncertainties during establishment as *Miscanthus* is sensitive in the first winter and it takes about 3 years until the full potential can be exploited, iii) immature technologies for planting, harvesting and processing, and iv) uncertain biomass quality,

that largely depends on harvesting point, genotype, abiotic-/ biotic stresses, and soil quality. Major progress has been achieved by extensive breeding programs. Development of high-yielding seed-based hybrids pave the way for adoption of *Miscanthus* into agriculture (Clifton-Brown et al., 2017). *Miscanthus* has considerable potential for various applications in thermochemical conversion such as direct combustion, gasification, pyrolysis (Jayaraman & Gökalp, 2015), and liquefaction (Hafez & Hassan, 2015) or in biochemical conversion like anaerobic digestion (Kiesel & Lewandowski, 2017; Whittaker et al., 2016) or enzymatic hydrolysis (Brosse et al., 2012). The ability of technology to utilise *Miscanthus* within economic and environmental constraints will finally decide about acceptance and expansion of *Miscanthus* as feedstock. Therefore, a deep understanding of the technology and the *Miscanthus* biomass is of utmost importance.
The biomass quality of *Miscanthus* has a strong influence on the conversion process itself. For example, the heating value of biomass for combustion tightly correlates with lignin content. Minerals like K, Na, Si, Ca, P, and Mg (ash) and moisture may cause fouling, corrosion or result in high particulate matter or emission of NO_x and SO_x during combustion (Baxter et al., 2014; Sommersacher et al., 2012). In turn, the harvesting time of *Miscanthus* is crucial for moisture and ash content (Iqbal & Lewandowski, 2016), whereas the lignin content tightly depends on the *Miscanthus* genotype (da Costa et al., 2014). The major limitation for biological conversion remains cell wall recalcitrance which is largely conferred by lignin. Various pretreatment technologies on *Miscanthus* have been reported to break down the lignin structure to enhance its enzyme digestibility (Brosse et al., 2012). In addition, breeding programs have been aiming to reduce cell wall recalcitrance by exploiting the large genetic and phenotypic variation in *Miscanthus* species (Slavov et al., 2014). Programs like the European OPTIMISC (Optimizing Miscanthus Biomass Production; Lewandowski et al., 2016) or the Bioeconomy Research Program from the state of Baden-Württemberg pursue a more collaborative and holistic approach, attempting to optimise the entire value chain. For example, OPTIMISC identified suitable *Miscanthus* genotypes for a certain cultivation area and conversion technology considering environmental and economical constrains (Lewandowski et al., 2016).

1.3 The plant cell wall

Every plant cell is surrounded by an extracellular matrix called cell wall, which clearly distinguishes plants from animals. The cell wall is a dynamic structure with various functions, that plays an eminent role at each step during the life cycle of a plant. The rigidity of the cell wall withstand the extremely high osmotic turgor pressure of up to 10 bar, sup-

porting plant stability to develop plant organs and to stand upright. At the same time the cell wall is flexible enough to allow cell elongation, confronting plants with a permanent dilemma between flexibility and stiffness. The cell wall is a selective filter controlling plant cell homeostasis. It allows diffusion of water, ions, and small molecules, facilitating cell to cell signalling but tightly regulates uptake of larger molecules. Furthermore, the cell wall separates the plant from its environment, protecting it from biotic and abiotic stresses.
Each plant cell is surrounded by up to three layers, in order from outside to inside, middle lamella (ML) as part of the primary cell wall (PCW), secondary cell wall (SCW), and plasma membrane (PM) as visualised in Figure 1. The ML consists of a pectic polysaccharide, that forms the outer layer of a cell and fastens neighbouring cells together, securing structural integrity of plant tissues and organs. The PM is made up of a phospholipid bilayer separating extra- and intracellular matrix. The PM is responsible for the basic function of a membrane, serving as semi-permeable gatekeeper of the cell. The PCW is formed and extended as a layer between ML and PM in growing plant cells. The driving force of cell expansion is turgor pressure, that is counteracted by the mechanical properties of PCW, which as a consequence eventually defines cell shape and size. The mechanical properties of the PCW are depended on polysaccharides like crystalline cellulose microfibrils, hemicellulose (xylogucan in dicots and arabinoxylose in monocots), and pectin (prominently represented by rhamnogalacturonans I and II) and their arrangement within the thin PCW matrix.

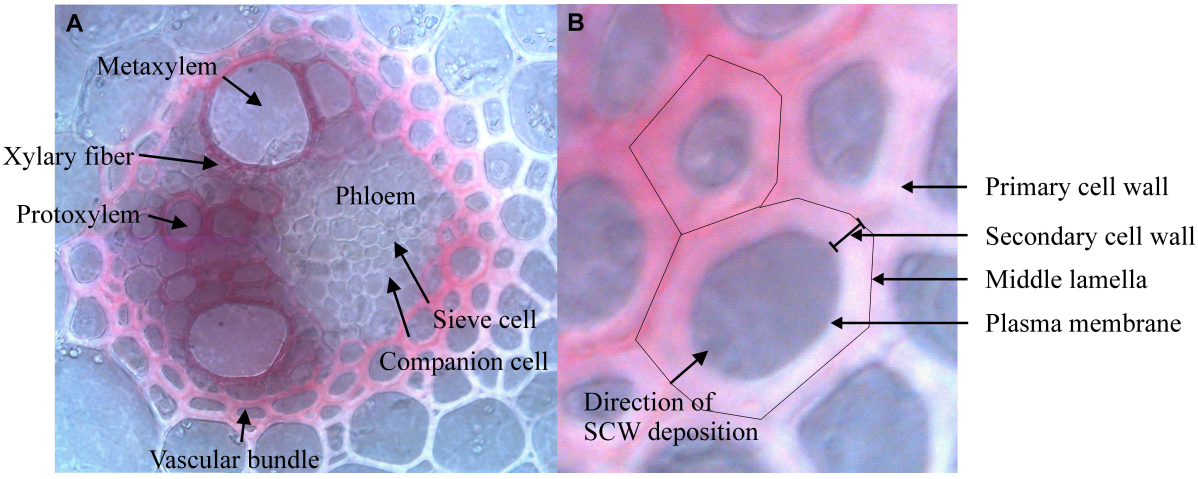

Figure 1: Morphology and secondary cell wall structure of a vasculature from *Miscanthus sinensis* stem.

(A) Morphology of vasculature of a *Miscanthus sinensis* stem. The cross-section was stained for lignin with HCl-phloroglucinol. (B) Structural layers of a cell wall by the example of a bundle sheath fiber cell.

1.3.1 Secondary plant cell wall

The SCW is formed in specialised cell types such as fibers and tracheary elements following cessation of cellular growth (Figure 1). SCW are composed of cellulose, hemicellulose, and lignin. However, the precise composition of cellulose, hemicellulose, and lignin and also the proportion of each component largely depend on the plant species, the tissue type, and its developmental stage. SCWs are deposited between the PCW and the PM to provide strength to the cell wall, that serves as mechanical support. Particularly strong SCW formation occurs in fibers, in which it can occupy most of the cell lumen. Fibers are present in diverse tissue types such as phloem, extraxylary, and interfascicular tissue to confer protection and structural support (Figure 1). In water conducting tissue, SCWs fulfil probably their most important function. SCW formation enables tracheary elements to resist the negative pressure generated by water transpiration stream, that is regarded as a key innovation of vascular plants to conquer terrestrial habitats. Incorporation of the aromatic polyphenol lignin into SCWs impregnates tracheary elements against water (Figure 1), constituting efficient water transport. SCWs are also present in seed coats of various plants providing protection of the seed against mechanical damage. In most flowering plant species, SCW formation in endothecia is critical for generation of the tensile forces necessary for dehiscence of anthers to release pollen (Mitsuda et al., 2005).
Comparison of cell wall composition of dicots and monocots nicely illustrates the large variability of cell walls among plant species. For example, SCWs from commelinid grasses, including *Miscanthus*, contain xylans with glucuronic acid- and arabinose side chains, which are not found in hemicelluloses of dicots (Harris & Trethewey, 2010; Vogel, 2008). Correlated with the unique chemistry of glucuronoarabinoxylan in grasses, ferulic acid, which is ester-linked to the hemicellulose is highly abundant while it represents a minor component in dicots (Harris & Trethewey, 2010). Another specific trait of grass cell walls is the incorporation of minor but significant amounts of H units into lignin compared to dicotyledonous lignins (Barrière et al., 2007).

1.3.2 Cellulose

The structural polysaccharide cellulose is made of β-1,4-linked D-glucosly residues polymerised to long, linear β-glucan chains. These can vary in length, strongly depending on plant species and tissue type usually several thousand glucose residues. β-glucan chains can crystallise to insoluble microfibrils through formation of hydrogen bonds and Van der Waals forces. Orientation, angle, length, and crystallisation of microfibrils are important

determinants of the physical wall cell properties (Cosgrove, 2016). While the exact structure of microfibrils are still under debate, a microfibril probably contains between 18 and 24 glucan chains with a diameter of about 3 nm (Newman et al., 2013; Turner & Kumar, 2018).

Cellulose is synthesised by a large membrane-bound cellulose synthase complex (CSC) at the PM. The CSC forms a hexameric rosette structure, that consists of cellulose synthase subunits (CesAs). The exact number of CesAs in a single CSC is still under debate but probably between 18 and 36 CesAs (Schneider et al., 2016). CSC are usually assumed to contain three different CesAs, which belong to glycosyltransferase family GT2 (McFarlane et al., 2014). In *Arabidopsis thaliana*, CesA1, CesA3, and CesA6 are implicated in synthesis of the PCW, whereas for CesA4, CesA7, and CesA8 a role in SCW synthesis has been demonstrated. It has been shown that CesAs function non-redundantly, as mutation of either CesA1, CesA3, or CesA6 results in defects of cell morphology in early plant development (Desprez et al., 2007). However, mutation of CesA4, CesA7, or CesA8 lead to collapsed vessel phenotype due to reduced cellulose content and SCW formation (N. G. Taylor et al., 2003). In other plant species, involvement of CesAs in PCW and SCW synthesis seems to be similar (Nairn & Haselkorn, 2005).

CesAs are synthesised by endoplasmic reticulum-bound ribosomes before they assemble to CSCs in the endoplasmic reticulum and the Golgi apparatus. After assembly, the CSCs are actively trafficked to the PM via small vesicles along the F-actin cytoskeleton (McFarlane et al., 2014). Cortical microtubules are known to target secretory vesicles to the PM (Paredez, Wright & Ehrhardt, 2006; Vukašinović et al., 2017). In addition, the association of CSC with cortical microtubules via CSI and POM2 proteins determines direction of CSC movement (Bringmann et al., 2012; E. Li et al., 2012; Watanabe et al., 2015). Thereby cortical microtubules control deposition of cellulose, typically perpendicular to the growth axis in elongating cells (Paredez, Somerville & Ehrhardt, 2006), which determine anisotropic growth and cell shaping (Landrein & Hamant, 2013).

Isoxaben

The potent broad leaf herbicide isoxaben was found as cellulose biosynthesis inhibitor. Isoxaben specifically inhibits cellulose biosynthesis by targeting CesA3 and CesA6 leading to clearance of CSCs from plasma membrane (Paredez, Somerville & Ehrhardt, 2006). In *Arabidopsis*, a missense mutations in the C-terminus of either CesA3 or CesA6 is sufficient to confer resistance against isoxaben (Desprez et al., 2002; Scheible et al., 2001). Isoxaben treatment was found to disrupt cell wall integrity. As a consequence, an ethylene-

and jasmonic acid-mediated defense response is activated which mimics a pathogen attack and results in ectopic lignin formation (Ellis et al., 2002; Tsang et al., 2011).

1.3.3 Hemicellulose

Hemicelluloses comprise a heterogeneous group of structural polysaccharides. They are believed to cross-link cellulose microfibrils through hydrogen bonds, and thereby providing mechanical stiffness to the cell wall matrix. In contrast to cellulose, hemicellulose synthesis occurs inside the Golgi apparatus. Hemicelluloses are transported to the PM via the *trans*-Golgi network, secreted to the apoplast, and incorporated into the cell wall. The polysaccharide xylan is the major hemicellulose in PCW of grasses and SCW of grasses and dicots. Structurally the backbone of xylan is made of β-1,4-linked D-xylosyl residues with various side chains. Based on the side chains, xylans can be classified into glucuronoxylan (GX) and acetylated glucuronoarabinoxlyan (GAX), that are predominantly found in dicot and monocot species, respectively. GX largely consists of α-1,2-linked glucuronic acid and 4-O-methylglucuronic acid residues. By contrast, GAX contains substantial amounts of α-1,2- and α-1,3-linked arabinofuranosyl residues, that form ester-bonds to hydroxycinnamic, ferulic, or *p*-coumaric acid (Rennie & Scheller, 2014). It has been postulated, that more side chains of GAX, as found in PCW lead to weaker interaction with cellulose. By contrast GAX with fewer side chains forms stronger interaction to cellulose contributing to recalcitrance of SCWs (Costa et al., 2016). Another unique characteristic of some grasses, including *Miscanthus*, is the occurrence of small amounts of mixed-linkage glucan, a β-1,3; 1,4-linked D-glucosyl polysaccharide (Kulkarni et al., 2012). Mixed-linkage glucan is considered as a structural component in young, expanding- and mature tissues (Vega-Sanchez et al., 2012).

1.3.4 Lignin

Lignin is a heterogeneous aromatic polymer predominantly derived from three hydroxycinnamyl precursors, namely *p*-coumaryl-, coniferyl-, and sinapyl alcohol. The hydroxycinnamyl alcohols are transported to the apoplast where they oxidatively polymerise to *p*-hydroxyphenyl (H), guaiacyl (G), and syringly (S) units (Figure 2). Lignin is mainly deposited in SCW and coats the cell wall polysaccharide matrix, providing resistance to degradation, mechanical support, and hydrophobicity. The lignin content, composition, and inter-unit linkage is extremely variable between species, tissue types, developmental

stages, and across cell wall layers. For example, lignins of angiosperms are largely composed of S and G units, whereas lignins of gymnosperms contain besides S and G units also minor but significant amounts of H units. Lignin content is strongly dependent on the developmental stage and varies considerably between different *Miscanthus* genotypes from about 17 % to 25 % of dry cell wall biomass (da Costa et al., 2014).

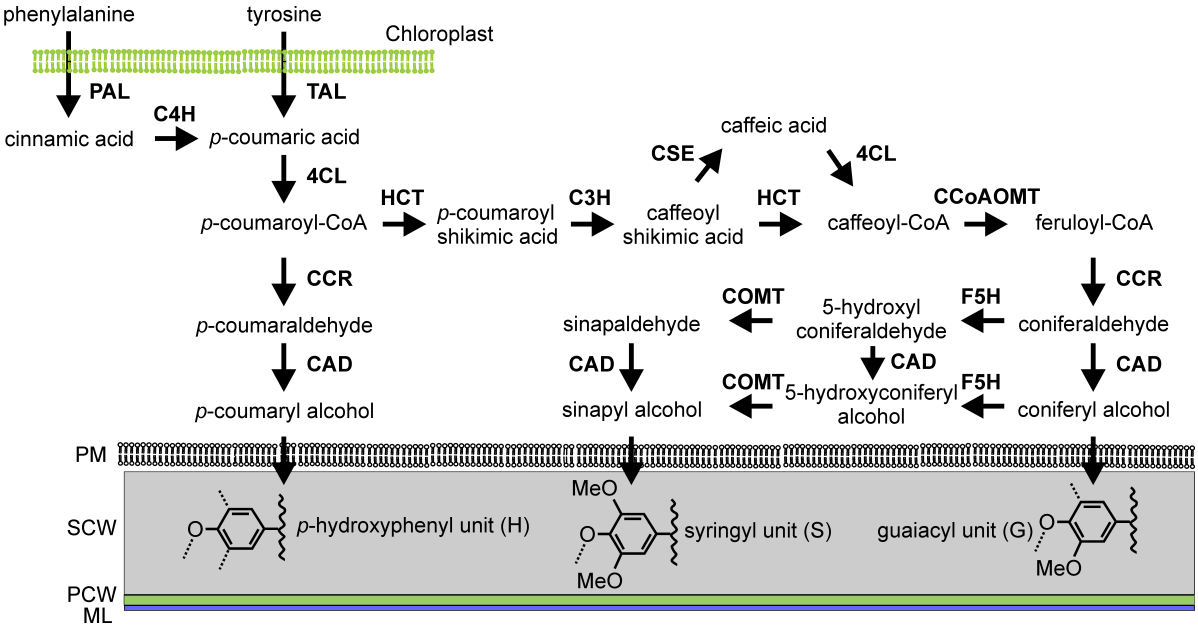

Figure 2: Biosynthetic pathway of monolignols via phenylpropanoid pathway.

Phenylalanine and tyrosine derived from the shikimate pathway from chloroplasts are converted to three monolignols, namely p-coumaryl, sinapyl, and coniferyl alcohol. The monolignols are transported from the cytosol to the apoplast and oxidised to the lignin polymer. Phenylalanine ammonia-lyase (PAL), tyrosine ammonia-lyase (TAL), cinnamic acid 4-hydroxylase (C4H), 4-coumarate:CoA ligase (4Cl), *p*-hydroxycinnamoyl transferase (HCT), *p*-coumarate 3-hydroxylase (C3H), caffeoyl-CoA *O*-methyltransferase (CCoAOMT), cinnamoyl-CoA reductase (CCR), and cinnamyl alcohol dehydrogenase (CAD). Middle lamella (ML), primary cell wall (PCW), secondary cell wall (SCW), and plasma membrane (PM).

The biosynthesis of monolignols starts with phenylalanine, which is derived from shikimate pathway from plastids and converted by phenylalanine ammonia-lyase (PAL), cinnamic acid 4-hydroxylase (C4H), and 4-coumarate:CoA ligase (4Cl) to *p*-coumaroyl-CoA (Figure 2). From this point *p*-coumaroyl-CoA is ultimately shuffled into several branches leading to formation of many secondary metabolites such as flavonoids and monolignols (Vogt, 2010). The monolignol-specific pathway starts with activation of *p*-coumaroyl shikimic acid to feruloyl-CoA by *p*-hydroxycinnamoyl transferase (HCT), *p*-coumarate 3-hydroxylase (C3H), and caffeoyl-CoA *O*-methyltransferase (CCoAOMT). Following activation of the precursors, feruloyl-CoA is reduced by two successive steps by cinnamoyl-CoA reductase (CCR) and cinnamyl alcohol dehydrogenase (CAD) to coniferyl and sinapyl alcohol. A

unique feature of grasses, tyrosine ammonia-lyase (TAL) and bifunctional ammonia-lyases (PTALs) were recently found to use additionally to phenylalanine, tyrosine as precursor for the synthesis of S lignin units (Barros et al., 2016).
Subsequent to synthesis in the cytosol, monolignols are combinatorially coupled, glycosylated, and either stored in the vacuole or transported to the apoplast (Dima et al., 2015). Transport of monolignols via the Golgi apparatus seems to be negligible (Kaneda et al., 2008). The glycosylation status of monolignols is proposed to determine transport and compartmentation by ABC transporters (Miao & Liu, 2010). However, monolignol glucosides probably do not constitute direct precursors of lignin (Chapelle et al., 2012). Radical polymerisation of monolignols to lignin gives rise to a wide range of linkages between subunits with β-aryl ether (β-*O*-4), resinols (β-β), and phenylcoumarans (β-5) as most abundant linkages (Vanholme et al., 2012). Peroxidases and/or laccases present in the cell wall matrix use H_2O_2 as co-substrate to create monolignol radicals, that polymerise into the lignin polymer (Vanholme et al., 2008). Another unique aspect of grasses is that they accumulate high amounts of ferulic and *p*-coumaric acid, that form cross-links to hemicellulose and serve as initiation site for lignin deposition (Ralph et al., 1995), highlighting different lignification mechanisms in grasses and dicots.
Even within the same plant, lignification shows distinct mechanisms. Sclerenchyma cells such as xylary fibers and sclereids control the whole process of lignification by their own from biosynthesis of monolignols to polymerisation of lignin in the cell wall. They undergo cell-autonomous lignification (Smith et al., 2013). In sharp contrast, programmed cell death occurs early in vessel development and as a consequence vessels cannot ensure their own lignification. They undergo non-cell autonomous lignification or the so-called 'good neighbours' scenario (McCann et al., 2001; Smith et al., 2013; Voxeur et al., 2015). Xylem parenchyma cells (good neighbours) allocate monolignols and H_2O_2 to vessel cells, that are required for lignification of the SCWs (Ros Barceló, 2005).

1.4 Transcriptional regulation of secondary cell wall biosynthesis

In *Arabidopsis*, formation of SCW cellulose, hemicellulose, and lignin is regulated by a sophisticated network of transcription factors (TFs), that is organised in a multi-tiered hierarchical manner by NAM, ATAF1,2, and CUC2 (NAC) and MYB TFs. Thereby the network coordinately integrates developmental aspects and environmental cues for the SCW formation, which is vital for the structural integrity of the plant.

1.4.1 NAC transcription factors

The plant-specific NAC proteins comprise one of the largest group of TFs in plants. They are usually represented by more than 100 members in angiosperm species and can be generally classified into 21 subfamilies (Zhu et al., 2012). They have been reported to participate in various processes including plant growth, development, and biotic and abiotic stresses (Olsen et al., 2005). NAC proteins share a highly conserved NAC binding domain at the N-terminus, that is important for nuclear localisation, DNA-binding, and homo-/heterodimer formation. However, the variable C-terminal domain is involved in transcriptional activation (Olsen et al., 2005).
The phylogenetically closely related NAC TFs of the subfamily Ic are regulators of the first-tier of the hierarchical network and its members are considered as master switches of SCW formation. Among the best studied NAC TFs are NAC SECONDARY WALL THICKENING PROMOTING FACTOR1, 2 (NST1, NST2), SECONDARY WALL-ASSOCIATED NAC DOMAIN1 (SND1/ NST3), VASCULAR-RELATED NAC-DOMAIN6 (VND6), and VND7. NST1, NST2, and SND1/NST3 have been reported to redundantly regulate the SCW formation in fibers or endothecia of anthers (Mitsuda et al., 2007; Mitsuda et al., 2005; Zhong et al., 2006; Zhong et al., 2007b), whereas VND6 and VND7 are implicated in the SCW deposition of tracheary elements (Kubo et al., 2005). Besides their regulatory function in SCW biosynthesis, they also control the machinery for its patterned deposition (Oda & Fukuda, 2013) and induction of programmed cell death (Yamaguchi et al., 2011). They were shown to bind an imperfect palindromic 19-bp consensus sequence designated as secondary wall NAC binding element (SNBE), present in promoter sequences of direct target genes (Zhong et al., 2010c).
NAC TF master switches regulating SCW formation have been identified in many vascular plant such as *Brachypodium*, *Picea*, *Oryza*, *Sorghum*, *Zea*, *Vitis*, *Eucalyptus*, *Medicago*, *Populus*, and *Carica* (Valdivia et al., 2013; Yoshida et al., 2013; Zhao et al., 2010; Zhong, Lee, McCarthy et al., 2011; Zhong et al., 2010a; Zhong et al., 2015; Zhu et al., 2012), indicating a high conservation of the regulatory network of SCW formation.

1.4.2 MYB transcription factors

MYB proteins build a large family of TFs in plant kingdom, where they are most abundantly represented by R2R3 MYB TF. They are characterised by a highly conserved MYB DNA-binding domain, that contains imperfect sequence repeats (R) of about 52 amino acids. Characteristic for the repeats is the formation of a helix-turn-helix structure with regular

tryptophan residues comprising the hydrophobic core (Stracke et al., 2001). Binding specificity is conferred by the third α-helix, that intercalates directly with its DNA target (Jia et al., 2004). MYB TFs function in a wide range of plant-specific developmental processes and environmental cues including cell fate and identity, primary and secondary metabolism, and biotic and abiotic stress responses.

In *Arabidopsis*, MYB46 and MYB83 were identified as second-tier regulators of SCW formation. They redundantly regulate expression of genes involved in SCW biosynthesis including cellulose, xylan, and lignin-related genes. In turn the expression of MYB46 and MYB83 is controlled by NAC TFs (Kim et al., 2014; McCarthy et al., 2009; Zhong et al., 2007a). MYB TFs from *Eucalyptus*, *Pinus*, and *Populus* including EgMYB2, PtMYB4, PtMYB8, PtrMYB2, PtrMYB3, PtrMYB20, and PtrMYB21 were found to perform the same or very similar function as MYB46/MYB83 from *Arabidopsis* (Bomal et al., 2008; Goicoechea et al., 2005; Patzlaff et al., 2003; Zhong et al., 2013). EgMYB2 and PtMYB4 specifically bind to three 7 bp DNA-binding elements, so called AC elements (Goicoechea et al., 2005; Patzlaff et al., 2003). Similarly, MYB46/MYB83 from *Arabidopsis* bind to the same AC elements and five additional variants designated as secondary wall MYB-responsive element (SMRE), that are present in all direct target genes (Zhong & Ye, 2012).

Downstream targets of MYB46 and MYB83 comprise a number of MYB TFs, that are considered as third-tier TFs to fine-tune transcriptional regulation of SCW formation. Among them MYB58, MYB63, and MYB85 are specifically involved in regulation of lignification, while MYB103 specifically gives rise to syringyl lignin by regulating the expression of ferulate 5-hydroxylase (Öhman et al., 2013). Many other third-tier TFs are reported to be involved in SCW formation such as MYB42, MYB52, MYB54, MYB69, MYB83, SND2, and SND3, although their precise roles are not fully understood (Ko et al., 2009; Zhong et al., 2008). Notably, the expression of some enzymes of cellulose, hemicellulose, and lignin biosynthesis are targeted by TFs from different tiers, creating strong feed-forward loops to ensure efficient activation of SCW formation (Taylor-Teeples et al., 2015). Besides these positive regulators of SCW formation, KNAT7, MYB4, MYB7, and MYB32 have been proposed as transcriptional repressors of lignification and SCW formation (Jin et al., 2000; E. Li et al., 2012; Preston et al., 2004).

As mentioned above, studies on tree species like poplar or *Eucalyptus* have suggested that the structure of the multi-tiered regulatory network controlling SCW biosynthesis is conserved among plant species. Considering the huge differences between the SCW formation in the herbaceous *Arabidopsis* and wood formation in poplar, it seems less of a surprise, that poplar has evolved a more complex regulatory network (Zhong, McCarthy, Lee & Ye, 2011). In support of this hypothesis, the extensive differences of SCW composition and structure between monocots and dicots (Section 1.3.3, 1.3.4) probably indicate distinct regulatory networks of SCW formation. Indeed, *Arabidopsis* MYB63 and the close

relatives in rice and sorghum (OsMYB58, OsMYB63, and SbMYB60) were reported to have different target gene profiles (Noda et al., 2015; Scully et al., 2018; Scully et al., 2016).

1.4.3 Lignin engineering

The bulk of plant biomass bears a large potential as sustainable and renewable energy resource substituting fossil energy sources. Driven by cell wall recalcitrance-based limitation in biomass processing, optimisation of plant biomass has been focused on altering lignin content, composition, and structure exploiting the natural plasticity of lignin (Section 1.3.4). Lignin engineers have been aiming for lignins: i) with reduced hydrophobicity, ii) with a lower degree of polymerisation, iii) with less cross-linking to other cell wall constituents, iv) with novel monolignols introducing chemically labile linkages, and v) with high value-added chemical moieties because lignin also represents a potential source of high-value aromatic chemicals (Lan et al., 2015; Ragauskas et al., 2014; Sainsbury et al., 2013; Smith et al., 2017; Stewart et al., 2009; Wilkerson et al., 2014).
Attempts to alter lignin composition, content or structure often result in undesirable phenotypes such as dwarfism, collapsed xylem vessels, or higher susceptibility against pathogens (Bonawitz & Chapple, 2013). However, the underlying mechanisms causing dwarfism are only poorly understood. It has repeatedly been suggested, that insufficient cell wall integrity is the reason for collapsed xylem vessels that ultimately results in dwarfism. Nonetheless, it seems more likely, that signalling accounts for the growth penalty, and circumventing the signalling feedback could prevent unfavourable phenotypes (Bonawitz et al., 2014; Gallego-Giraldo et al., 2011). Another explanation is that accumulating byproducts have an inhibitory feedback on growth or constitute toxic compounds (Bonawitz & Chapple, 2013). Designer lignins seem to meet the biological requirements avoiding undesired growth phenotypes, but at the same time improving biomass utilisations and comprising novel compounds with distinct chemical properties for new applications in biorefinery (Mottiar et al., 2016).

1.5 Research Objectives

The desire to use lignocellulosic biomass as a renewable energy and material resource has intensified research efforts to understand secondary cell wall formation, mainly because of two reasons. Firstly, cell wall recalcitrance is largely conferred by coating of the

polysaccharide matrix with lignin. Secondly, the heterogeneous aromatic polymer lignin has recently gained more importance as raw material for lignin-derived products. Hybrids of the genus *Miscanthus* have emerged as leading candidates for the production of lignocellulosic biomass in temperate climates. However, nothing is known about molecular players regulating secondary cell wall biosynthesis or lignin biosynthesis in *Miscanthus*. Knowledge about key regulators of secondary cell wall formation are likely to facilitate exploration of the regulatory network. Furthermore, key regulators are considered as potential targets for breeding of tailored biomass. Since lignin engineering has gained momentum, specific regulators of lignin biosynthesis probably present attractive targets for biomass improvements. Therefore, this study aimed at identification and characterisation of molecular regulators of secondary cell wall formation with a strong focus on lignification in *Miscanthus sinensis*.

Chapter 2

Material and Methods

2.1 Plant material

2.1.1 Plant genotypes

Experiments were carried out on *Miscanthus sinensis* (identification number: Sin-13) collected in Honshu, Japan (Clifton-Brown & Lewandowski, 2002). For transient expression *in planta*, *Nicotiana benthamiana* wildtype was used. *Arabidopsis thaliana* (L.) Heynh. had the ecotype Columbia. Arabidopsis *snd1 nst1* double mutant seeds (Mitsuda et al., 2007) were obtained from the Nottingham Arabidopsis Stock Center (NASC). In the double mutant the respective genes have been knocked-out by tDNA insertion containing a selection marker. Arabidopsis *snd1 nst1* double mutant have been genetically and phenotypically verified (Section 3.4).

2.1.2 Plant Cultivation

On Soil

Arabidopsis thaliana, *Nicotiana benthamiana* and *Miscanthus sinensis* were grown on standardised soil ED-73 from seeds in glasshouse under 8/16-hr (light/dark) photoperiod at 22-25 °C. The soil composition is listed below (Table 1).

Table 1: Soil composition (ED-73)

3 g l^{-1}	KCl
0.6 g l^{-1}	K_2O
0.3 g l^{-1}	N
0.3 g l^{-1}	P_2O_5
	pH 6.0 ($CaCl_2$)

On Agar Plates

For selection and plant treatment, seeds were surface-sterilised according to Section 2.1.3 and subsequently grown on half-strength MS plates supplemented with 25 µg l^{-1} hygromycin, 7.5 µg l^{-1} glufosinate ammonium or isoxaben (Sigma-Aldrich) in concentrations indicated in the corresponding experiment.

MS plates (Murashige & Skoog)

2.2 g l^{-1}	Murashige & Skoog with vitamins (Duchefa)
3 % (w/v)	Sucrose (Roth)
0.8 % (w/v)	Agar (Duchefa)
	pH 5.7 (KOH)

2.1.3 Surface-Sterilisation of Plant Seeds

A. thaliana

To grow *A. thaliana* on agar plates, seeds were collected in 1.5 ml Eppendorf tube and shaken by hand with 1 ml sterilisation solution for 2 minutes. Subsequently, the seeds are washed twice for 1 minute with 100 % ethanol (v/v) and dried in a sterile bench.

Sterilisation Solution

1.3 % (v/v)	Sodium hypochlorite
70 % (v/v)	Ethanol

M. sinensis

To ensure sterile growth condition on agar plates, *M. sinensis* seeds were surface-sterilised by shaking about 20 seeds in 70 % ethanol (v/v) for 1 minute. Ethanol was replaced with 1 % sodium hypochlorite (v/v) containing 0.1 % Tween-20 (v/v) and shaken by hand for another 10 minutes. Afterwards the sodium hypochloride was discarded and the seeds were washed three times with 1 ml sterile ddH_2O to remove residual sodium hypochloride.

2.1.4 Plant treatment

For identification of direct and indirect targets of MsSND1, 10 day old transgenic mCherry-GR-MsSND1 Arabidopsis seedlings were pretreated for 2 hours in half-strength MS liquid medium (Section 2.1.2) supplemented with 10 µM cycloheximide (CHX). To activate mCherry-GR-MsSND1, the seedlings were transferred to fresh half-strength MS liquid medium containing either 10 µM dexamethasone (DEX) and/or 10 µM CHX solution for 4 h. Excessive medium was quickly removed with paper tissue before flash freezing in liquid nitrogen.

2.2 Microbiological and Biomolecular Methods

2.2.1 Bacteria strains, Plasmids and Oligonucleotides

For cloning, mutagenesis, and preparation of plasmids the bacteria strains *Escherichia coli (E. coli)* XL1-blue, DH5α, and DB3.1 were used (Table 2). The bacteria strains facilitate easy transformation and allow efficient selection of successful transformants. Transformation of *N. benthamiana* for transient expression studies or stable transformation of *A. thaliana* were achieved with *Agrobacterium tumefaciens*.

Table 2: Bacterial strains and plasmid vectors/constructs used in this study

Strains	**Description**	**Reference**
A. tumefaciens ASE (pSOUP$^+$)	pSOUP$^+$ helper plasmid that confers replicase activity for pSa replication origin on pGreen-derived plasmids. Chl^r, Tet^r and Kan^r	Hellens et al., 2000
A. tumefaciens C58C1 (P14)	35S:p14 silencing suppressor from Pothos latent virus (PoLV). Kan^r, Rif^r, Tet^r	Mérai et al., 2005
E. coli XL1-Blue	*rec*A1, *end*A1, *gyr*A96, *thi*-1, *hsd*R17(r_K, m_K+), *sup*E44, relA1, lac, [F', *pro*AB+, lacI^{q}ZΔM15, ::Tn10 (tet^r)]	Bullock et al., 1987
E. coli DH5α	F$^-$ $\varphi 80$*lac*ZΔM15 Δ (*lac*ZYA-*arg*F U169 *rec*A1 *end*A1 *hsd*R17 (rk$^-$, mK$^+$) *pho*A *sup*E44 λ^- *thi*-1 *gyr*A96 *rel*A1	Woodcock et al., 1989
E. coli DB3.1	F$^-$ *gyr*A462 *end*A1 Δ(*sr*1-*rec*A) *mcr*B *mrr* *hsd*S20(r_B^-, m_B^-) *sup*E44 *ara*14 *gal*K2 *lac*Y1 *pro*A2 *rps*L20(Sm^r) *xyl*5 Δ*leu* *mtl*1	Bernard and Couturier, 1992

Plasmids:

Vector	**Description**	**Reference**
pART7_GW	Overexpression plasmid for bombardement, Amp^r	Höll, 2014
pLUC_GW	Firefly luciferase plasmid for bombardement, Amp^r	Höll, 2014
pPGA10	At*SND1* promoter	this study
pGGA004	35S promoter	Lampropoulos et al., 2013
pGGA006	UBQ10 promoter	Lampropoulos et al., 2013
pGGB003	B-Dummy	Lampropoulos et al., 2013
pGGB021	mCherry-Glucocorticoid receptor-linker	A kind gift from Dr. Miotk (Heidelberg University)
pPGC11	Ms*SND1*	this study
pPGC12	At*SND1* (At1g32770)	this study
pPGC13	Ms*MYB20*(*SCM1*)	this study

pPGC14	Ms*MYB43*(*SCM3*)	this study
pPGC15	Ms*MYB63*(*SCM4*)	this study
pPGC16	Ms*MYB85*(*SCM2*)	this study
pPGC17	Ms*MYB103*	this study
pGGC087	C-Dummy	Lampropoulos et al., 2013
pGGD002	D-Dummy	Lampropoulos et al., 2013
pGGE001	RBCS terminator	Lampropoulos et al., 2013
pGGE009	UBQ10 terminator	Lampropoulos et al., 2013
pGGF001	pMAS::Basta^r::tMAS	Lampropoulos et al., 2013
pGGF005	pUBQ10::Hygromycin^r::tOCS	Lampropoulos et al., 2013
pGGF026	pUBQ::mCherry::tRBS pNOS::Kan^r::tNOS	Lampropoulos et al., 2013
pGGZ003	destination vector	Lampropoulos et al., 2013

GreenGate Constructs:

Complementation Constructs	
pPGA10	At*SND1* promoter
pGGB003	B-Dummy
pPGC11/12	Ms*SND1* or Ms*VND7*
pGGD002	D-Dummy
pGGE009	UBQ10 terminator
pGGF001	pMAS::Basta^r::tMAS
pGGZ003	destination vector
Overexpression Constructs	
pGGA004	35S promoter
pGGB003	B-Dummy
pPGC11-16/ pGGC087	Ms*SND1*, At*SND1*, C-Dummy (control), Ms*MYB20*, Ms*MYB43*, Ms*MYB63* and Ms*MYB85*
pGGD002	D-Dummy
pGGE001	RBCS terminator
pGGF026	pUBQ::mCherry::tRBS pNOS::Kan^r::tNOS
pGGZ003	destination vector
Inducible Construct	

pGGA006	UBQ10 promoter
pGGB021	mCherry-Glucocorticoid receptor-linker
pPGC11	Ms*SND1* or Ms*VND7*
pGGD002	D-Dummy
pGGE001	RBCS terminator
pGGF005	pUBQ10::Hygromycin^r::tOCS
pGGZ003	destination vector

Table 3: Oligonucleotides used for PCR, qRT-PCR and sequencing

Transcript	Forward (5'-3')	Reverse (5'-3')	Length (bp)
Miscanthus sinensis qPCR			
PP2A	GCTAGCTCCTGTCATGGGTC	TCATGTTCGGAACCCTGTCC	89
Clath	ACAATCAAGGAATTGGGCCG	GCACCGAAAACACTCTTGACT	65
UBC	CTGAACCAGACAGCCCACTT	CTCTGATATCACCCGACCGC	63
TIP	ACTGTGGGAGTGATGCTGTG	CTCCCAACACAAAGTGCTGC	80
SND1	GACATCCAAGAGAAGTGCCG	CGTCGGGTACTTCTTGTCCT	84
MYB63	ACATAGCAAGCTTCAGCCCA	CCACCAGGAGTTCAGGTTCC	105
MYB85	GCAGCCCTACGGAATCGA	CCAGCGGGTCTTGGTCAT	93
MYB43	AAGGCAGCTTCCTCACAGTC	GCTGGACTGCTCCGATGAAT	132
HCT	GGAGCACTGGATAGGATGGA	AAGTCGGCATCATGGATAGG	161
CCoAOMT	ACGCCGACAAGGACAACTAC	GTCACGGTAGAAGCGGATGT	155
Arabidopsis thaliana qPCR			
Clath	TCGATTGCTTGGTTTGGAAGAT	GCACTTAGCGTGGACTCTGTTTGC	61
MYB46	TTCGCTTTCATTCCATCCTCG	CAATCGTGCTGCAATCTGAGA	53
MYB83	AACGTGGATCCTTCTCTCCTC	AGCCGAGTAGCTATTTGAGACC	91
CesA4	CTGTGGTTATGAAGAGAAGACTGAA	TGCATTCTAAATCCAGTGAGGA	93
CesA7	ATGCCACCGATAAGCACATT	TTCCTCAATGCTAACTCCGC	108

CesA8	GATTCCTACCCAACAGCACAT	ACAGAGCCAAGATGATCAACC	149
LAC4	GGTAGATATCCAGGTCCCACA	GTTATGTAAGCAGGCCCATCA	149
IRX7	AAAACATCAGTGGACGCTTCT	TTGCCGTTGGAGATAAAACCT	92
IRX8	GGCTTGGAGGAGGACTAACAT	GTTTGGACATGACCGTGGAAA	132
4Cl1	CTAATGCCAAACTCGGTCAGG	AGCTCCTGACTTAACCGGAAA	104
CCoAOMT	CTCACAAGATCGACTTCAGGG	ACGCTTGTGGTAGTTGATGTAG	137
XCP1	TCCACAAAGAAGATGATTACCCTTA	TCACACGTTCCACATCCTCTT	78

Cloning

AtSND1p fwd	aacaGGTCTCAacctCGCGATTATTTGTGCTGAAG
AtSND1p rev	aacaGGTCTCTtgttTCAGCCATTAACGAAGATAGCA
AtSND1 fwd	aacaGGTCTCAggctCACGTTAATGGCTGATAATAAGGTCA
AtSND1 rev	aacaGGTCTCTctgaTCATACAGATAAATGAAGAAGTGGGT
MsSND1 fwd	aacaGGTCTCAggctCAATGAGCATCTCGGTGAACG
MsSND1 rev	aacaGGTCTCTctgaCTAGAAGTTGTTCATCGTCAAGTCC
MsMYB20 fwd	aacaGGTCTCAggctCAAGAGAGATGGGCAGGCAG
MsMYB20 rev	aacaGGTCTCTctgaCTAGCTAGAATTTTGCTCCGTTTG
MsMYB43 fwd	aacaGGTCTCAggctCAATGGGGAGACAGCCATGC
MsMYB43 rev	aacaGGTCTCTctgaTTAGAAGTTTGATCCATTTGAGGC
MsMYB63 fwd	aacaGGTCTCAggctCAATGGGGCGAGGGCGAG
MsMYB63 rev	aacaGGTCTCTctgaTCATAGCAGAACGGCAGATG
MsMYB85 fwd	aacaGGTCTCAggctCAATACAGGTTGGGATGGGTCG
MsMYB85 rev	aacaGGTCTCTctgaCTAGCTAGCTAGAATTTTGCTCCG
MsMYB103 fwd	aacaGGTCTCAggctCAATCTAGCATGGGGCATCACT
MsMYB103 rev	aacaGGTCTCTctgaCACCAAGCAGCTTTTCATCA

2.2.2 DNA Amplification via Polymerase Chain Reaction (PCR)

The polymerase chain reaction (PCR) was performed with genomic DNA, complementary DNA or plasmid DNA as template for *in vitro* amplification of DNA fragments. Primers to specify the DNA fragments (Table 3) were designed with Primer3 software and synthesised by Eurofins (Munich, Germany). The thermocycles were carried out by a Mastercycler® RealPlex 2 from Eppendorf (Hamburg, Germany).

Standard PCR reaction mix

0.1 to 100 ng µl^{-1}	DNA
10 µM	Forward Primer & Reverse Primer (Table 3)
10 mM	dNTP mix
2 or 4 µl	10×/5× Reaction buffer
0.1 or 0.2 µl	Taq-/Q5-polymerase
ad 20 µl	ddH_2O

Standard PCR cycle

Initial denaturation	95 °C	5 min	
Denaturation	95 °C	0.5 to 2 min	35 to 40 cycles
Primer annealing	58 to 72 °C	30 s	
Elongation	72 °C	0.5 to 3 min	
Terminal elongation	72 °C	5 min	
Cool down	4 °C		

2.2.3 DNA Cloning

GreenGate

A DNA fragment was amplified (Section 2.2.2) with gene-specific primers (Table 3) including *Eco*31I restriction site and module code. PCR product was column purified with GeneJET PCR Purification Kit (Thermo Fisher). About 0.2 µg purified PCR product and up to 1 µg empty entry vector were digested together with *Eco*31I FD (Thermo Fisher) at 37 °C for 10 min. After another column purification, about 5 µl digestion product were ligated for 1 h with T4 DNA ligase and T4 buffer (Thermo Fisher) in a total volume of 10 µl and transformed according to Section 2.2.6. Correctness of entry construct was tested by check-PCR using appropriate primers (Table 3). Positve colonies were transferred to liquid culture and plasmid were prepared with GeneJET Plasmid Miniprep Kit (Thermo Fisher) and sent to sequencing.

To create destination constructs, 1.5 µl of each module (A-F), 1 µl empty destination vector, 2 µl FastDigest buffer, 1.5 µl 10 mM ATP, 1 µl T4 DNA ligase and 1 µl *Eco*31I FD were mixed and incubated in a PCR thermocycler as described in Lampropoulos et al., 2013

and the table below. 5 µl of the resulting reaction mix were transformed into *E. coli* DH5α and correctness of constructs were examined as described above.

GreenGate reaction cycle

37 °C	2 min	50 cycles
16 °C	2 min	
50 °C	5 min	
80 °C	5 min	
4 °C	∞	

Gateway™

A DNA fragment was amplified (Section 2.2.2) with gene-specific primers (Table 3) including Gateway-compatible attB-overhangs. PCR product was column purified with GeneJET PCR Purification Kit (Thermo Fisher). 75 ng pDONR201 were combined with approximately 3 µl purified PCR product and 1 µl BP clonase II mix (Invitrogen) to a total volume of 10 µl and incubated for at least 1 h at RT. The reaction was stopped by adding 1 µl Proteinase K and incubating at 37 °C for 10 min before it was transformed into *E. coli* and selected on Kanamycin plates. Positive clones were identified by check-PCR followed by plasmid preparation and sequencing. The LR recombination reaction into pART7 or pLUC were conducted similar to BP reaction but with about equal molar ratios of entry and destination vectors and LR clonase II mix.

2.2.4 Cultivation of Bacteria

E. coli and *A. tumefaciens* cultures were grown under aerobic conditions at 37 °C and 28 °C, respectively in low salt LB medium. For selection of positive transformants media were supplemented with corresponding antibiotics as listed in Section 2.2.4, Table 4.

Low salt LB medium

1 % (w/v)	tryptone (BD Biosciences)
0.5 % (w/v)	yeast extract (Roth)
0.5 % (w/v)	NaCl
	pH 7.0 (NaOH)
(2 % (w/v)	Agar)

Antibiotics

To select for positive transformants, selection marker i.e. resistance genes were encoded on plasmids and vectors. Thus, media were supplemented with antibiotics (Table 4). Prior addition of antibiotics all media were autoclaved at 121 °C for 20 min.

Table 4: Antibiotics used in media for selection of *E. coli* and *A. tumefaciens*

Antibiotic	Concentration in medium
Ampicillin (Amp)	100 µg ml^{-1}
Rifampicin (Rif)	50 µg ml^{-1}
Kanamycin (Kan)	50 µg ml^{-1}
Spectinomycin (Spec)	50 µg ml^{-1}
Chloramphenicol (Clm)	34 µg ml^{-1}
Tetracycline (Tet)	12.5 µg ml^{-1}

2.2.5 Production of Competent Bacteria Cells

E. coli

The production of competent *E. coli* cells was achieved using the Inoue method by Sambrook and Russell, 2006. For the production of competent *E. coli* cells 25 ml LB medium (Section 2.2.4) were inoculated with 0.2 ml of an over night culture from a single colony and incubated at 37 °C till an OD_{600} of 0.6 was reached. After cooling down the suspension to 4 °C it was centrifuged for 10 min, 4 °C and 2,500 *g*. Thereafter the pellet was

resuspended in 100 ml Inoue buffer and centrifuged as before. The bacteria cells were resuspended in 20 ml Inoue buffer and 1.5 ml of DMSO was mixed into the cells by swirling. The cell suspension was aliquoted into 50 µl aliquots, snap frozen in liquid nitrogen and stored at −80 °C until use.

Inoue Buffer

55 mM	$MnCl_2$
2.5 M	KCl_2
15 mM	$CaCl_2$
10 mM	PIPES (pH 6.7)

Inoue buffer was sterilised by filtration through 0.45 µm filter prior to use.

A. tumefaciens

For the production of competent *A. tumefaciens* strain ASE cells 200 ml YEB medium were inoculated with 2 ml of an over night culture and incubated at 30 °C to an OD_{600} of 0.95. After spin down of the cells for 10 min, 4 °C and 2,500 *g* the pellet was washed twice with 10 % glycerol containing 1 mM HEPES pH 7. The cells were resuspended in 2 ml of the same solution and aliquoted into 50 µl aliquots, flash frozen in liquid nitrogen and stored at −80 °C until use.

2.2.6 Transformation of Bacteria Cells

E. coli

One aliquot competent *E. coli* cells was thawed on ice and carefully mixed with plasmid DNA (about 1 µg) or 5 ml ligation mix and incubated on ice for 15 min. To accelerate the uptake of DNA the cells were heat-shocked at 42 °C for 90 s in a water bath. Subsequently the cells were cooled down on ice for 5 min before adding 1 ml SOC medium. After regeneration for 1 h at 37 °C at 180 rpm cells were streaked out LB plates containing antibiotics for selection (Section 2.2.4/Antibiotics) and incubated over night at 37 °C.

A. tumefaciens

An aliquot of chemical competent *A. tumefaciens* ASE cells were thawed on ice for 45 min and mixed with 1 µg DNA. After 10 min incubation on ice the cells were flash frozen in liquid nitrogen. The following heat-shock at 37 °C for 5 min in a water bath accelerates the uptake of DNA. After heat shock bacteria were supplemented with 1 ml SOC medium and incubated at 28 °C and 180 rpm for 3 h. For selection of positive transformants cells were plated on LB plates containing appropriate antibiotics (Section 2.2.4/Antibiotics) and incubated at 28 °C for 2 days.

SOC Medium

0.5 % (w/v)	yeast extract (Roth)
2 % (w/v)	tryptone (BD Biosciences)
10 mM	NaCl
10 mM	$MgCl_2$
10 mM	$MgSO_4$
2.5 mM	KCl
20 mM	Glucose
	pH 7.0 (NaOH)

2.2.7 Transformation of Plants

N. benthamiana

For overexpression of transcription factors *in planta* about 4 week old *N. benthamiana* plants were transformed with *A. tumefaciens*.
For a pre-culture about 3 ml LB medium containing appropriate antibiotics (Section 2.2.4/ Antibiotics) were inoculated with either a single colony or with a small piece of glycerol culture *A. tumefaciens* and grown for 2 days at 28 °C and 180 rpm. The cells were harvested after incubation over night at 3,000 *g* for 10 min (RT). The supernatants were discarded and the pellets were resuspended in Agro buffer. An OD_{600} of 0.1 for P14 cells and 0.4 for Agrobacteria containing respective constructs were mixed with Agro buffer. The bacteria suspensions were incubated for at least 2 h at RT. Tobacco leaves were slightly cut with a razor blade and the suspension was injected with a 2 ml sterile needleless syringe until the whole leaf was infiltrated. The leaves were harvested after 4 to 6 days of expression.

Agro Buffer

10 mM	$MgCl_2$
10 mM	MES
150 µM	Acetosyringone (solved in DMF)
	pH 5.6 (KOH)

A. thaliana

A. thaliana plants were stably transformed by the floral dip method as described in Clough and Bent, 1998. Briefly, *A. tumefaciens* carrying respective construct were grown to an OD_{600} of 2 as described in Section 2.2.4. The cell suspension was centrifuged 3,000 *g* for 10 min. The supernatant was replaced with an equal amount of Dipping Medium. The bacteria suspension was directly pipetted onto young, unopened *A. thaliana* flower buds. Seeds were collected and selected on agar plates containing corresponding herbicide.

Dipping Medium

2.2 g l^{-1}	Murashige & Skoog (Serva)
2.5 mM	MES (pH 5.7)
10 % (w/v)	Sucrose (Roth)
0.05 % (v/v)	Silwet (Lehle Seeds)

Transient Promoter Assay

Transient promoter assay was conducted on *Vitis vinifera* cv. 'Chardonnay' (Höll, 2014). Therefore, a 5 day old cell suspension of *V. vinifera* was transferred to a filter paper to remove excessive medium and equilibrate cells on GC plates for 2 h. 1.6 µm gold particles (Bio-Rad) were coated with 0.5 µg of respective plasmids but not more than 2 µg total plasmid DNA as described elsewhere Czemmel et al., 2009. As internal transformation control 50 ng pRluc plasmid encoding a *Renilla* luciferase was used. After 2 h incubation, cells were bombarded with coated gold particles using Model PDS-1000/He Biolistic Particle Delivery System from Bio-Rad with 4481 kPa helium pressure, a vacuum of 86 kPa and a distance of 9.5 cm. Cells were incubated in the dark for 48 h at RT before they were harvested and ground in 200 µl 2x Passive Lysis Buffer (Promega) on ice. After centrifugation for 1 min at 11,000 *g*, 10 µl of the lysate supernatant were mixed with 25 µl LARII supplemented with firefly substrate beetle luciferin and Stop & Glo® (Promega). Light emission

was detected with a Lumat LB 9507 Luminometer of both firefly and renilla luciferase and ratio was calculated.

GC Medium

3.2 g l^{-1}	Gamborgs B5 with minimal organics (Sigma)
30 g l^{-1}	Sucrose (Roth)
0.25 g l^{-1}	Casein hydrolysate
0.93 g l^{-1}	Kinetin
0.54 g l^{-1}	1-Naphthaleneacetic acid (NAA)
	pH 5.8 (KOH)

2.2.8 Isolation of genomic DNA from *A. thaliana*

Isolation of genomic DNA (gDNA) from plant tissue was performed according to the method by Edwards et al., 1991. For that one leaf was potted to homogeneity using a plastic pestle with 500 µl Extraction buffer in a 1.5 ml Eppendorf tube and centrifuged at 11,000 *g* at 4 °C for 5 min. 400 µl supernatant was transferred into a new Eppi with the same amount of Roti®-Phenol/Chloroform/Isoamyl alcohol (Roth), inverted a few times and centrifuged again. 350 µl from the upper phase was transferred into a new Eppi and mixed with 350 µl 100 % isopropanol. A pellet of gDNA was sedimented after another centrifugation step at 11,000 *g* for 10 min. The pellet was washed once with 70 % and once with 100 % ethanol before it was eluted in 50 µl sterile ddH_2O. The isolated gDNA was used for knock-out and stable transformation screening of *A. thaliana* mutants (Section 2.1.1, 2.2.7).

Extraction Buffer

400 mM	LiCl
200 mM	Tris
25 mM	EDTA
1 % (w/v)	SDS
	pH 9.0 (HCl)

2.2.9 Gene Expression Analysis*

Developing Miscanthus leaves were cut at their node, dissected and immediately frozen in liquid nitrogen. Total RNA was isolated from ground plant material from 100 µg Arabidopsis seedlings or 30 µg Miscanthus leaves using GeneMatrix Universal RNA Purification Kit (EURx/ roboklon) including an on column DNase I digestion. cDNA was synthesised according to manufacturer's instructions of Superscript III Reverse Transcriptase (Invitrogen) for Arabidopsis samples and RevertAidFirst Strand cDNA Synthesis Kit (Thermo Fisher) for Miscanthus samples with oligo dT primer and 1 µg RNA. qPCR reactions were prepared in 15 µl volume containing 2 µl of 1:8 diluted cDNA, 1 µl 5 µM of each forward and reverse primer, 0.3 µl 10 mM dNTPs, 0.3 µl of 1:400 diluted SYBR® Green I (Sigma-Aldrich), 0.3 µl of JumpStart™ Taq DNA Polymerase with 1.5 µl of the corresponding buffer (Sigma-Aldrich) and 8.6 µl H_2O. Ct values, primer efficiencies and melting curves were measured in a Rotor-Gene Q machine and evaluated by Q Series Software Q (Qiagen). Primer sequences can be found in Table 3. Gene expression in Arabidopsis was normalised against clathrin adaptor subunit (At5g46630) described in (Czechowski et al., 2005). During the course of the leaf gradient cytoskeleton reference genes like tubulin or actin were differentially expressed in leaf base and tip. In search for a stable reference gene in *Miscanthus sinensis* four genes, protein phosphatase 2A subunit 3A (PP2A), clathrin adaptor AP2M (Clath), peroxin 4 (UBC21) and TIP41-like protein (TIP) were examined. Because PP2A and UBC21 were found to be most stable they were selected for normalisation. The qPCR products were either sequenced and/or checked on acrylamide gel in cases of small amplicons.

2.3 Tissue Staining and Microscopy

2.3.1 Lignin Staining

Basic fuchsin

Lignin was stained according to Valdivia et al., 2013. Briefly, plant tissue was fixed and destained in methanol for 2 h or until white at RT under mild shaking. Methanol was replaced with 10 % (w/v) NaOH and incubated at 65 °C for 2 h. Thereafter, plant tissue was stained in 0.01 % (w/v) basic fuchsin until the red/pinkish colour disappeared. Excessive

*Section is adapted from Golfier et al., 2017

basic fuchsin was removed with 50 % (v/v) Ethanol before the tissue is mounted on glass slides with 50 % (v/v) Glycerol and sealed with nail paint.

HCl-phloroglucinol

As described in Section 2.3.1/Basic fuchsin, plant tissue was cleared in methanol before it was transferred into staining solution for a few minutes until a pinkish colour became visible. To avoid fading of the colouration tissue was mounted in staining solution on glass slides.

HCl-phloroglucinol

0.1 % (w/v)	Phloroglucionol
16 ml	HCl conc.
ad 100 ml	Ethanol

2.3.2 Hemicellulose Staining with LM11 Antibody

Hemicelluloses were detected with xylan and arabinoxylan specific LM11 as primary (McCartney et al., 2005) and Alexa 488-conjugated donkey anti-rat IgG (H+L; Thermo Fisher) as secondary antibody. Therefore tobacco leaves were cut into thin stripes and embedded in 6 % (w/v) agarose. The embedded tissue was cut into thin sections with a sharpe razor blade. The best hand sections were sorted under a binocular microscope and transferred into methanol for 10 min. Subsequently, the sections were equilibrated with 1x PBS buffer for 15 min. To block unspecific binding sites the sections were incubated with blocking solution for 1 h at mild shaking. A 1:2000 dilution of LM11 primary antibody in blocking solution was applied for 1 h. Excessive antibodies were removed by three washing steps with 1x PBS for 5 min. Thereafter a 1:1000 dilution of Alexa 488 secondary antibody in PBS buffer was applied to the section followed by three washing steps with 1x PBS for 5 min. The sections were mounted in antifade medium on a glass slide.

10x PBS Buffer

1.37 M	NaCl
27 mM	KCl
100 mM	Na_2HPO_4
18 mM	KH_2PO_4
	pH 7.4 (HCl)

Blocking solution

1x	PBS
1 % (w/v)	BSA
0.05 % (w/v)	Tween-20

2.3.3 Cellulose and Cell Wall Staining

Cellulose was stained with the flurochrome Calcofluor White M2R (fluorescent brightner 28) according to the procedure described in McCartney et al., 2003 with minor modifications. Briefly, Tobacco cross sections were equilibrated in 10 mM Tris-HCl pH 9 for 10 min. 0.25 µg ml^{-1} in 10 mM Tris-HCl pH 9 was applied to sections for 5 min. As Calcofluor White requires an alkaline pH for binding, sections were mounted in 70 % antifade medium with 30 % 10 mM Tris-HCl pH 9.
To stain entire cell walls, Arabidopsis seedlings were mounted in SR2200 staining solution on glass slides (Musielak et al., 2015).

SR2200 Staining Solution

0.1 % (v/v)	SR2200
1 % (v/v)	DMSO
0.05 % (w/v)	Triton-X100
5 % (w/v)	Glycerol
4 % (w/v)	Paraformaldehyde
	in PBS buffer (pH 8.0, Section 2.3.2)

2.3.4 Microscopy and Image Analysis*

HCl-phloroglucinol staining was imaged under brightfield with a 20.0 x 0.40 NA objective on a Leica DM IRB inverted microscope with a DFC320 colour camera. Fluorescent images were captured with a confocal Leica TCS SP5II microscope equipped with a 40.0 x 1.25 NA objective. Basic fuchsin-, SCRI Renaissance-and Calcofluor White-stained tissues were excited at 561 nm, 405 nm and with UV irradiation to detect emission at 593/40 nm and with DAPI filter, respectively. Immunolabeled tissues with LM11 and anti-rat Alexa 488 conjugate were exited using the 488 nm Argon laser line to detect emission

*Section is adapted from Golfier et al., 2017

with Alexa 488 filter settings. The fluorescent protein mCherry was imaged at 543 nm excitation and 600/80 nm detection. Orthogonal sections and scale bars were produced with ImageJ software.

2.4 Chemical Lignin Analysis

2.4.1 Acid Hydrolysis (Klason Lignin)

Tobacco samples were collected, dried for 2 days at 45 °C in an oven, finely ground with a spice mill and wrapped in small paper pockets. Sample pockets were placed in a Soxhlet apparatus where they were repeatedly flooded and washed with acetone overnight. When complete sample pocket were allowed to dry in fume hood until acetone was evaporated, dried at 105 °C overnight and cooled down in an desiccator. Clean sintered-glass crucibles were dried overnight at 105 °C. Crucibles were removed from oven, and placed in desiccator to cool for 20 min. After 20 min, the exact weight was recorded and crucible were placed back in 105 °C oven for 1 h. The weight of each crucible were determined at least three times. About 100 mg oven-dried extractive free sample were weighed into a serum bottle and exact weight was recorded. Exactly 3 ml 72 % (w/w) H_2SO_4 were added to samples. Samples were macerated with glass rods every 10 min for 2 h to facilitate acid hydrolysis reaction. After 2 h, exactly 112 ml ddH_2O were applied by weight to dilute acid to 4 %. Serum bottles were capped with rubber septum and sealed with aluminium caps using crimper. To determine soluble sugars and estimate loss by decomposition, four sugar controls with 30 ml, 10 ml, 5 ml and 2 ml sugar stock and 3 ml 72 % (w/w) H_2SO_4 were filled up to 115 ml with ddH_2O. Samples and sugar controls were autoclaved for 1 h at 121 °C. Serum bottles were allowed to cool down to room temperature before the hydrolysates were vacuum-filtered through pre-weighed crucibles. 10 ml of flow through was captured and solids remaining in serum bottle were washed out with ddH_2O. Crucibles were dried overnight at 105 °C and weight was determined again three times as previous described. The percentage of acid insoluble lignin was calculated according to $Acid\ Insoluble\ Lignin\ \% = [(M_{\text{lignin+crucible}} - M_{\text{crucible}}/M_{\text{sample}}) \times 100]$. Acid soluble lignin were measured by determine absorbance of flow-through at 205 nm on UV/Vis spectrophotometer using quartz cuvettes. The percentage of acid soluble lignin was calculated according to $Acid\ soluble\ Lignin\% = Absorbance/110 \times dilution\ factor \times [Final\ volume(\text{ml})/amount\ of\ starting\ material(\text{mg})] \times 100$. To determine soluble sugars, 950 mg of flow-through were supplemented with 50 mg internal fucose standard (5 g l^{-1}) and filtered into a HPLC vial. Samples were analysed by an anion exchange

high-performance liquid chromatography (HPLC) Dionex DX-600 equipped with a Carbopac PA20 column and an electrochemical detector. To determine sugar concentration, the area of respective peaks were integrated by Chromeleon^{TM} software and normalised against the loading control.

Sugar Stock Solution

2.4 g l^{-1}	Glucose
0.7 g l^{-1}	Xylose
0.2 g l^{-1}	Galactose
0.1 g l^{-1}	Mannose
80 mg l^{-1}	Arabinose
50 mg l^{-1}	Rhamnose

2.4.2 Lignin Monomer Composition by Thioacidolysis

To analysis lignin monomer composition, 20 mg of ground, extracted, oven-dried at 105 °C overnight and desiccator-cooled leaf tissue as described in Section 2.4.1 was weighed into a vial with teflon-lined screw cap and exact weight was recorded. Dioxane was distilled under N_2 (10 psi) until desired volume was reached and mixed with 2.5 % (v/v) boron trifluoride etherate (Sigma-Aldrich) and 10 % (v/v) ethanethiol (Sigma-Aldrich) to obtain the reaction mixture. 1 ml of reaction mixture was added to each vial and purged with N_2 before the lid was sealed tightly. Vials were incubated on a dry heating block at 100 °C for 4 h, with periodic manual agitation of each vial. After 4 h, the reaction were halted by placing vials in the −20 °C freezer for 5 min. As internal standard 200 µl methylene chloride containing 5 g l^{-1} tetracosane were added to each vial. To extract the reaction products 1 ml methylene chloride and 2 ml ddH_2O were pipetted to each vial, recapped, vortexed, and allowed to settle into upper (aqueous) and lower (organic) phases. In order to clean and dry samples, 1 ml of the lower phase was transferred onto a Pasteur pipette packed with filter paper and $NaHCO_3$. The flow-through was evaporated in a Vacufuge (Eppendorf) and resuspended in 700 µl methylene chloride. The samples were derivatise for 2 h in the dark at RT by combining 20 µl sample with 20 µl pyridine, 100 µl N,O-bis(trimethylsilyl) acetamide. The GC/MS analysis was conducted as described in Robinson and Mansfield, 2009. 1 µl of each sample was analysed by a ThermoFinnigan Trace GC-PolarisQ ion trap system equiped with an AS2000 auto-sampler, a split/splitless injector and a low-bleed Restek Rtx-5MS column. The corresponding area for G- and S-units with an approximate retention time of 29 and 32 min, respectively, were integrated and the ratio was calculated.

Chapter 3

Results

Cell wall recalcitrance is one of the major limitations to explore lignocellulosic biomass as renewable resource. *Miscanthus* has emerged as leading candidate crop for the production of lignocellulosic feedstock in temperate climates. However, nothing is known in *Miscanthus* about the molecular players involved in cell wall biosynthesis to facilitate breeding efforts towards tailored biomass. This work was dedicated to identify and characterise important molecular regulators of secondary cell wall formation with a particular focus on lignification in *Miscanthus*.

3.1 Is *Miscanthus* susceptible to the herbicide isoxaben?

The broad spectrum herbicide isoxaben was found as a potent inhibitor of cellulose synthesis complex in plants that causes lignification (Caño-Delgado et al., 2003). Because isoxaben specifically targets cellulose synthase A3 or A6 (CesA3/ 6) a point mutation in the C-terminus of CesA3 or CesA6 can be sufficient to confer resistance against isoxaben in *Arabidopsis* (Desprez et al., 2002; Scheible et al., 2001). Grasses like *Brachypodium distachyon* were shown to be isoxaben tolerant probably due to grass-specific cell wall characteristics (Brabham et al., 2017). A defined treatment to induce lignification in *Miscanthus* could greatly facilitate exploring and identification of processes and players involved in lignification. A *Miscanthus* transcriptome survey after induction of lignification could identify up- and downregulated genes. However, because a comprehensive *Miscanthus* genome is not available yet, gene annotations would be based on sorghum, rice, or maize genome. As a first step, the capability of isoxaben to induce ectopic lignification in *Miscanthus* should be assessed.

3.1.1 The growth of *Miscanthus sinensis* is inhibited by isoxaben

Treatment with the herbicide isoxaben could provide a valuable tool to understand lignin formation in *Miscanthus*. So far it is unclear whether *Miscanthus* is a susceptible genus or not. To test the potency of isoxaben on *Miscanthus sinensis*, the average length increase of *Miscanthus* plantlets were monitored 7 days prior and after isoxaben treatment in various concentrations (Figure 3).

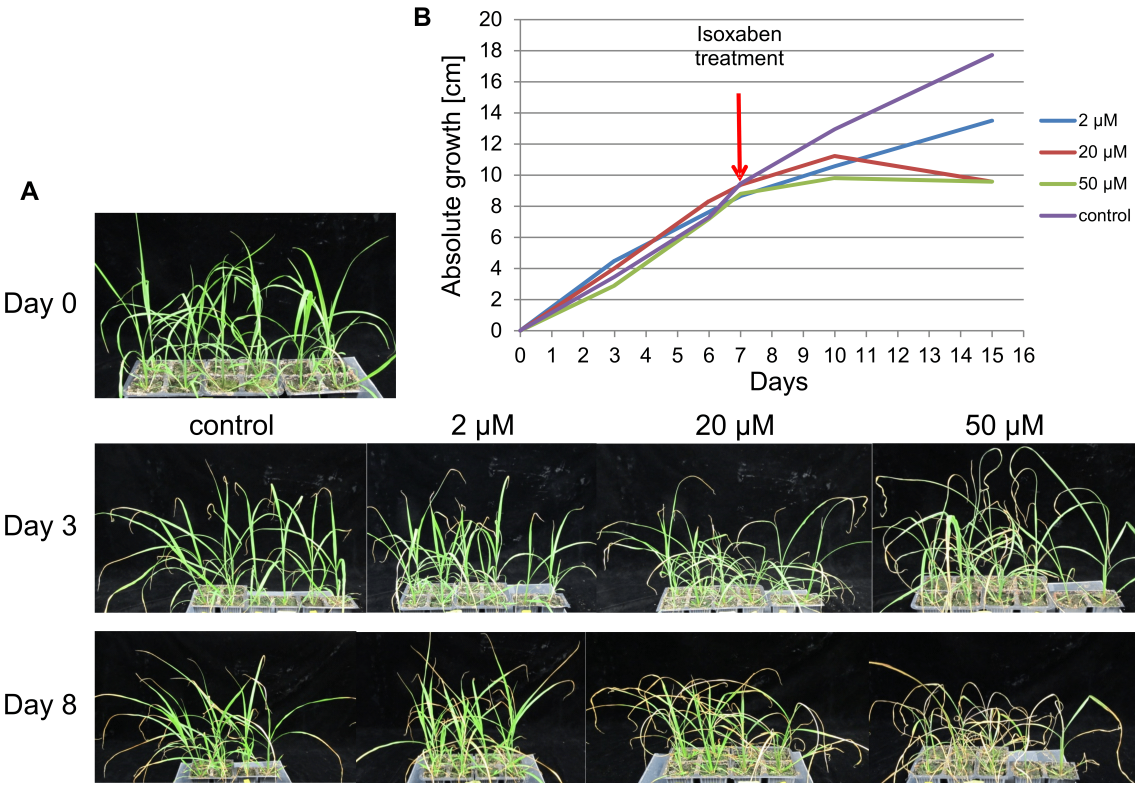

Figure 3: Isoxaben treatment inhibit growth of *Miscanthus* plantlets.

(A) Pictures of *Miscanthus sinensis* plantlets before treatment and 3 days and 8 days after treatment, respectively. (B) Average growth/length increase [cm] of 6 week old *Miscanthus* plantlets were monitored over a time course of 14 days, 7 days prior and after they were watered with different concentrations of isoxaben (solvent control, 2, 20, and 50 µM, n $\geq$ 8).

Three days after treatment with high concentrations of 20 µM and 50 µM leaves became limp and their tips dry (Figure 3A). This phenotype was more pronounced after eight days, whereas no or only little effect was observed after treatment with 2 µM isoxaben compared to control treatment. The visual observation was confirmed by length measurements. Before treatment, plantlets showed very similar and steady growth rates of about 1.2 cm/ day (Figure 3B). After treatment with 20 µM and 50 µM, growth of *Miscanthus* plantlets was effectively inhibited within 3 days. 2 µM isoxaben caused a reduction of the growth rate

but did not completely inhibit growth of plantlets. The control was just treated with solvent (DMSO), which had no effect on the growth rate of *Miscanthus* plantlets. In summary, isoxaben had an inhibitory effect on the growth of *Miscanthus* plantlets.

3.1.2 Isoxaben treatment increases expression of lignin-related genes

To further evaluate the capability of isoxaben to induce lignin formation in *Miscanthus*, expression of genes involved in lignification should be determined by quantitative real-time PCR. Expression of Ms*SCM4*, a close relative of At*MYB63* and Sb*MYB60* (Section 3.2, Figure 7B) and putative Ms*HCT* were found to be approximately 40 % higher after treatment with 100 nM isoxaben for 48 h (Figure 4). The putative genes Ms*CCoAOMT* and Ms*CesA7* also revealed stronger expression of about 25 % by isoxaben treatment. Ms*SCM2* was just slightly induced, whereas expression of Ms*SND1* showed no significant difference after isoxaben treatment.

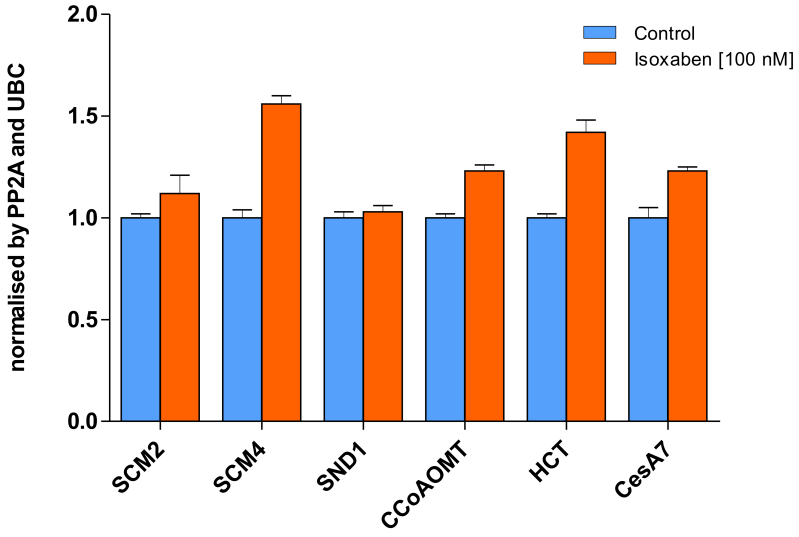

Figure 4: Isoxaben treatment causes upregulation of lignin-related transcripts in *Miscanthus* seedlings.

Miscanthus seedlings grown on MS plates were transferred for 48 h to MS plates containing 100 nM isoxaben and solvent, respectively. *Miscanthus* root tissue were employed for quantitative real-time PCR analysis. Two biological replicates were combined and normalised against two reference genes (PP2A and UBC) by geometric means. Bars depict means + SE from three technical replicates.

3.1.3 HCl-phloroglucinol and basic fuchsin stains *Miscanthus* seedling roots after isoxaben treatment

To evaluate the capability of isoxaben to promote ectopic lignification in *Miscanthus*, *Miscanthus* seedlings were germinated and grown on MS plates supplemented with different concentrations of isoxaben for 10 days before they were stained for lignin with either HCl-phloroglucinol or basic fuchsin (Figure 5).

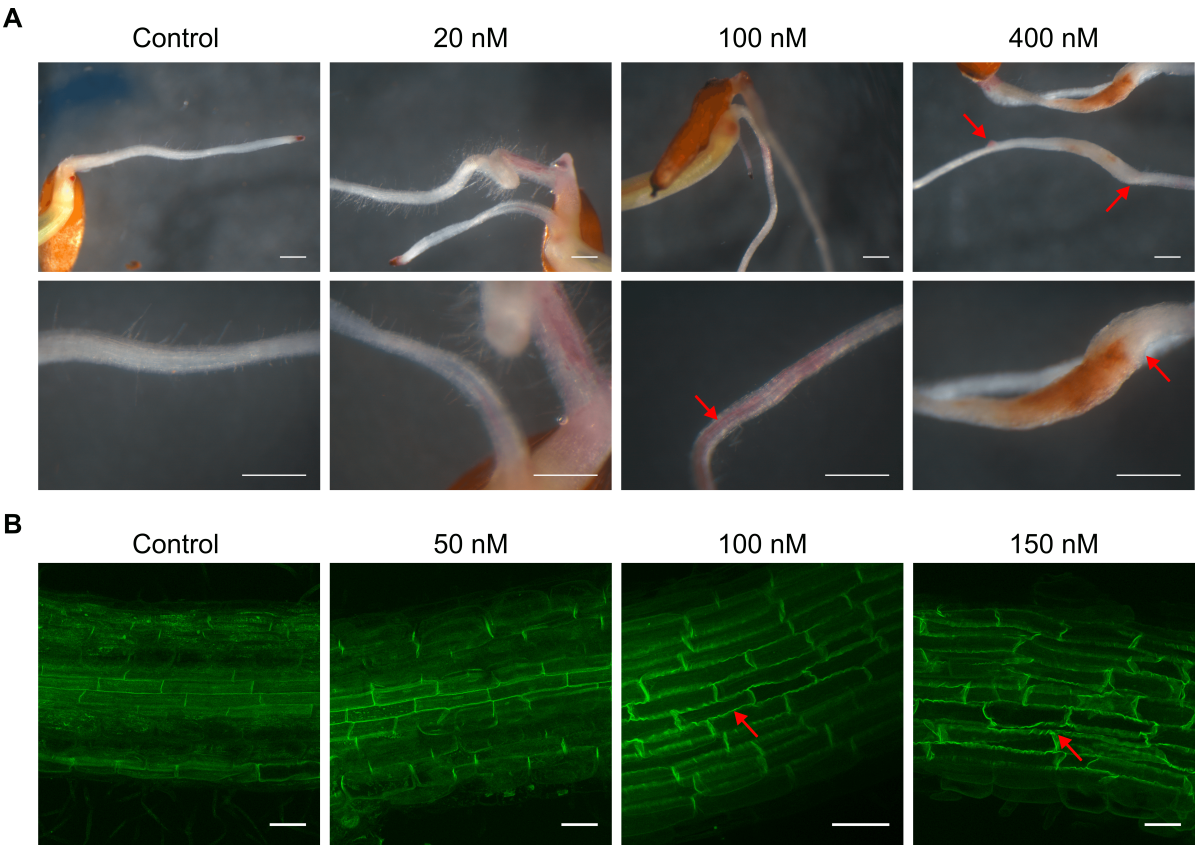

Figure 5: Isoxaben treatment induces ectopic lignification in *Miscanthus* seedling roots.

Miscanthus seedlings grown on MS plates supplemented with increasing concentrations of isoxaben for 10 days were stained for lignin with HCl-phloroglucinol (A) or basic fuchsin (B) and detected under a stereo microscope (A) or confocal microscope (B). Scale bar 0.5 mm (A) and 50 µm (B), respectively.

Root-tips of unstained *Miscanthus* seedlings appeared pinkish-red which remained unchanged after staining. Comparable to the ectopic deposition in *Arabidopsis* roots (Caño-Delgado et al., 2003), 20 nM or 100 nM isoxaben provoked lignification of longitudinal stripes in *Miscanthus* seedling roots, illustrated by pink colour (Figure 5A). Treatment with 400 nM isoxaben caused severe defects on root morphology and growth, confirming susceptibility of *Miscanthus* to isoxaben. The diameter of *Miscanthus* seelding roots were enlarged in some parts of the root that were in contact with MS-plates supplemented with

isoxaben (Figure 5A, red arrows). In addition, growth of lateral roots were diminished shortly after appearance. Staining with HCl-phloroglucinol revealed brown-reddish colour in parts of enlarged roots, indicating a distinct lignin composition. Upon reaction of phloroglucinol in ethanol-hydrochloric acid with 4-*O*-linked coniferyl and sinapyl aldehyde units contained in lignins the dye turns pinkish-red, whereas 4-*O*-linked hydroxybenzaldehydes results in red-brown colour (Pomar et al., 2002).
Although *Miscanthus* roots stained with basic fuchsin appeared with a relative high background, cell walls of the central cylinder showed a distinct fluorescent signal in the control as expected for a Casparian strip (Figure 5B). In line with HCl-phloroglucinol staining, after treatment with isoxaben cortical/parenchyma cell walls showed an ubiquitous fluorescent signal which was not observed in the control. Moreover, 100 nM and 150 nM isoxaben caused disturbance of cell shape with a wavy phenotype that was more pronounced in 150 nM than in 100 nM (Figure 5B). Taken together, HCl-phloroglucinol and basic fuchsin staining indicate formation of lignin in *Miscanthus* roots after isoxaben treatment.

3.1.4 Isoxaben treatment increases Klason lignin content and structural xylose in *Miscanhtus* seedling roots

Previously, it could be shown that *Miscanthus* is susceptible to isoxaben. Lignin staining with either HCl-phloroglucinol and basic fuchsin indicate, that isoxaben provokes lignification in *Miscanthus* seedling roots. Together with the finding that isoxaben induces expression of putative lignin-related genes these results suggest, that isoxaben is capable to induce lignification in *Miscanthus*. To further validate this hypothesis, about 2 g of dry *Miscanthus* roots were harvested to chemically analyse the cell wall composition of isoxaben treated and untreated roots.

Sulfuric acid hydrolysis were applied the root samples to determine Klason lignin. In *Miscanthus* roots the proportion of Klason lignin increased from 4 % to 6 % of total biomass when treated with isoxaben, which represents an increase of about 50 % compared to the control sample. Simultaneously, the content of soluble lignin slighty decreased in the isoxaben treated sample (Figure 6A). Monosaccharide released by acid hydrolysis were measured by high-performance liquid chromatography (HPLC). The amount of structural xylose increased by isoxaben treatment from approx. 90 µg/mg dry tissue to about 110 µg/mg dry tissue in the control. Concomitant with higher xylose content glucose content went down from 270 µg/mg dry tissue to 240 µg/mg dry tissue (Figure 6B). Notably, in *Miscanthus* roots rhamnose could not be detected. The lignin monomer composition measured by thioacidolysis and gas chromatography-mass spectrometry (GC-MS)

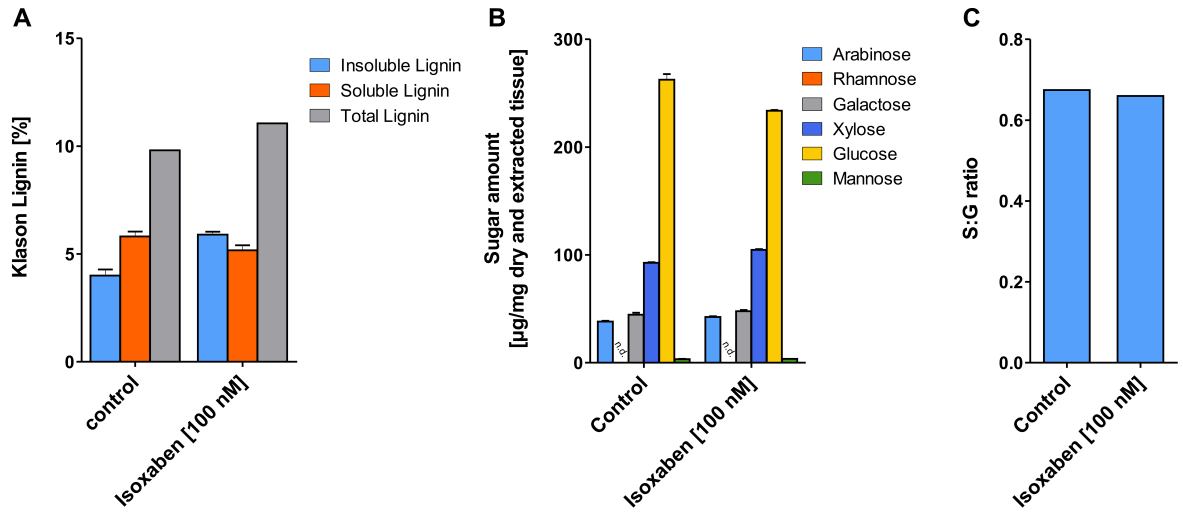

Figure 6: Isoxaben treatment changes cell wall composition of *Miscanthus* roots.

Miscanthus seedlings grown vertically on MS plates with and without 100 nM isoxaben for 17 days. Seedling roots were dried at 45 °C for 2 days and finely grounded before chemical analysis. Cell walls were analysed for Klason lignin (A), monosaccharide content (B), and S/G lignin monomer ratio (C). Values are + SE of two technical replicates.

remained unchanged by isoxaben treatment, even though *Miscanthus* roots tend to possess with a ratio of 0.68 more G monomers than S monomers.

The presented results suggest *Miscanthus sinensis* as susceptible species against the herbicide isoxaben. Expression of lignin-related genes were increased after isoxaben treatment. In accordance, lignin was detected via lignin staining in *Miscanthus* seedling roots when grown on isoxaben. Chemical analysis of cell wall composition confirmed accumulation of ectopic lignification following isoxaben treatment. As a next step, a transcriptome survey could be undertaken to obtain a more complete picture of processes and players involved in lignification in *Miscanthus sinensis*.

3.2 Identification of *Miscanthus sinensis* transcription factors through phylogenetic analysis*

In *Miscanthus* molecular players involved in cell wall biosynthesis are still unknown. New genomic resources for *Miscanthus* are increasingly available to explore its fundamental biology by exploiting knowledge from other plant species. A homology-based approach allows rapid identification of putative homologous genes involved in cell wall formation

*Section is adapted from Golfier et al., 2017

(Zhong et al., 2010a). The previously published *Miscanthus* transcriptome by Barling et al., 2013 were mined for candidate transcription factors involved in cell wall formation using known factors from *Arabidopsis thaliana* and other plants. A phylogenetic analysis of NAC TFs from different angiosperm lineages showed that the subfamily Ic may be further divided into three classes (Figure 7A). Members of classes II and III are implicated in xylem differentiation (Kubo et al., 2005; Zhou et al., 2014), whereas members of class I are described to be involved in fiber differentiation (Zhong et al., 2006). Formation of secondary cell wall is thought to be regulated by a multi-tiered hierarchical network of TFs. Lower-tier MYBs are proposed to fine-tune transcriptional regulation of secondary cell wall (SCW) formation, in particular lignification (Öhman et al., 2013; Zhou et al., 2009). MYB TFs known to be involved in lignification, especially from *Arabidopsis* (Zhong et al., 2008), served as query to search the *Miscanthus* transcriptome for putative candidate genes. The phylogenetic analysis revealed an ambiguous relationship of *Miscanthus* candidate MYBs to AtMYBs; therefore, they were named *Miscanthus sinensis* SECONDARY CELL WALL MYBs 1-4 (MsSCM1-4; Figure 7B). MsSCM1-3 fall into the clade of AtMYB20, AtMYB43, and AtMYB85, respectively, whereas MsSCM4 is most closely related to AtMYB63 and AtMYB58 (Figure 7B, Zhong et al., 2008;

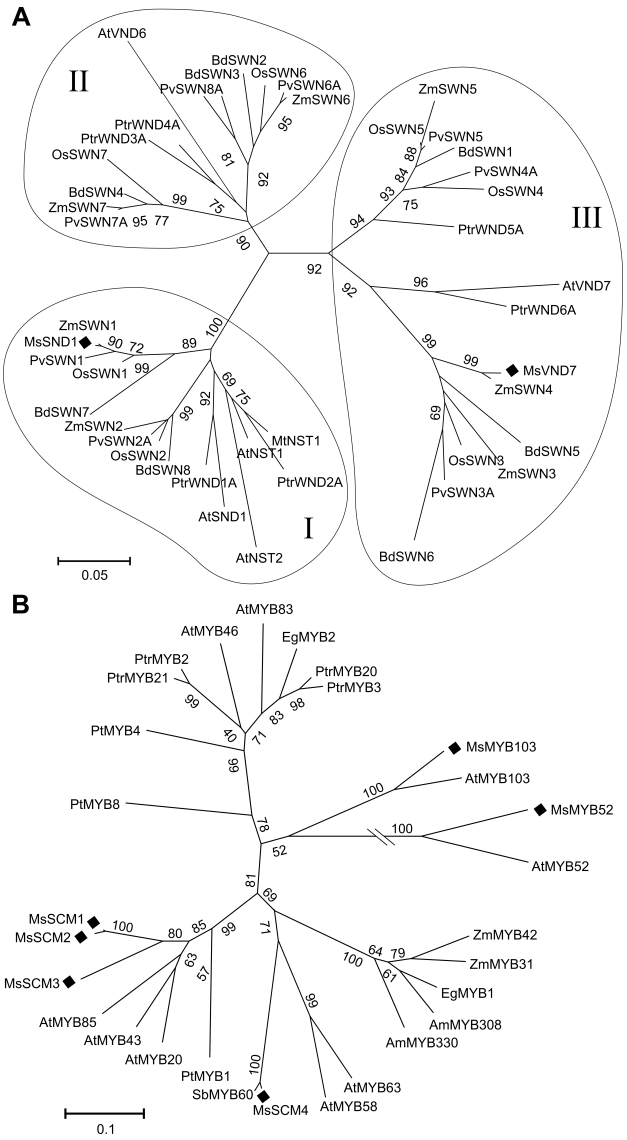

Figure 7: Phylogenetic tree of NAC and MYB transcription factors from *Miscanthus* (adapted from Golfier et al., 2017).

Neighbor-joining phylogeny of the NAC transcription factors MsSND1 and MsVND7 (A) and a series of MYB transcription factors (B) in relation to the transcription factor from angiosperm lineages *Antirrhinum*, *Arabidopsis*, *Brachypodium*, *Eucalyptus*, *Panicum*, *Pinus*, *Populus*, *Oryza*, and *Zea*. Amino acid sequences were aligned with ClustalW, and the neighbor-joining phylogenetic tree with 1000 bootstraps was conducted using MEGA6 software (Tamura et al., 2013). The evolutionary distance is indicated by the scale bar.

Zhou et al., 2009).
The predicted proteins AtSND1 and MsSND1 share 41.5 % identity and 51.5 % similarity on amino acid level (Figure S1), whereas the predicted proteins of *Miscanthus* MYB transcription factors and their closest putative *Arabidopsis* homologs fall in the range of 43.9 % identity and 51.9 % similarity for MsMYB103 and AtMYB103 or 53.2 % identity and 64.0 % similarity for MsSCM3 and AtMYB85. The alignment of AtSND1 and MsSND1 or AtMYB85 and MsSCM3 in Figure S1 and S2 reflect exemplarily alignments for investigated NAC and MYB TFs from *Miscanthus*. The structurally and functionally essential N-terminal DNA-binding motif (Figure S1, S2), known as the NAC and MYB domain, respectively shows the highest similarity in the range of 90 to 95 % within the amino acid sequence, suggesting that MsSND1/VND7/SCM1-4/MYB52, and MYB103 from *Miscanthus* may possess similar DNA-binding characteristics to the respective TF in *Arabidopsis*. In all TFs, the C-terminus that contains the transcriptional activation domain is more divergent, probably reflecting different activation properties. In the case of MsSND1 the C-terminus is 63 amino acids longer compared to AtSND1. In summary, the phylogenetic analysis indicates a close relationship between NAC and MYB TFs from *Miscanthus* and their related TFs in *Arabidopsis*.

3.3 *Miscanthus* leaf gradient: a model to understand developmental processes involved in SCW formation*

In addition to apical and lateral meristems present in dicots, grasses possess a third type, the intercalary meristems. The intercalary meristems are situated at stem nodes, where they account for leaf elongation. As a result of the intercalary meristem, leaf differentiation follows a linear pattern from the leaf sheath toward the leaf blade, resulting in a continuous developmental gradient along the leaf. To explore the role of Ms*SND1* and Ms*SCM*s in *Miscanthus* development, three leaves were sampled according to Figure 7A and the expression profiles of Ms*SND1* and Ms*SCM*s, together with those of putative cell wall-related biosynthetic genes were determined along the developmental gradient in the leaf, and visualised in Figure 7B, C. The likely transcripts of lignin biosynthesis and polymerisation genes were identified in the *Miscanthus* transcriptome in the same manner as described for Ms*SND1* and Ms*SCM*s. Along the leaf developmental gradient, the expression of Ms*SND1* was highest at the leaf sheath and decreased rapidly over the following two leaf segments (Figure 7B, C). The expression of *Miscanthus* SCM TFs, as

*Section is adapted from Golfier et al., 2017

well as that of lignin biosynthesis genes peaked in the second segment to decline toward the leaf blade at different rates depending on the gene. The expression profiles of the putative SCW-related genes were correlated with SCW differentiation in leaf segments of *Miscanthus*. Therefore, cross-sections of the first three *Miscanthus* leaves segments were stained for lignin with HCl-phloroglucinol (Figure 7E-G). At the leaf sheath, the basic organisation of vasculature is established very early in development but it is still in a juvenile stage. Maturation of the vasculature started with lignification of protoxylem cells in the first segment, which may be required to secure integrity of the tissue during early stages of leaf maturation. In the second segment, the SCWs of vascular bundle appeared thicker and lignification seemed stronger than in sclerenchyma fibers (Figure 7F). In the third leaf segment, tracheary elements and sclerenchyma fibers (extraxylary fibers) revealed strong lignification (Figure 7D-G). Extraxylary fibers, the adaxial threads of sclerenchyma fibers that are in contact with the outer bundle sheath, and the thin abaxial subepidermal strip of sclerenchyma fibers seemed to lignify and deposit SCWs in a similar fashion, different from vascular cells.

In order to obtain a higher magnification and a better resolution of lignification, that occurs along the leaf gradient, lignin was stained with basic fuchsin and analysed by Confocal Laser Scanning Microscopy (CLSM). The cross-section depicted in Figure 8 corresponded to the third segment (Figure 7D, G) and was very similar to following segments. Surprisingly, basic fuchsin was able to stain cells in the vascular tissue but was unable to stain sclerenchyma fibers (Figure 8A, C). While the bright-field images showed strong SCW deposition of both vascular tissue and sclerenchyma fibers (Figure 8B, D). Basic fuchsin has been widely used as a staining for lignified cell walls, although the specific targets and the underlying reaction mechanism of the dye remain unclear.

The high expression of Ms*SND1*, candidate MYB TFs, and lignin biosynthesis genes that occurs concurrently with differentiation and SCW formation of xylary and extraxylary elements suggests a possible involvement of the investigated genes in this process.

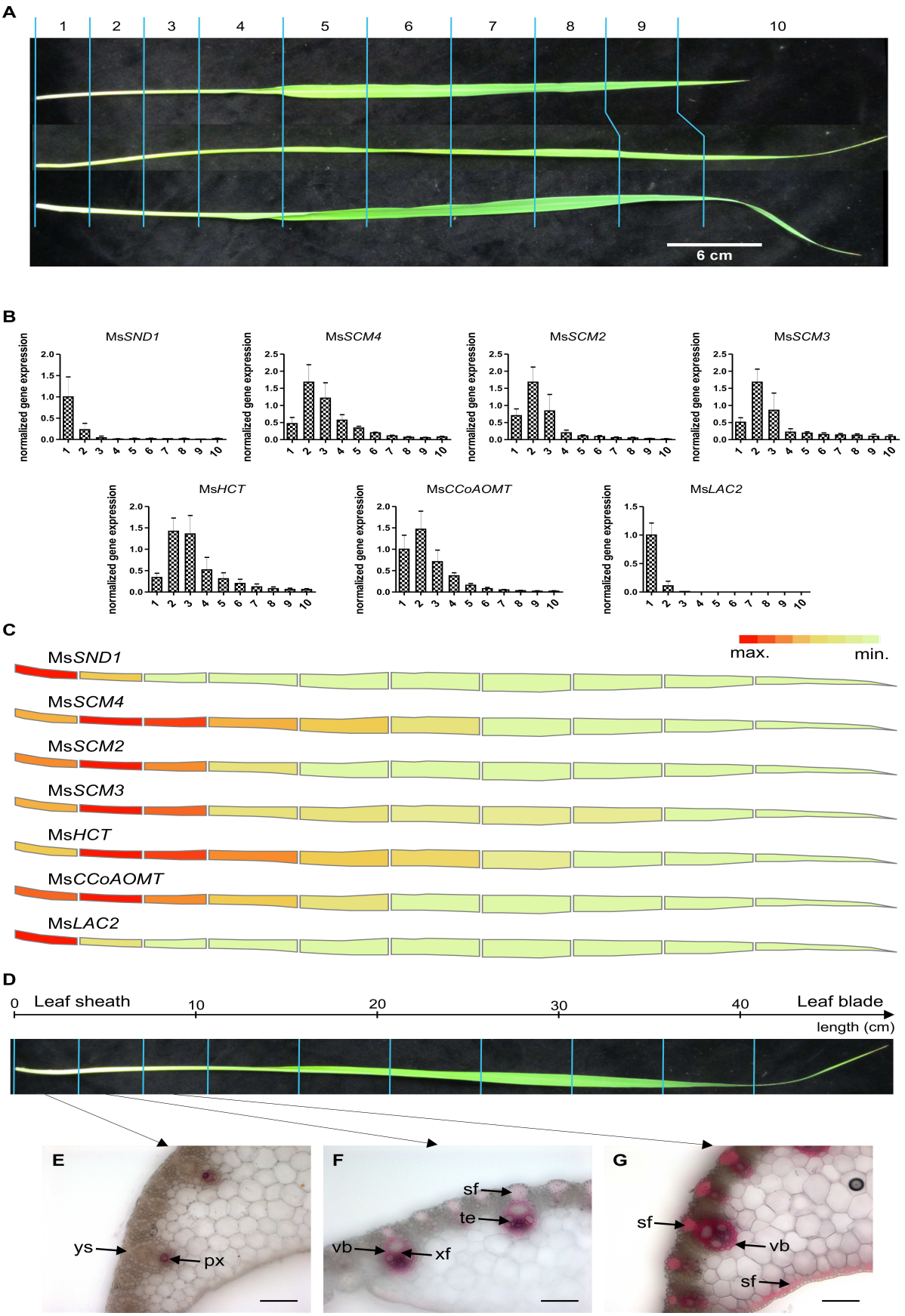
A
1
2
3
4
5
6
7
8
9
10
6 cm
B
MsSND1
MsSCM4
MsSCM2
MsSCM3
MsHCT
MsCCoAOMT
MsLAC2
normalized gene expression
C
max.
min.
MsSND1
MsSCM4
MsSCM2
MsSCM3
MsHCT
MsCCoAOMT
MsLAC2
D
0
Leaf sheath
10
20
30
40
Leaf blade
length (cm)
E
ys
px
F
sf
te
vb
xf
G
sf
vb
sf

Figure 7: Ms*SND1* expression is correlated with expression of its putative target genes and vascular development along *Miscanthus sinensis* leaves (Golfier et al., 2017).

(A) Sampling scheme of three *Miscanthus sinensis* leaves, that were used for gene expression analysis (B, C) Gene expression profiles of the indicated genes over ten developmental zones as obtained by quantitative real-time PCR. The results of three biological replicates were combined, normalised against two reference genes (PP2A and UBC) and visualised as heat map in (C). Cross-sections of the first three basal zones (E-G) from the *Miscanthus* leaf depicted in (D) were stained for lignin with HCl-phloroglucinol, indicating that the expression of Ms*SND1* and its putative targets is concomitant with the onset of vascular development. Scale bar 100 µm. px, protoxylem; sf, sclerenchyma fibers (extraxylary fibers); te, tracheary elements; vb, vascular bundle; xf, xylary fibers; ys, young sclerenchyma.

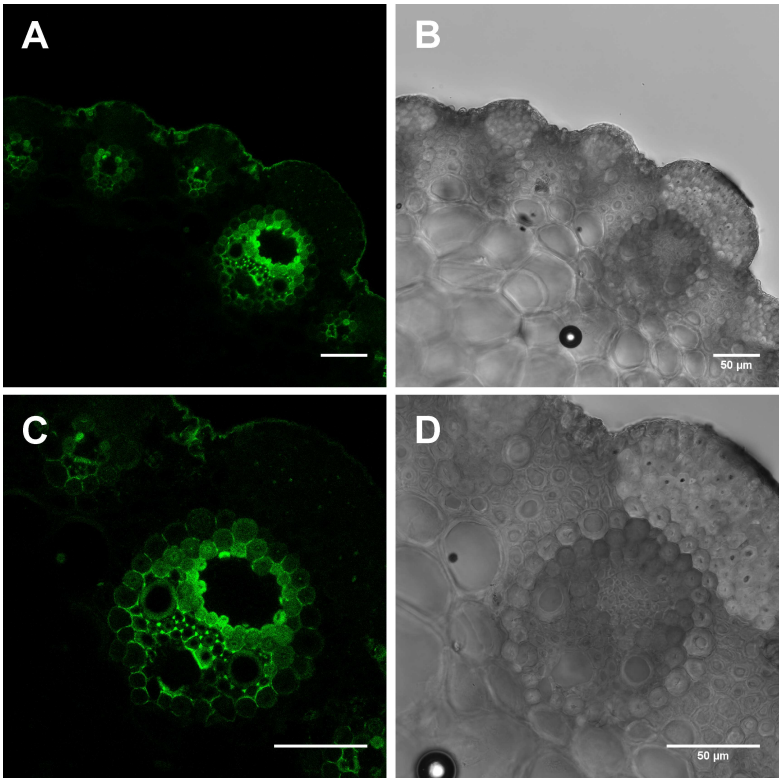

Figure 8: *Miscanthus* leaf cross-sections from the third segment (Figure 7C, F) stained with basic fuchsin to observe fluorescence (A, C) and white light images (B, D). Scale bar 50 µm (Golfier et al., 2017).

3.4 Ms*SND1*, Ms*SND2*, and Ms*VND7* rescue *Arabidopsis snd1 nst1* phenotype

To substantiate the hypothesis that *Miscanthus* MsSND1, MsSND2, and MsVND7 are functionally equivalent to AtSND1, it was tested whether they could complement the pendant stem phenotype caused by SCW defects of interfascicular fibers in the *Arabidopsis snd1 nst1* double mutant when expressed under control of the At*SND1* promoter (Figure 10A; Mitsuda et al., 2007).

3.4.1 Genetic validation of *Arabidopsis snd1 nst1* double mutant

Homozygous *Arabidopsis snd1 nst1* double mutant seeds were obtained from the Nottingham Arabidopsis Stock Center (NASC). Before using them for complementation experiments they were genetically verified via PCR by detecting tDNA insertion. Gene-specific primers for *nst1* and *snd1* led to bands with theoretical size of 852 bp and 976 bp, respectively in the wildtype but not in the double mutant (Figure 9B, C). On the other hand, PCR with the tDNA-specific LBa1 did not result in a product with wildtype but resulted in strong bands in the double mutant (Figure 9B). Taken together, the double mutant was genetically verified as such.

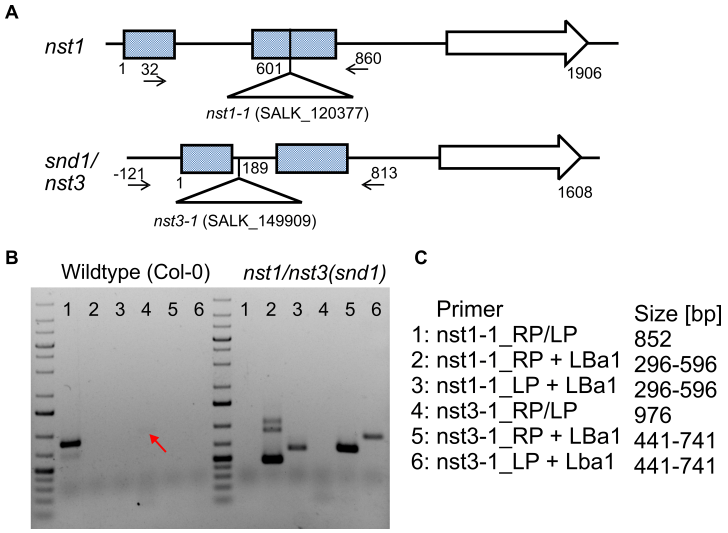

Figure 9: Genetic screeing of *Arabidopsis snd1 nst1* double mutant.

gDNA from wildtype and *snd1 nst1* double mutant were tested via PCR with tDNA- and gene-specific primer combination. (A) Illustration of theoretical locus of *nst1* and *snd1* with sizes, exons, introns, and primer binding sites. (B) Gel picture after DNA separation via gel-electrophoresis. (C) Primer combination and theoretical sizes of PCR products.

3.4.2 Ms*SND1*, Ms*SND2*, and Ms*VND7* complement the SCW deficiency of the *Arabidopsis snd1 nst1* double mutant*

MsSND1, MsSND2, and MsVND7 were capable to rescue the vertical growth of *Arabidopsis snd1 nst1* mutant similar to AtSND1 (Figure 10A). Cross-sections of inflorescence stems stained for lignin with HCl-phloroglucinol confirmed that Ms*SND1*, Ms*VND7*, and At*SND1* are able to complement the *snd1 nst1* double mutant and fully restore loss of lignin in stem fiber cells (Figure 10D). Expression of Ms*SND2* under control of At*SND1* promoter could alleviate the pendent phenotype but lignin staining of the cross-section of the inflorescence stem revealed that the SCW defect was restored in less interfascicular fibers compared to AtSND1 or MsSND1. Notably, complementation with Ms*VND7* led to formation of xylem-like structures with SCWs in the cortex of inflorescence stem (Figure 10G). As improvement of fibers is a desirable breeding target and MsSND1 appeared to be functional equivalent to the fiber-specific AtSND1 a strong focus was placed on MsSND1 with a more profound functional characterisation to shed light on its regulatory role in SCW formation.

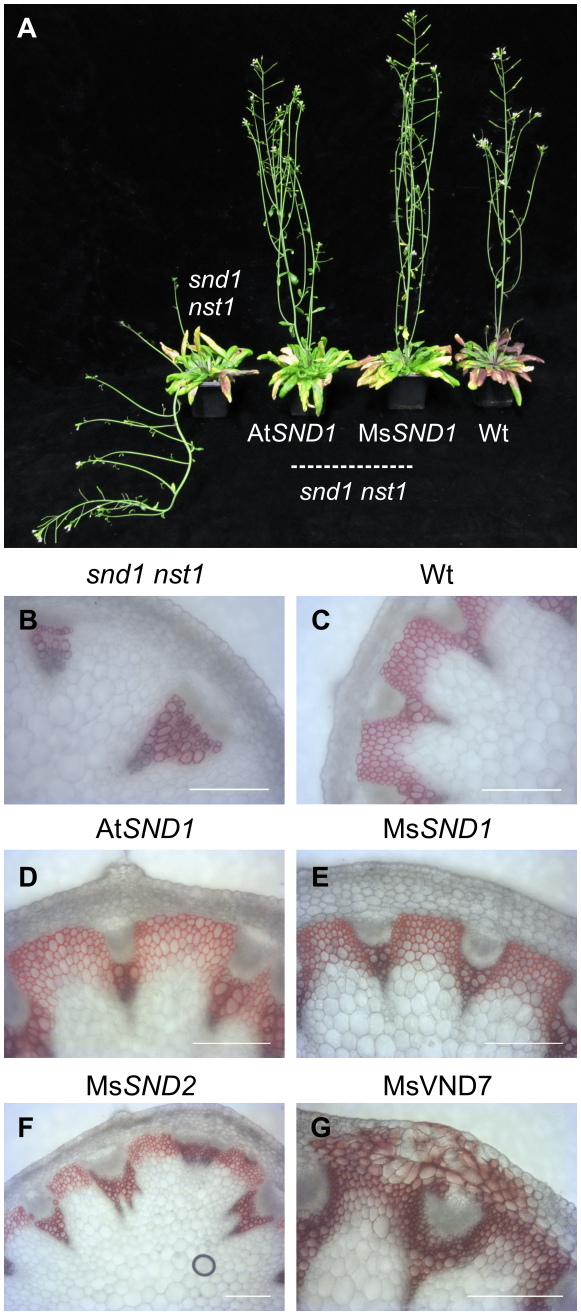

Figure 10: Ms*SND1* can replace *Arabidopsis SND1* (Golfier et al., 2017).

Complementation of *Arabidopsis snd1 nst1* double mutant by expression of Ms*SND1*, Ms*SND2*, and Ms*VND7* under At*SND1* promoter. Ms*SND1*, Ms*SND2*, and Ms*VND7* restored vertical growth (exemplary for Ms*SND1* in A) and lignification of secondary cell walls in the interfascicular fibers even though similarity was highest for Ms*SND1* to the positive control At*SND1* (B-G). Cross-sections of inflorescence stems were stained with HCl-phloroglucinol for lignin. Scale bar 100 µm.

*Section is adapted from Golfier et al., 2017

3.5 Expression of Ms*SND1* leads to strong ectopic SCW deposition in tobacco leaves*

In order to examine the ability of Ms*SND1* to stimulate SCW formation, Ms*SND1* was transiently overexpressed in *Nicotiana benthamiana* leaves. After 6 days of incubation, leaf cross-sections were stained for lignin with basic fuchsin, cellulose with Calcofluor white, and hemicellulose with LM11 antibodies and observed using Confocal Laser Scanning Microscopy (CLSM). Overexpression of Ms*SND1* and At*SND1* led to patterned ectopic deposition of lignified SCW in epidermis, palisade, and spongy mesophyll cells, depicted in Figure 11 by strong fluorescent signals. Transformation with an empty vector control did not result in lignification or hemicellulose deposition in tobacco leaves (Figure 11C, I). In addition the fluorescent signal in the control after Calcofluor white staining was less intense and not patterned (Figure 11F).

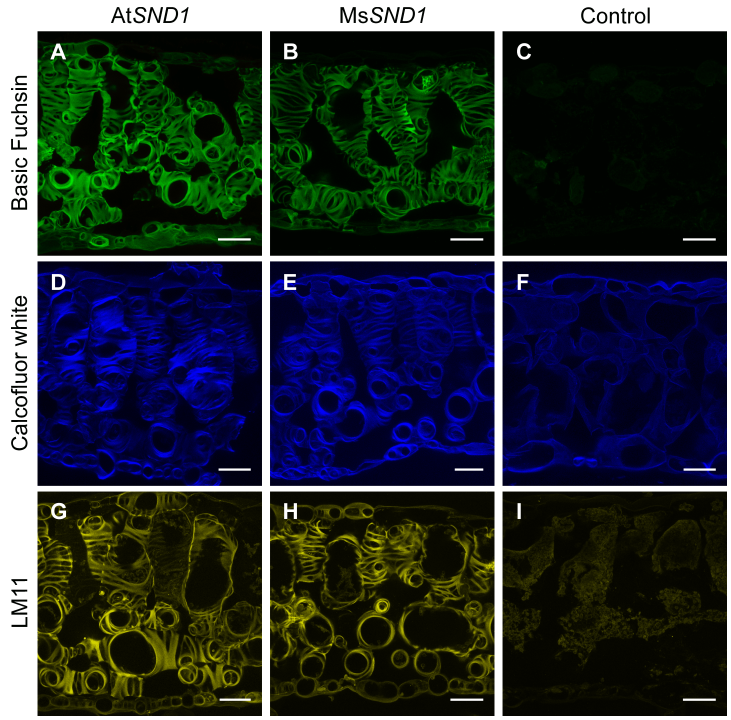

Figure 11: Expression of Ms*SND1* is sufficient to induce ectopic secondary cell wall deposition and patterning (Golfier et al., 2017).

Ectopic deposition of secondary cell wall components in *Nicotiana benthamiana* leaves induced by transient expression of At*SND1* and Ms*SND1*. Cross-sections of tobacco leaves stained for lignin with basic fuchsin (A-C), for cellulose with Calcofluor White (D-F), and for xylan and arabinoxylan with LM11 as primary and Alexa 488 as secondary antibody (G-I). The control leaves were transformed with an empty vector control (C, F, I). Scale bar 40 µm.

*Section is adapted from Golfier et al., 2017

In sharp contrast to the patterned ectopic SCW formation after transient expression of At*SND1* and Ms*SND1*, expression of Ms*SCM1-3* (related to At*MYB20*, At*MYB43*, and At*MYB85*) and Ms*SCM4* (related to At*MYB63* and At*MYB58*) (Figure 7) resulted in uniform lignin deposition around *N. benthamiana* mesophyll cells without apparent SCW pattern (Figure 12).

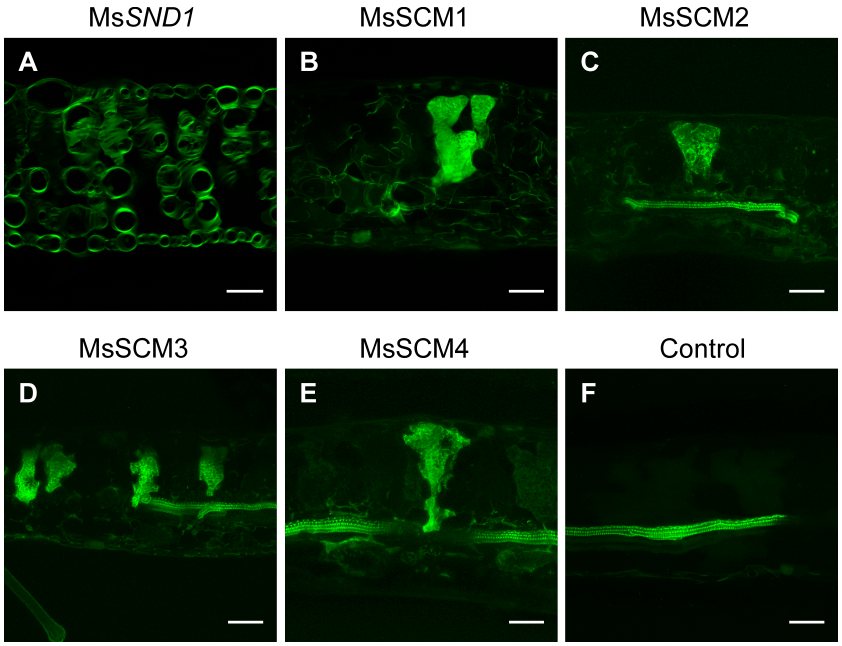

Figure 12: Ectopic secondary cell wall patterning differs between MsSND1 and downstream MYB factors (Golfier et al., 2017).

Ectopic deposition of lignin in tobacco leaves induced by transient expression of Ms*SND1*, Ms*SCM1*, Ms*SCM2*, Ms*SCM3*, and Ms*SCM4* in *Nicotiana benthamiana* leaves. Cross-sections of leaves were stained for lignin with basic fuchsin. The control leaves were transformed with an empty vector control. Scale bar 50 µm.

3.6 Expression of *Miscanthus* TFs change cell wall composition of tobacco leaves

Transient expression of the NAC and MYB TFs in tobacco leaves resulted in ectopic deposition of cellulose, hemicellulose, and/or lignin (Section 3.5). To further investigate the cell wall changes that are associated with transient expression of NAC and MYB TFs, cell wall composition of tobacco leaves after 5 days expression of the respective TFs was chemically analysed. The chemical lignin analysis was carried out in the group of Shawn D. Mansfield at the Faculty of Forestry, Vancouver, Canada.

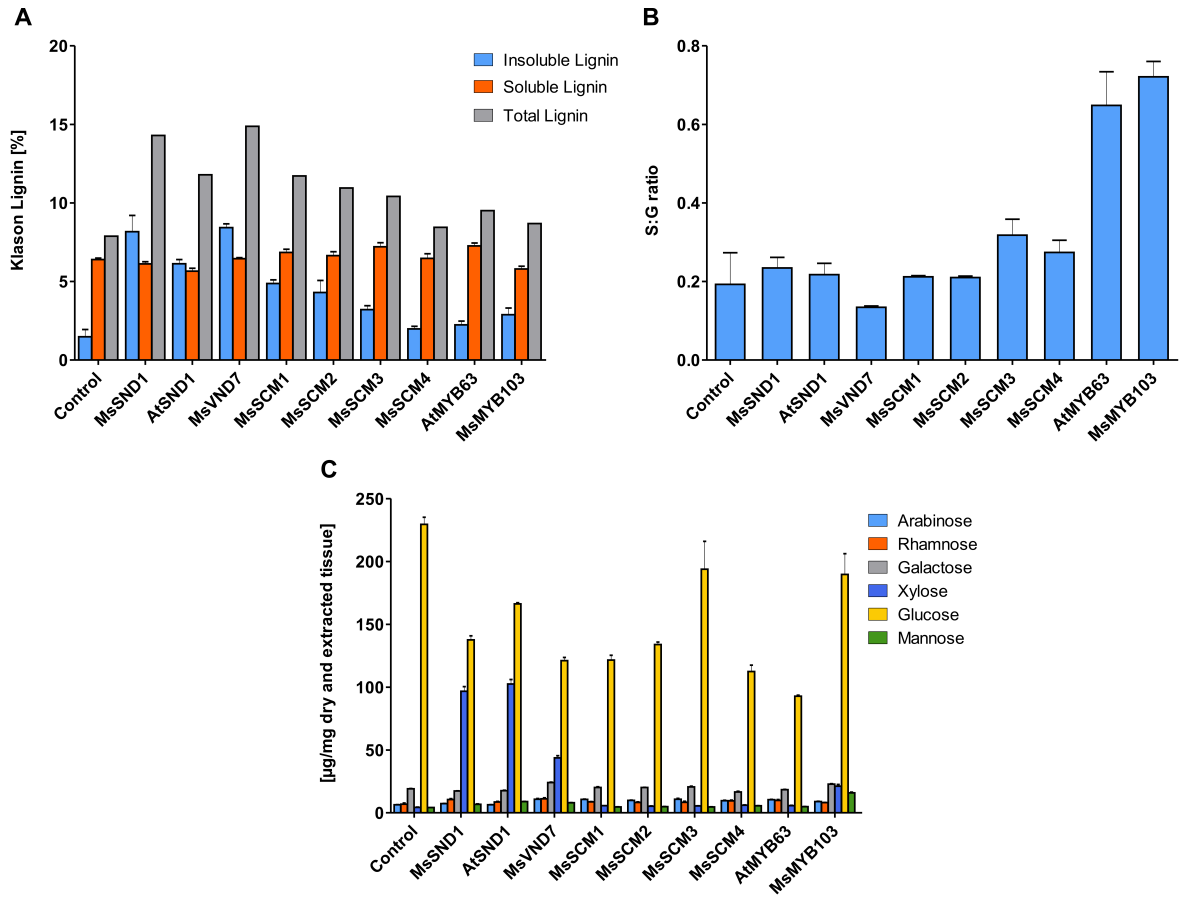

Figure 13: Transient expression of NAC and MYB TFs causes changes in cell wall composition in tobacco leaves.

Tobacco leaves were investigated for Klason lignin (A), S/G lignin ratio (B), and monosaccharide content after transient expression for 5 days of NAC and MYB TFs. The control leaves were transformed with an empty vector control. Values are means + SE for $n = 3$ biological replicates, each consisting of at least 5 pooled leaves and two technical replicates for Klason lignin (A).

Dried and methanol extracted cell wall pellets from leaves were subjected to hydrolysis with sulfuric acid to determine acid insoluble lignin (Klason lignin) and acid soluble lignin. Klason lignin content was determined by weight, whereas acid soluble lignin was spectrophotometrically measured at OD_{205}. The acid soluble lignin is considered to contain low molecular weight lignin and lignin-carbohydrate complexes, resulting from hydrolysis with sulfuric acid (Matsushita et al., 2004). In contrast, Klason lignin is the high molecular weight lignin.

With about 1.5 % of acid insoluble lignin in the control the contribution of lignin to dry leaf biomass is very low (Figure 13A). Transient expression of MsSND1, AtSND1, and MsVND7 in tobacco leaves resulted in an increased amount of Klason lignin of 8.5 % of total dry leaf biomass. Expression of various MYB TFs elevated the Klason lignin content ranging from 2 to 4.9 % of total dry leaf biomass after. In contrast to Klason lignin the

proportion of soluble lignin remained with about 7 % almost unchanged in all samples. Even though Klason lignin was only slightly increased in AtMYB63 and MsMYB103 with 2.2 and 2.9 %, respectively, the ratio of syringyl to guaiacyl (S/G ratio) was considerably higher with 0.65 and 0.72 compared to the control with 0.19 (Figure 13B).
Interestingly, AtMYB103, a putative homolog of *Miscanthus* MYB103 was found to be a central regulator of ferulate-5-hydroxylase (F5H) that determines S/G ratio by providing sinapyl alcohol (Öhman et al., 2013). In other samples the S/G ratio ranged from 0.13 to 0.3. Monosaccharides released by acid hydrolysis showed a strongly increased abundance of the structural carbohydrate xylose in MsSND1, AtSND1, and MsVND7, that went up from 6 µg per mg dry tissue in the control to about 100 or 50 µg per mg dry tissue in MsSND1, AtSND1, and MsVND7, respectively (Figure 13C). Monosacchardies like arabinose, rhamnose, galactose, and mannose represented with less than 5 % only a minor fraction of cell wall sugars which did not differ much between the samples, although MsMYB103 contained slightly more mannose.

3.7 *Miscanthus* transcription factors can activate *Arabidopsis* and *Miscanthus* promoters

A promoter activation assay was applied to investigate the regulatory network underlying SCW formation from *Miscanthus*. The capability of *Miscanthus* NAC and MYB TFs to induce lignin-related promoters from *Arabidopsis* and *Miscanthus* was examined. Therefore, transient promoter activation assay was conducted on *Vitis vinifera* cv. 'Chardonnay' suspension cell culture. Promoter of interest controlling expression of a firefly luciferase were co-bombarded with a constitutively expressed TF into grapevine cells. After two days incubation, transformed grapevine cells were crushed to extract proteins. The extract was used to detect a light signal following successive application of firefly and *Renilla* luciferase substrates. The *Renilla* luciferase signal served as internal transformation control.

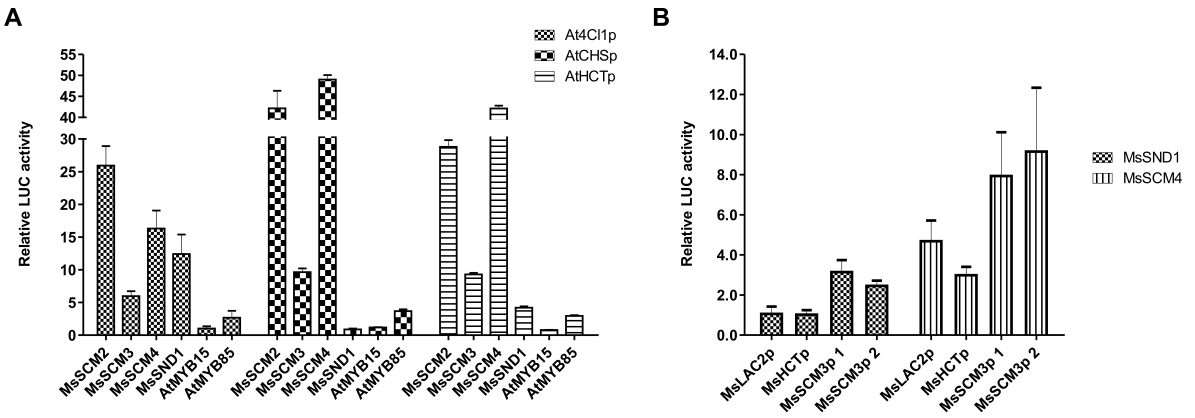

Figure 14: *Miscanthus* TFs are able to activate promoters of *Arabidopsis* and *Miscanthus*.

(A,B) Transient promoter activation assay in *Vitis vinifera* cv. 'Chardonnay' suspension cell culture following particle bombardment. Respective promoters linked to a firefly luciferase were co-bombarded with expression constructs 35S:TF and pRluc plasmid, containing a *Renilla* luciferase as an internal control. The relative LUC activity is the ratio of firefly to *Renilla* luciferase signal correlated to promoter background. Values are means + SE for $n = 3$ (A) or $n = 5$ (B) biological replicates.

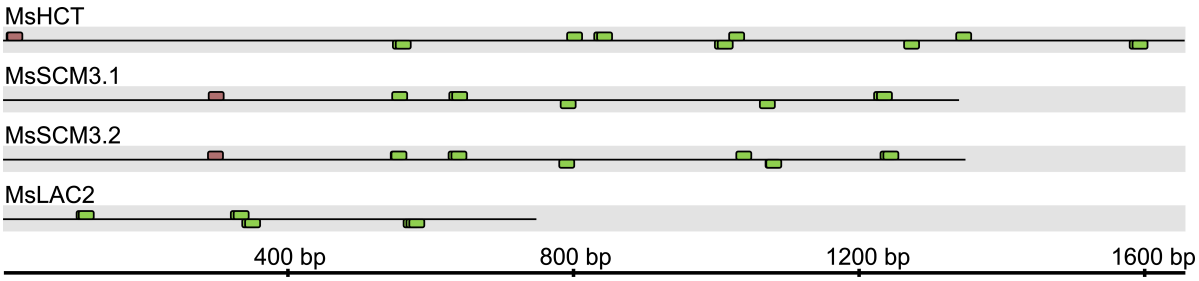

Figure 15: Cis-elements in promoter sequences of *Miscanthus*.

The promoter sequences from Ms*LAC2*, Ms*HCT*, Ms*SCM3.1*, and Ms*SCM3.2* were searched with MatInspector for known secondary wall-associated NAC (brown box) and MYB (including SMRE sites and AC-elements (green box; Zhong and Ye, 2012) binding sites.

MsSCM2-4 were able to activate the promoters of the general phenylpropanoid pathway enzyme At*4Cl1*p, the first enzyme of flavonol biosynthesis pathway At*CHS*p, and the lignin-specific enzyme At*HCT*p ranging from 5-fold to 50-fold (Figure 14A). However, MsSND1 activated At*4Cl1*p about 12-fold and At*HCT*p about 4-fold but no activation was observed with At*CHS*p. The negative control AtMYB15, an activator of the Shikimate pathway (Chen et al., 2006) was not able to activate any promoter. However, AtMYB85, which is described as an lignin-specific activator (Zhong et al., 2008) induced all three promoters, even though induction was only between 3 and 4-fold (Figure 14A). Similar to AtMYB85, the TFs MsSCM2-4 were capable to activate promoters from genes from phenylpropanoid-, flavonol-, and lignin biosynthesis pathway, indicating functional similarities.

Analysis of *Miscanthus* promoters could reveal new insight about regulation of SCW formation in *Miscanthus*. Until now, the genome of *Miscanthus* is not sequenced. In order to extract regulatory elements like promoter sequences of *Miscanthus*, a partial genome database were created from *Miscanthus sinensis* variant Sin-13 (Reference: Clifton-Brown and Lewandowski, 2002). Promoter sequences were retrieved by a homology-based search with amino acid sequences from *Arabidopsis* for Ms*LAC2*p (laccase) and Ms*HCT*p (hydroxycinnamoyl-coenzyme A shikimate/quinate hydroxycinnamoyltransferase). In order to increase the chances to clone an active promoter/isoform of HCT, the best hits for At*HCT* were aligned against sorghum and maize genome to identify an active locus and probably a functional and active promoter. In case of Ms*SCM3*p the cloned nucleotide sequence of the gene plus promoter (from the genome database) was aligned against sorghum genome with a 94 % match to Sb07g024970. Primers were designed according to the sorghum sequence, to amplify two very similar promoter fragments of about 1.3 kb, that probably indicate two alleles.
MatInspector algorithm (Cartharius et al., 2005) detected MYB binding sites including SMRE sites and AC-elements, that are documented to be involved in SCW formation (Zhong & Ye, 2012) in promoter sequences of MsHCTp, MsSCM3.1/.2p, and MsLAC2p (Figure 15). Additionally, a secondary wall-associated NAC binding site was recognised in MsSCM3.1/.2p and MsHCTp. As depicted in Figure 14B, MsSCM4 activated the promoters Ms*LAC2*p, Ms*HCT*p, and two Ms*SCM3*p more than 3-fold. However, MsSND1 was only able to activate Ms*SCM3*p but not Ms*LAC2*p or Ms*HCT*p.
The promoter activation assay revealed the capability of MsSND1 and MsSCM4 to activate promoters of putative lignin-related genes from *Miscanthus*.

3.8 Establishment of a precise posttranslational induction system of mCherry-GR-MsSND1 or mCherry-GR-MsVND7*

To further evaluate the function of MsSND1 and MsVND7, a posttranslational induction system was established in *Arabidopsis* consisting of either MsSND1 or MsVND7 fused to the fluorophore mCherry and the ligand-binding domain of the rat glucocorticoid receptor (GR; Figure 16). Briefly, the heat-shock protein 90 (HSP90) prevents the fusion proteins, in this case mCherry-GR-MsSND1/VND7 from entering the nucleus by forming a cytosolic complex with GR. Upon application of the synthetic steroid ligand dexamethasone (DEX)

*Section is adapted from Golfier et al., 2017

the protein complex disassociates allowing mCherry-GR-MsSND1/VND7 to enter the nucleus and act as transcriptional regulator. Under normal growth conditions for 10 days, transgenic *Arabidopsis* carrying a constitutively expressed mCherry-GR-Ms*SND1* or mCherry-GR-MsVND7 construct exhibited no obvious differences to wild-type plants concerning germination, growth, or development (Figure 16, 17). In contrast, activation of mCherry-GR-MsSND1 or mCherry-GR-MsVND7 with DEX led to an arrest of growth in seedlings of three and two independent transgenic *Arabidopsis* lines, respectively (Figure 16B, 17). While in mCherry-GR-MsSND1 lines growth was completely arrested after 7 days of DEX induction, in mCherry-GR-MsVND7 lines 3 days of induction were sufficient to inhibit growth (Figure 16B, 17). Furthermore, induction of mCherry-GR-MsSND1 and mCherry-GR-MsVND7 resulted in cell death, as indicated by loss of chlorophyll. The transgenic lines 16-2 and 2-2 seemed to show the strongest activation of mCherry-GR-MsSND1 and mCherry-GR-MsVND7, respectively, as growth was immediately arrested and loss of chlorophyll was the fastest, and thus were chosen for subsequent experiments. Nonetheless, cell death after mCherry-GR-MsSND1 activation occurred much slower than observed in mCherry-GR-Ms*VND7* lines (Figure 17). In untreated mCherry-GR-MsSND1 seedlings, detection of the mCherry signal in root tips revealed a cytosolic localisation of the fusion protein mCherry-GR-MsSND1 (Fig-

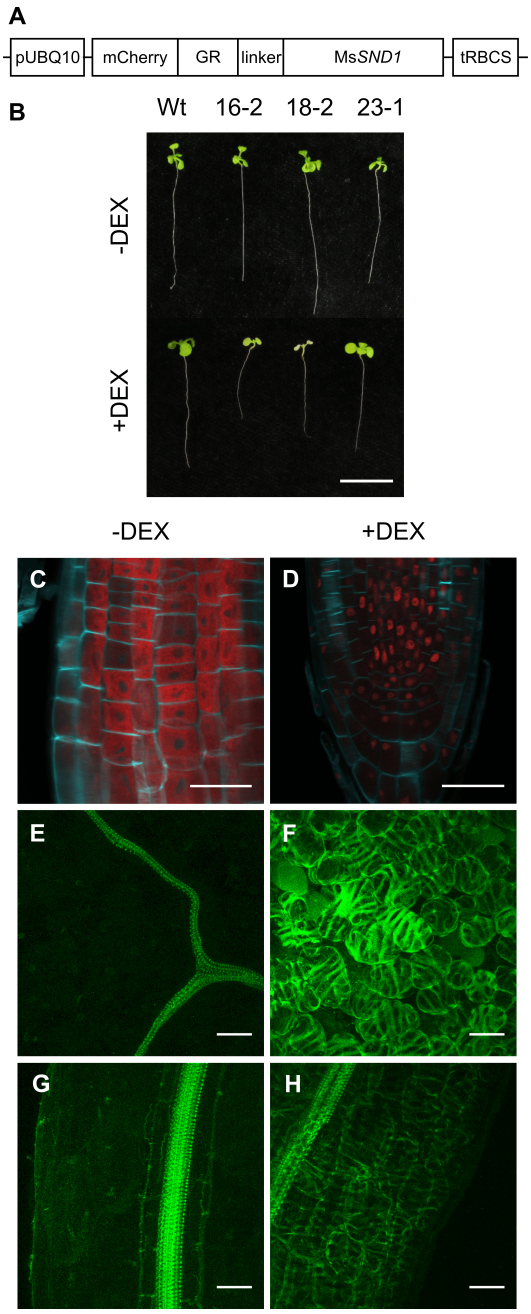

Figure 16: Induction of MsSND1 leads to secondary cell wall differentiation in *Arabidopsis*. (A) Schematic of inducible mCherry-GR-MsSND1 construct. Transgenic *Arabidopsis* mCherry-GR-MsSND1 seedlings (line 16-2) were treated with (+DEX) and without (-DEX) dexamethasone for 7 days (B), 4 days (E-H), and 24 hr (C, D), respectively. (C, D) The root tip cell walls were stained with SCRI Renaissance 2200, and lignin was stained with basic fuchsin. pUBQ10, ubiquitin-10 promoter; mCherry, synthetic fluorophore; GR, ligand-binding domain of the rat glucocorticoid receptor; tRBCS, ribulose-1,5-bisphosphate carboxylase small subunit terminator (from pea). Scale bar 1 cm (B) and 30 µm (C-H), respectively (Golfier et al., 2017).

ure 16C). After 24 h of DEX treatment, the mCherry signal was exclusively detected in nuclei of root cells (Figure 16D). Lignin staining with basic fuchsin revealed, that in the absence of DEX, only vascular elements in leaves and roots were lignified in mCherry-GR-MsSND1 seedlings (Figure 16E, G). In contrast, application of 10 µM DEX to *Arabidopsis* mCherry-GR-MsSND1 or mCherry-GR-MsVND7 seedlings for 4 days led to ubiquitous SCW deposition in the seedling including leaf mesophyll cells and root ground tissue (Figure 16F, H, S8). The establishment of a precisely inducible mCherry-GR-MsSND1 and mCherry-GR-MsVND7 *Arabidopsis* lines allow localisation and tracking of the fusion protein and corroborates the finding that MsSND1 and MsVND7 is capable of activating the SCW program resulting in patterned SCW deposition reminiscent of xylem elements.

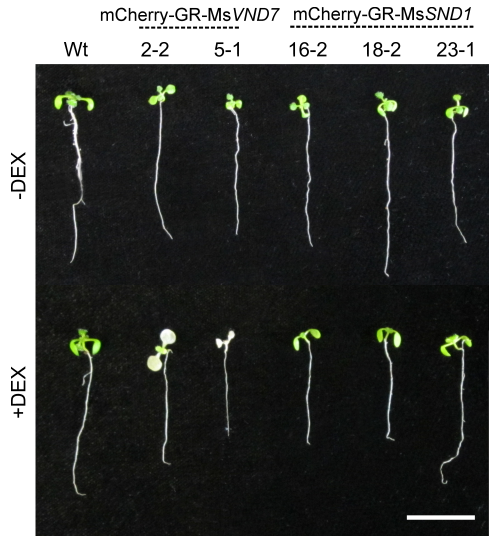

Figure 17: Faster phenotypic response after induction of mCherry-GR-MsVND7 compared to mCherry-GR-MsSND1. (Golfier et al., 2017).

10 day old *Arabidopsis* mCherry-GR-MsVND7 and mCherry-GR-MsSND1 seedlings were induced with DEX for 3 days to observe chlorosis and cell death. Scale bar 1 cm.

3.9 Assessment of mCherry-GR-MsSND1 to act as transcriptional regulator of genes involved in SCW formation*

With the establishment of an inducible system for MsSND1, the ability of MsSND1 to act as transcriptional regulator in SCW formation was addressed. To this end, mCherry-

*Section is adapted from Golfier et al., 2017

GR-Ms*SND1 Arabidopsis* lines were induced with or without pretreatment with the protein translation inhibitor cycloheximide (CHX), to determine direct and indirect targets. As shown in Figure 16C, D, application of DEX releases mCherry-GR-Ms*SND1* fusion protein from the cytosolic retention, to act as transcriptional regulator in the nucleus. Addition of CHX should prevent synthesis of proteins, including TFs, which in turn influence gene expression. Expression levels of selected genes involved in SCW formation were measured via qRT-PCR and normalised against *Clathrin Adaptor Subunit* (At5g46630; Figure 18).

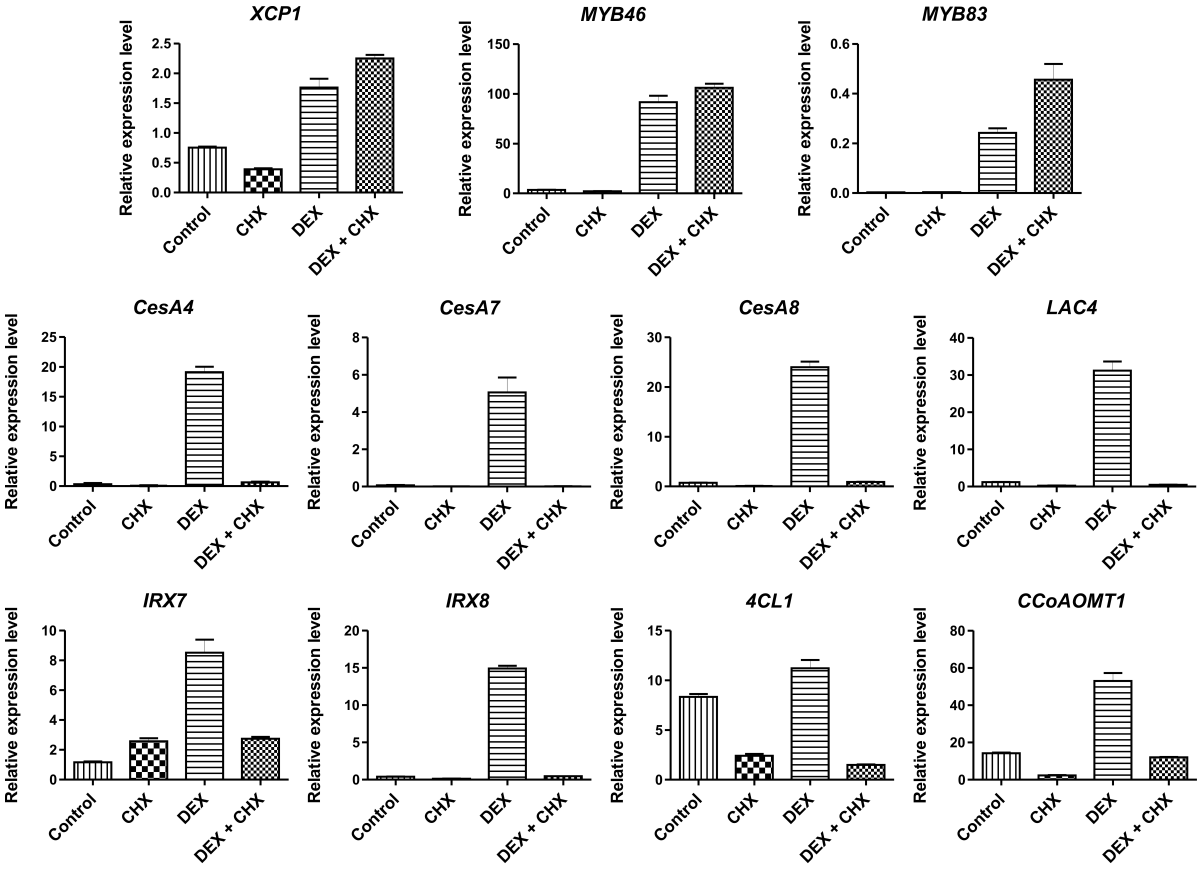

Figure 18: Induction of mCherry-GR-MsSND1 activates expression of genes involved in SCW formation (Golfier et al., 2017).

Expression analysis by qRT-PCR of candidate genes directly and indirectly targeted by MsSND1. Ten-day-old heterozygous *Arabidopsis* mCherry-GR-Ms*SND1* seedlings (line 16) were treated with cycloheximide (CHX) and/or dexamethasone (DEX). Gene expression is normalised against *Clathrin Adaptor Subunit* (At5g46630). Bars depict means + SE from three technical replicates.

Activation of mCherry-GR-MsSND1 with DEX elevated the transcript levels of genes associated with cellulose biosynthesis (*CesA4*, *CesA7*, and *CesA8*), xylan biosynthesis (*IRX7* and *IRX8*), lignin biosynthesis (*4CL1* and *CCoAOMT1*), cell death (*XCP1*), lignin polymerisation (*LAC4*), and MYB TFs (*MYB46/83*). In case of *CesA7*, gene expression was strongly upregulated up to 70-fold (Figure 18). In the presence of both DEX and CHX,

transcript levels of just *XCP1*, *MYB46*, and *MYB83* were increased, suggesting that expression is directly regulated by MsSND1. On the contrary, incubation of seedlings with DEX and CHX did not change transcript levels of *CesA*s, *IRX7/8*, *4CL1*, *CCoAOMT1*, and *LAC4* compared to the values obtained by CHX treatment, indicating indirect regulation by MsSND1. Except for *XCP1*, *4Cl1*, and *CCoAOMT1*, the background expression levels in the controls were very low. The independent mCherry-GR-MsSND1 line 18 exhibited the same activation pattern as mCherry-GR-MsSND1 line 16 but with generally lower relative values (Figure S9). Induction of mCherry-GR-MsSND1 activates directly and indirectly expression of genes involved in SCW formation.

Chapter 4

Discussion

The increasing demand for sustainably produced energy and materials has drawn attention to lignocellulosic biomass from short rotation coppice such as willow or poplar and perennial grasses like switchgrass or *Miscanthus*. However, *Miscanthus* has emerged as a leading candidate crop cross Europe because of higher yields of up to 23 t ha^{-1} depending on factors like growing site, genotype, and fertilisation compared to 13 t ha^{-1} for willow or 10 t ha^{-1} for switchgrass (Aylott et al., 2008; Heaton et al., 2004; Iqbal & Lewandowski, 2014). In addition, *Miscanthus* is suitable for production of biomass on marginal land due to modest nutrient and water requirement (Lewandowski et al., 2016). Thereby *Miscanthus* avoids competition for high grade agricultural land.

Cell wall recalcitrance is still one of the major limitations to exploit its huge potential as renewable resource. In order to improve biomass yield and composition, global breeding programs have been aiming to exploit the huge genetic and phenotypic diversity of *Miscanthus* by molecular assisted selection of desirable traits and cell wall profiling (da Costa et al., 2017; Robson et al., 2013; Slavov et al., 2014). However, understanding the mechanisms underlying secondary cell wall (SCW) formation has not received much attention in *Miscanthus* but may complement breeding efforts to improve quantity and quality of lignocellulosic biomass. This work was dedicated to identify and characterise important molecular players and regulators involved in cell wall biosynthesis to facilitate breeding efforts towards tailored biomass.

4.1 *Miscanthus sinensis* is susceptible to the herbicide isoxaben

A treatment to precisely induce lignification in *Miscanthus* could greatly facilitate exploration of underlying processes and players involved in lignification. The potent broad spectrum herbicide isoxaben belongs to a family of cellulose biosynthesis inhibitors, that induces clearance of cellulose synthase A (CesA) from the plasma membrane (Debolt & Brabham, 2013). In *Arabidopsis* roots and mesophyll cells of *Zinnia elegans*, application of isoxaben provoked ectopic lignification (Caño-Delgado et al., 2003; J. G. Taylor et al., 1992). A missense mutation in the highly conserved C-terminus of either CesA3 or CesA6 can be sufficient to confer resistance against isoxaben in *Arabidopsis* (Desprez et al., 2002; Scheible et al., 2001). Isoxaben had an inhibitory effect on the growth of switchgrass and sorghum, albeit they tolerate about 15- and 20-times higher isoxaben concentration compared to *Arabidopsis* (Petti et al., 2013). *Brachypodium distachyon* is considered as isoxaben tolerant because it tolerates about 100-times higher isoxaben concentrations compared to *Arabidopsis* (Brabham et al., 2017). However, comparative genomics could not identify a synonymous missense mutation in putative CesA genes in sorghum, *Brachypodium* or *Miscanthus*. *Brachypodium* did not metabolise isoxaben but a knockdown mutation of *Cellulose synthase-like F*6 increased sensitivity to isoxaben, suggesting mixed-linkage glucans as important cell wall component to confer isoxaben tolerance (Brabham et al., 2017). To assess whether *Miscanthus* is a susceptible genus or not, *Miscanthus* plantlets were watered with different concentrations of isoxaben, following the experimental approach by Heim et al., 1993 and growth was monitored. The concentration dependent inhibition of growth point out susceptibility of *Miscanthus* against isoxaben. Cross-sections of *Miscanthus* stems and leaves stained for lignin with HCl-phloroglucinol exhibited no unusual deposition of lignin.

4.1.1 Isoxaben increases expression of lignin-related genes in *Miscanthus* seedling roots indicating induction of lignification

To gain deeper insights into the response of *Miscanthus* to isoxaben treatment, 10 day old *Miscanthus* seedlings were exposed to 100 nM isoxaben for 48 hours to measure expression of lignin-related genes. Isoxaben treatment strongly elevated the expression of Ms*CCoAOMT*, Ms*HCT*, and Ms*SCM4*, which is closely related to At*MYB63*. Strikingly, a time-course experiment of isoxaben-treated *Arabidopsis* seedlings revealed a very similar

pattern of differential expressed genes (Figure S3). Although the response of *Arabidopsis* is much stronger, probably due to higher susceptibility and treatment was performed with higher isoxaben concentration. It is noteworthy that Ms*SND1* was not differentially expressed, meaning that if lignification is induced by isoxaben the route of activation does not seem to involve SND1. In contrast, the putative Ms*CesA7* gene is upregulated by isoxaben treatment, while *CesA*s in *Arabidopsis* were negatively regulated or unaffected (Figure S3; Bischoff et al., 2009; Manfield et al., 2004), highlighting differences of *Miscanthus* and *Arabidopsis* in response to isoxaben. In *Arabidopsis* CesA1, 3, and 6 are involved in primary cell wall biosynthesis (Desprez et al., 2007; Persson et al., 2007), while CesA4, 7, and 8 are important for SCW formation (N. G. Taylor et al., 2003). The effects of isoxaben on CesAs in *Miscanthus* remains elusive, thus it can only speculate about if redundancy of *CesA*s plays a role and if MsCesA7 could actually compensate deficiencies of other CesAs.

4.1.2 HCl-phloroglucinol and basic fuchsin staining indicate capability of isoxaben to induce lignification in *Miscanthus*

Lignin staining with HCl-phloroglucinol and basic fuchsin confirmed the postulated hypothesis that isoxaben induces ectopic lignification in *Miscanthus*. Cell walls of root cortex cells exhibited ectopic lignification when grown on isoxaben (Figure 5B). Moreover, increasing isoxaben concentrations resulted in intensifying disturbance of the cell shape (Figure 5B). In *Arabidopsis* it was proposed that the mode of action of isoxaben is disturbance of CesA complex trafficking by internalisation CesAs into small bodies, although CesA3 and CesA6 seemed to be directly targeted because missense mutations in C-terminus confers resistance to isoxaben (Desprez et al., 2002). It is conceivable that inhibition of cellulose biosynthesis by isoxaben lead to thinner and weaker cell walls, which are less resistant to the internal turgor pressure (Heisler et al., 2010). Intriguingly, isoxaben treatment led to a wavy cell phenotype in *Miscanthus* roots, suggesting decreased stiffness of the cell walls and thus less resistance to the internal turgor pressure. It is tempting to speculate that the wavy cell phenotype is a result of an inhibitory effect on CesAs in *Miscanthus* similar to *Arabidopsis*. However, the cell size and growth seemed to be largely unaffected, probably indicating that not all CesAs are targeted by isoxaben in *Miscanthus*.

Notably, disruption of cellulose biosynthesis or cell wall integrity are documented to induce plant defence mechanisms (Bischoff et al., 2009; Caño-Delgado et al., 2003; Ellis

et al., 2002), suggesting strengthening of cell walls with lignin as a defensive response to a pathogen attack. Indeed, the cellulose biosynthesis inhibitor isoxaben was found to elevate a number of genes involved in jasmonic acid- (JA), salicylic acid- (SA) and ethylene-dependent plant defence such as VSP1, VSP2, PR1, PR5 and PDF1.2 to name but a few (Bischoff et al., 2009). It is possible that isoxaben also triggers a plant defence response in *Miscanthus* leading to induction of lignification.

4.1.3 Analysis of cell wall composition reveals induction of lignification by isoxaben in *Miscanthus* seedling roots

Previously, treatment of Miscanthus with isoxaben indicated that i) Miscanthus is a susceptible species, ii) isoxaben provokes ectopic lignification in seedling roots illustrated by lignin staining and iii) isoxaben causes upregulation of putative genes involved in lignification. To corroborate the previous findings, the cell wall compositions of isoxaben treated and untreated Miscanthus roots were chemically analysed. Consistent with HCl-phloroglucinol and basic fuchsin lignin staining, Klason insoluble lignin increased considerably from 4 % to 6 % of total biomass concomitant with a slight decrease of soluble lignin in Miscanthus seedling roots when treated with isoxaben. This observation corroborate the assumption that an increase in insoluble lignin correlates with a decrease in soluble lignin, which may polymerise into the lignin polymer. The ratio of G and S units that are released from the lignin polymer by chemically cleavage of β-*O*-4 bonds were unchanged by isoxaben treatment (Figure 6C). A S/G ratio of 0.68 is comparable to lignin composition of internodes (S/G 0.64) but higher compared to lignin from leaves (S/G 0.43) of *Miscanthus x giganteus* (Le Ngoc Huyen et al., 2010). The highly induced expression of Ms*SCM4* by isoxaben treatment is consistent with no change of S/G ratio in *Miscanthus* because transient expression of Ms*SCM4* did not change S/G ratio in tobacco leaves either (Section 3.6), suggesting MsSCM4 as important player of lignification in *Miscanthus*. The S/G ratio remained unchanged after treatment of Miscanthus with 100 nM isoxaben. It seems possible that higher isoxaben concentrations may alter lignin composition because HCl-phloroglucinol staining indicated a distinct lignin after treatment of *Miscanthus* with 400 nM isoxaben (Section 4.1.2, Figure 5A). It should be noted, that Klason lignin content in *Miscanthus* seedling roots is certainly low with 4 % compared to up to 20 % in fully grown roots (Amougou et al., 2011) making young roots an attractive tool to detect even small differences in Klason lignin, despite labour intense generation of sufficient plant material for analyses. As isoxaben belongs to a family of cellulose biosynthesis inhibitors, it is not surprising that isoxaben treatment reduced the structural glucose content in *Miscanthus* seedling roots. However, the increased content of xylose, one of the main component

of hemicelluloses seemed like a compensatory response to inhibition of cellulose biosynthesis, as proposed by Caño-Delgado et al., 2000 but rather contradicts the hypothesis that isoxaben provokes lignification as defence response (Caño-Delgado et al., 2003). Clearly, more work is needed to understand the connections between isoxaben treatment and induction of ectopic lignin deposition in *Arabidopsis* and *Miscanthus*.
Taken together, *Miscanthus sinensis* has proven to be a susceptible species against the herbicide isoxaben. Furthermore, isoxaben was found to increase expression of lignin-related genes in Miscanthus seedling roots. In accordance, lignin staining with either HCl-phoroglucinol or basic fuchsin and analysis of cell wall composition provided clear evidence, that isoxaben induces ectopic lignification. As a next step, a *Miscanthus* transcriptome survey could facilitate identification of players involved in lignin formation. However, because a comprehensive *Miscanthus* genome is not available yet, gene annotations would rely on sorghum, rice, or maize genome as reference genome.

4.2 Identification of *Miscanthus sinensis* NAC and MYB transcription factors through phylogenetic analysis*

In the life cycle of higher plants, secondary cell wall formation (SCW) is crucial in plant development as SCWs provide mechanical strength, environmental protection, and impregnate water conducting tissues. As SCW deposition is irreversible the formation of SCW is spatio-temporally tightly regulated by a sophisticated multi-tiered hierarchical network of transcription factors (TF). Identification of master regulators is highly interesting because they are able to active the entire biosynthetic cell wall program (Zhong et al., 2010b; Zhong et al., 2015), which on the one hand can facilitate identification of genes involved in this program and on the other hand might be exploited to improve overall SCW formation. Regulators of the lowest tier have been proposed to fine-tune transcriptional regulation of the SCW formation, in particular lignification (Öhman et al., 2013; Zhong et al., 2008), which makes them designated targets for quality improvements.
Screening of a *Miscanthus* transcriptome allowed rapid identification of putative homologous TFs from different tiers of the regulatory network controlling SCW formation. Phylogenetic analysis suggested that MsSND1 and MsVND7 belong to the NAC subfamily Ic that could be further divided into three classes. Members of classes II and III are implicated in xylem differentiation (Kubo et al., 2005; Zhou et al., 2014), whereas members of class I are described to be involved in fiber differentiation (Zhong et al., 2006). MsVND7

*Section is adapted from Golfier et al., 2017

fell into class III, however MsSND1 was assigned to class I. Grass species like maize, *Brachypodium*, and rice possess up to nine members of the NAC subfamily Ic. In the closely related grass species *Sorghum bicolor* 15 members were assigned to the NAC subfamily Ic consisting of seven putative SNDs and eight putative VNDs (Kadier et al., 2017), indicating the presents of more NAC factors in *Miscanthus*. The exact number of NAC TFs in *Miscanthus* remains elusive due to incomplete transcripts in the *Miscanthus* transcriptome and without a comprehensive *Miscanthus* genome.

MYB TFs belong to a large and functional very diverse family of DNA-binding proteins, most abundantly represented in plants by R2R3 MYB TFs (Dubos et al., 2010). Depending on plant species the group R2R3 MYB TFs is represented with usually more than 100 members (Feller et al., 2011). The large number of R2R3 MYB TFs in the *Miscanthus* transcriptome and the highly divergent C-terminus allowed classification into a clade but did not always allow a more precise allocation (Figure 7B). This was particularly the case while searching for a close relative of AtMYB46 or their orthologs from poplar, *Eucalyptus*, rice, and maize which showed an inconclusive result with many candidate genes.

The high degree of conservation within the amino acid sequence of the N-terminal DNA-binding domain of NAC and MYB TFs was remarkable with $\geq$ 90 %, even to further related species like *Arabidopsis*, indicating very similar DNA-binding characteristics. In contrast, the C-terminus of NAC and MYB TFs is highly divergent, which may reflect different activation properties. Although, the C-termini of TFs carry conserved islands that could represent motifs, that may be important for activation (Figure S4). Divergence of regulatory elements like Cis-elements play a major role in evolutionary change (Wittkopp & Kalay, 2012), probably because mutations in regulatory elements might allow finer nuances of effects. Similarly, divergence of the C-terminus may play an important role in evolutionary adaptation.

4.3 High Ms*SND1* and Ms*SCM*s expression coincide with sclerenchyma-, vasculature development and SCW formation in *Miscanthus* leaves*

In grasses like *Miscanthus*, at the leaf base, meristems give continuously rise to cells that differentiate into leaf sheath and blade. Therefore, each single leaf displays the full sequence of differentiation along its length, with distinct degree of differentiation at particular locations. To capture level of expression and anatomical states, *Miscanthus sinensis*

*Section is adapted from Golfier et al., 2017

leaves were cut into ten fragments (Figure 7A) and examined with qRT-PCR and lignin staining. Spence et al., 2014 proposed cytoskeleton genes like tubulin or actin as good reference genes. During the course of leaf gradient cytoskeleton reference genes were differentially expressed in dividing tissue and fully developed tissue (leaf base and tip), and hence unsuitable for gene expression normalisation. In order to identify stable reference genes, common housekeeping genes from *Arabidopsis* (Czechowski et al., 2005) were blasted against a *Miscanthus* transcriptome (Barling et al., 2013). Four putative genes referred to as *protein phosphatase 2A subunit 3A* (*PP2A*), *clathrin adaptor AP2M* (*Clath*), *peroxin 4* (*UBC21*) and *TIP41-like protein* (*TIP*) revealed to be excellent reference genes with *PP2A* and *UBC21* as most stable ones. Even though surveyed leaves slightly differed in length and width, the expression pattern proved to be very stable and reproducible, highlighting leaf gradient as excellent model to study developmental processes such as SCW formation. Ms*SND1* showed highest expression in the first segment before rapidly declining in the second part, indicating activity of MsSND1 might initiate differentiation during very early leaf development (Figure 7). In line with this hypothesis is that expression of putative downstream targets of MsSND1 followed shortly after Ms*SND1* expression. Ms*LAC2* exhibited co-expression to Ms*SND1* that could suggest Ms*LAC2* as an direct target of MsSND1 or as putative cell wall-related laccase, MsLAC2 is secreted and integrated into the cell wall early during development to remain active until completion. In support of the uncovered expression pattern along the leaf gradient, putative orthologues from maize and rice revealed very similar expression patterns (P. Li et al., 2010; L. Wang et al., 2014). These observations suggest evolutionary conservation of the SCW transcriptional network in accordance with previous reports (Zhong et al., 2010a), and demonstrate feasibility of a homology-based approach for identifying SCW-related genes in *Miscanthus*.

Secondary cell walls and lignification is established very early during development of vasculature. Lignification starts in protoxylem cells, shortly followed by tracheary elements and sclerenchyma fibers, probably illustrating the order of importance for the integrity of the tissue (Figure 7D). Lignification and SCW deposition in sclerenchyma fibers seemed to be different from vasculature. This was further confirmed by basic fuchsin staining of the leaf cross-sections. Basic fuchsin was able to stain cells in the vascular tissue but was unable to stain sclerenchyma fibers (Figure 8). Notably, sclerenchyma cells were found to possess a distinct lignin composition in alfalfa (Vallet et al., 1996), which is probably the result of different lignification mechanisms employed by xylary and extraxylary fibers (Smith et al., 2013). A possible explanation is that vascular tissue and sclerenchyma fibers require distinct lignins with optimised properties such as better waterproofing or higher mechanical strength, respectively. However, a much deeper understanding of lignin and lignification is needed before such questions might be answered. Nonetheless, this

observation nicely illustrates how accurately lignification is regulated in *Miscanthus* even between neighbouring tissues, highlighting sclerenchyma fibers as an attractive target for lignin manipulation without affecting vessels and associated severe growth penalties (Smith et al., 2017).
Expression analysis and lignin staining along the leaf gradient revealed a correlation of high expression of Ms*SND1*, Ms*SCM*s and putative lignin-related genes with sclerenchyma and vasculature development.

4.4 Ms*SND1*, Ms*SND2*, and Ms*VND7* complement *Arabidopsis snd1 nst1* double mutant suggesting functional similarity to At*SND1*[*]

Complementation of the *Arabidopsis snd1 nst1* double mutant has been proven as valuable tool to characterise NAC TFs from many species like rice, poplar, maize, switchgrass as functional equivalent to AtSND1 or AtNST1 (Yoshida et al., 2013; Zhong, Lee, McCarthy et al., 2011; Zhong et al., 2010b; Zhong et al., 2015; Zhou et al., 2014). The strong pendant stem phenotype of *Arabidopsis snd1 nst1* caused by SCW defects of interfascicular fibers enables rapid selection of complemented T1 transformants. Phenotypic evaluation and cross-sections of inflorescence stems stained for lignin with HCl-phloroglucinol confirmed that MsSND1, MsSND2, MsVND7 and AtSND1 were able to complement the *Arabidopsis snd1 nst1* double mutant (Figure 10). This finding supported the hypothesis that MsSND1, MsSND2, MsVND7 and AtSND1 are functionally similar, even though a previous study has revealed that only partial activation of the regulatory network is already sufficient to rescue the *snd1 nst1* mutant, albeit with compositional changes to the SCW (Sakamoto & Mitsuda, 2015), that may explain for the partial complementation with Ms*SND2*. In line with the phylogenetic analysis (Figure 7A), that suggested MsVND7 as a class III member of the NAC TF subfamily Ic, which are implicated in xylem differentiation (Kubo et al., 2005), complementation of *Arabidopsis snd1 nst1* mutant with Ms*VND7* resulted in xylem-like structures in the cortex of inflorescent stem. Contradictory, the native At*SND1* promoter is predominantly active in interfascicular fibers and not in cortex of stems (Mitsuda et al., 2007). Thus, the appearance of xylem-like structures are probably explained by diffusion of MsVND7 from interfascicular fibers into cortex or the transgenic MsVND7-construct was integrated into an cortex active site of *Arabidopsis* genome or at least in close proximity of it. Nonetheless, the complementation of *Ara-*

[*]Section is adapted from Golfier et al., 2017

bidopsis snd1 nst1 double mutant with *Miscanthus* NAC TFs corroborate the phylogenetic assessment to rapidly identify functional homologs.
Multiple sequence alignment of amino acid sequences from NAC and MYB TFs revealed a high degree of conservation of the N-terminal DNA-binding motif raising speculation about similar DNA-binding characteristics. Indeed, the capability of Ms*SND1*, Ms*SND2*, Ms*VND7* to complement *Arabidopsis snd1 nst1* double mutant supports the hypothesis that MsSND1, MsSND2, MsVND7 act on the same regulatory network as AtSND1 and consequently possibly act on the same genes. The function of SCW master switches seemed to be highly conserved between different taxa of vascular plants as well as *Miscanthus*, highlighting the great importance during evolution of NAC-mediated transcriptional regulation of SCW machinery in fibers and xylem.

4.5 Expression of Ms*SND1* leads to strong ectopic SCW deposition in tobacco leaves, contrasting with MsSCMs induced lignification patterns *

To further examine MsSND1 and its regulatory role in SCW formation, functional characterisation was continued by transient expression of Ms*SND1* in *Nicotiana benthamiana* leaves. Overexpression of Ms*SND1* and At*SND1* caused strong patterned ectopic deposition of lignin, cellulose, and hemicellulose in almost every cell of the leaf (Figure 11). Interestingly, the patterns of ectopic SCW deposition are reminiscent of tracheary elements which has been previously observed after induced expression of NAC and MYB SCW master switches from several species such as *Arabidopsis*, poplar, *Eucalyptus*, switchgrass, rice, maize, and *Brachypodium* (Kubo et al., 2005; McCarthy et al., 2009; Valdivia et al., 2013; Yoshida et al., 2013; Zhong, Lee, McCarthy et al., 2011; Zhong et al., 2010a, 2010c; Zhong et al., 2007a, 2007b). Cortical microtubules have long been known to play a crucial role in patterned deposition of SCW by guiding exocyst complex and secretory vesicles at the sites of SCW deposition (Baskin, 2001; Oda & Fukuda, 2013; Vukašinović et al., 2017; Watanabe et al., 2015; Wightman & Turner, 2008). Indeed, several genes involved in cytoskeleton organisation and vesicle transport like MIDD1, FRA1, kinesins, or tubulin were found to be regulated by NAC TFs (Ohashi-Ito et al., 2010; Yamaguchi et al., 2011; Zhong et al., 2010c). Therefore, it is tempting to speculate that ectopic expression of Ms*SND1* does not only activate the biosynthetic cell wall machinery but also impacts cytoskeleton organisation and vesicle transport resulting in the specific patterns of SCW

*Section is adapted from Golfier et al., 2017

deposition. Nonetheless, the discrepancy that a fiber-specific gene initiates formation of xylem-like elements remains unclear. Probably, the cell program of a fully differentiated mesophyll cell can be overwritten by transient expression but the cell fate and cell niche is maintained, limiting morphological adaption into a fiber cell. The high similarity of the observed SCW pattern and deposition after transient expression of At*SND1* and Ms*SND1* supports the assumption that they are functionally similar.

After six days of incubation, tobacco leaves transiently expressing Ms*SND1* or At*SND1* appeared still vital. In clear contrast, ectopic expression of Ms*VND7* for six days led not only to patterned ectopic formation of SCW similar to Ms*SND1* and At*SND1* (Figure S6) but also induced extensive cell death, indicated by loss of chlorophyll and leaves, that became limp and dried out. This has been previous observed for members of the NAC subfamily Ic class III (Valdivia et al., 2013), evincing a distinctive capability of class I and III members to activate programmed cell death.

In clear contrast to the patterned ectopic SCW formation following transient expression of Ms*SND1* or At*SND1*, induced expression of Ms*SCM1-4* in tobacco leaves gave rise to uniform lignification of mesophyll cells (Figure 12), demonstrating that individual SCW TFs differ in their functionality and target spectrum. It remains speculative, why transient expression of either Ms*SCM1-4* resulted in strong lignification of only individual cells and not like Ms*SND1* that showed SCW formation in almost every cell of the leaf, although relative expression level after 3 days incubation of Ms*SCM1* and Ms*SCM2* were 8-fold and 22-fold higher compared to Ms*SND1* (Figure S7). Only if certain requirements are given, that could be the case in some individual cells, transient expression of Ms*SCM*s lead to lignification of the cell wall. J. G. Taylor et al., 1992 proposed that lignification is ultimately dependent on the localisation and the amount of cellulose. Probably, if a specific cellulose structure is not given than lignification cannot occur. Furthermore, lignification requires a sequence of precisely coordinated processes like biosynthesis of precursors, transportation to the cell wall, and polymerisation to name just a few (Y. Wang et al., 2013). It is conceivable that the assumed narrower target spectrum of MsSCMs activates just a subset of the required processes. Notably, in many cases lignified cells were attached to vascular elements, that might possess a favourable conditions to lead to lignification of cell walls.

In summary, ectopic expression of Ms*SND1* in tobacco leaves demonstrates that Ms*SND1* is capable of initiating a SCW differentiation program resulting in ectopic deposition of patterned cellulose, hemicellulose, and lignin. In contrast, transient expression of Ms*SCM*s is capable of initiating lignification resulting in uniform ectopic lignin deposition contrasting the patterned SCW deposition of Ms*SND1*. Thus, lower-tier TFs constitute attractive targets for specific lignin manipulation.

4.6 Expression of Ms*SND1* and Ms*SCM*s change cell wall composition with distinct profiles in tobacco leaves

To follow the hypothesis that individual SCW TFs from *Miscanthus* differ in their functionally and target spectrum, cell wall composition was chemically analysed after transient TF expression in tobacco leaves. Previously, transient expression of Ms*SND1*, At*SND1*, and Ms*VND7* led to ectopic deposition of lignin and hemicellulose as demonstrated by staining with LM11 antibodies and basic fuchsin (Figure 11, S6). This finding is in line with changes of cell wall composition associated with transient expression of Ms*SND1*, At*SND1*, and Ms*VND7*. An increase of structural xylose and Klason lignin illustrated again the capability of Ms*SND1*, At*SND1*, and Ms*VND7* to induce SCW formation. Interestingly, elevated amounts of Klason lignin and structural xylose appeared concomitantly with reduced structural glucose (Figure 13), suggesting a balance between Klason lignin, hemicellulose and cellulose (Hu et al., 1999). Even though, Ms*SND1*, At*SND1* and Ms*VND7* were just transiently and not stably expressed it is possible that the carbon flux was redirected from cellulose- towards lignin- and hemicellulose biosynthesis.

Thioacidolysis and derivatisation followed by reductive cleavage liberate a fraction of monomers that are β-aryl ether (β-*O*-4)-linked to the lignin polymer (Lu & Ralph, 1997). The released fraction is quantified by GC-MS and constitutes a representative proportion of G and S units within the analysed lignin polymer (Robinson & Mansfield, 2009). The recovery yields of ether-linked monomers from lignin following transient expression of MsSND1 and AtSND1 revealed a slightly higher S/G ratio in cells expressing MsSND1 and AtSND1 compared to the control (Figure 13). Even though the change to the control is small, MsSND1 and AtSND1 seemed to behave similarly, supporting the hypothesis of functional similarity between MsSND1 and AtSND1. Xylary elements were previously reported in alfalfa, soft- and hardwood to possess higher abundance of G-lignin, in contrast to sclerenchyma fibers which are dominated by S-lignin (Musha & Goring, 1975; Vallet et al., 1996; Zhao et al., 2010). Indeed, expression of MsVND7 resulted in a reduction of S/G ratio in tobacco leaves, confirming its implication in xylem differentiation, while a higher S/G ratio of AtSND1 and MsSND1 rather follows the cell wall composition of fibers.

Ectopic expression of Ms*SCM1-4* in tobacco leaves revealed individual mesophyll cell uniformly lignified (Figure 12). This observation was substantiated by detection of cell wall composition of tobacco leaves, following transient expression of Ms*SCM1-4*, At*MYB63* and Ms*MYB103*. Klason lignin was increased, albeit less extensive than in MsSND1, AtSND1 and MsVND7 (Figure 13A), precisely reflecting conclusions from lignin staining. As observed for MsSND1, AtSND1 and MsVND7 elevated amounts of Klason lignin are accompanied by a reduction of structural glucose, although in MsSCM3 and MsMYB103

the reduction was less pronounced, probably indicating the capability of MsSCM3 and MsMYB103 to activate cellulose biosynthesis. Supporting this assumption is a slight increase of structural xylose and mannose in MsMYB103 (Figure 13C). Intriguingly, despite a rather small increase of Klason lignin in AtMYB63 and MsMYB103 the S/G ratios were substantially higher. Strikingly, *Arabidopsis* AtMYB58 or AtMYB63 overexpressors and sorghum co-ortholog SbMYB60 overexpressors were documented to possess higher S/G ratios (Scully et al., 2016; Zhou et al., 2009). However the S/G ratio of the closely related MsSCM4 (Figure 7) was only lightly increased compared to the control. It remains unclear whether this is attributed to the low Klason lignin that is just 0.5 % higher than the control or whether MsSCM4 is functional different than AtMYB58/MYB63 or SbMYB60. Characterisation of AtMYB103 knock-out lines demonstrated that AtMYB103 is a key regulator of ferulate-5-hydroxylase (F5H), modifying S-lignin formation (Öhman et al., 2013). A high S/G ratio of MsMYB103 suggests functional similarities of AtMYB103 and MsMYB103. In summary, ectopic expression of both master regulators of SCW formation and low tier lignin-specific MYB TFs in tobacco has revealed implications of NAC and MYB TFs on cell wall composition, especially lignin. It further supports the hypothesis, that NAC and MYB TFs are associated with certain lignin qualities, providing an attractive target for lignin manipulation.

4.7 Promoter activation of target genes with Ms*SND1* and Ms*SCM*s suggests complex regulatory network of SCW formation of *Miscanthus*

In *Arabidopsis*, secondary cell wall formation is controlled and regulated by a sophisticated, multi-tiered hierarchical network of transcription factors (Taylor-Teeples et al., 2015). To gain a deeper understanding of the regulatory network of SCW formation of *Miscanthus*, *Miscanthus* TFs were analysed for the capability to activate promoters of lignin-related genes and other TFs from *Arabidopsis* and *Miscanthus*. Therefore a grapevine cv. 'Chardonnay' cell suspension was transformed via particle bombardment with various TFs and selective promoters. In a promoter activation assay AtMYB85 were documented to activate At*4Cl1* promoter (Zhong et al., 2008), suggesting AtMYB85 as lignin-specific regulator. This assumption was only partially confirmed by promoter activation assay in grapevine cell suspension. As expected, AtMYB85 activated At*HCT*p but surprisingly, AtMYB85 was also able to regulate chalcone synthase (At*CHS*), an enzyme which shuffles resources from phenylpropanoid pathway into flavonoid pathway (Lanz et al., 1991), in-

dicating a broader target spectrum as proposed by Zhong et al., 2008. Similar to AtMYB85, the *Miscanthus* MYB TFs MsSCM2-4 activated the promoters of At*4Cl1*, At*HCT*, and At*CHS* but to a much stronger extend (Figure 13). The stronger activation of lignin-related promoters by MsSCMs in relation to AtMYB85 probably reflects stronger lignification of vegetative parts of *Miscanthus* compared to *Arabidopsis*. Following the results from lignin staining and cell wall composition analysis, MsSND1 was capable to activate At*4Cl1*p and At*HCT*p but not At*CHS*p.

A first indication on the complexity of the transcriptional network regulating lignification in *Miscanthus* was gained by promoter activation assay with *Miscanthus* TFs. Ms*SCM3* promoters were activated by MsSCM4, suggesting MsSCM4 as higher-tier regulator. Interestingly, Ms*SCM3.2* promoter was slightly stronger activated by MsSCM4 (Figure 14A), although the only difference between Ms*SCM3.1*p and Ms*SCM3.2*p is a small insert, containing a predicted MYB binding site (Figure 15). The ability of MsSCM4 to activate Ms*LAC2*p and Ms*HCT*p proposed both genes to be involved in lignification, confirming expression profiles along the leaf gradient (Figure 7B, C). Surprisingly, MsSND1 activated both Ms*SCM3* promoter but not Ms*LAC2*p or Ms*HCT*p. *In silico* identification of cis-acting elements provided a possible explanation for this. With about 800 bp the Ms*LAC2* promoter is relative short and might not contain important TF binding sites (NAC binding sites and/or MYB binding sites, Figure 15). Due to high evolutionary conservation of SCW formation, one might assume similar transcriptional mechanisms in grapevine. However, it cannot be excluded that activation of Ms*LAC2*p and Ms*HCT*p requires a complex of many factors such as bHLH- and WD40 proteins, which may be not present grapevine. It is also possible that the cloned Ms*LAC2*p and Ms*HCT*p are less active allelic variations with minor function in lignification that is reflected by little activation by MsSCM4.

The promoter activation assay revealed target genes of MsSND1 and MsSCMs in *Arabidopsis* and *Miscanthus*, illustrating a complex regulatory network of SCW formation.

4.8 Induction of mCherry-GR-MsSND1 or mCherry-GR-MsVND7 lead to transdifferentiation of xylem-like elements and allows localisation and tracking of the fusion protein*

In order to gain further insights into the regulatory properties of MsSND1 and MsVND7, a posttranslational induction system was established in *Arabidopsis* consisting of either MsSND1 or MsVND7 fused to the fluorophore mCherry and the ligand-binding domain of the rat glucocorticoid receptor (GR). Briefly, in the absence of the steroid ligand, the heat-shock protein 90 (HSP90) builds a cytosolic complex with GR, preventing the fusion protein, in this case mCherry-GR-MsSND1 or mCherry-GR-MsVND7 from entering the nucleus (Dalman et al., 1991). Upon application of the synthetic steroid dexamethasone (DEX), mCherry-GR-MsSND1 or mCherry-GR-MsVND7 are released from cytosolic retention and able to act as transcriptional regulator in the nucleus. Treatment with DEX for 7 days, the growth of mCherry-GR-MsSND1 seedlings was arrested and loss of chlorophyll indicated induction of cell death. Although, chlorosis and cell death appeared faster in mCherry-GR-VND7 lines, confirming previous observations by Yamaguchi et al., 2010, suggesting functional similarity of MsVND7 to class II or III NAC TFs like AtVND7 or BdSWN5. By contrast, the weaker induction of chlorosis and cell death by MsSND1 emphasises MsSND1 as a member of class I NAC TFs like AtSND1 or BdSWN8 (Valdivia et al., 2013). The sharp boundaries of the mCherry signal, excluding nuclei, in Figure 16C, D indicate that the mCherry-GR-MsSND1 fusion protein only marginally leaked into the nucleus, consistent with normal growth and development of noninduced seedlings. However, induction of mCherry-GR-MsSND1 is rapid and strong, suggested by the strong mCherry signal in nuclei 24 hours after DEX application. This was further validated by lignin staining using basic fuchsin in the absence and presence of DEX. In absence of DEX, exclusively vascular elements were lignified in mCherry-GR-MsSND1 seedlings. 4 days of DEX treatment was sufficient to ubiquitously induce strong SCW deposition in nearly every cell in both mCherry-GR-SND1 and mCherry-GR-VND7 seedlings (Figure 16, S8). Induction of mCherry-GR-MsSND1 and mCherry-GR-MsVND7 in *Arabidopsis* gave rise to patterns of SCW deposition reminiscent of tracheary elements, that is in line with similar patterns caused by transient expression of MsSND1 and MsVND7 in *Nicotiana benthamiana* leaves. This result again supports a high degree of conservation of the molecular mechanism involved in SCW patterning and biosynthesis throughout vascular plants (Bomal et al., 2008; E. Li et al., 2012; Zhong et al., 2010a).

*Section is adapted from Golfier et al., 2017

4.9 Induction of mCherry-GR-MsSND1 activates directly and indirectly expression of genes involved in SCW formation*

With an established posttranslational induction system, MsSND1 was assessed for the capability to directly and indirectly activate genes involved in SCW formation. Therefore, transgenic mCherry-GR-MsSND1 *Arabidopsis* seedlings were pretreated with or without the translation inhibitor cycloheximid (CHX) before mCherry-GR-MsSND1 was induced with DEX. Induction of mCherry-GR-MsSND1 with DEX in the presence of CHX promoted the expression of *XCP*, *MYB46*, and *MYB83*, while genes associated with cellulose biosynthesis (*CesA4*, *CesA7*, and *CesA8*), xylan biosynthesis (*IRX7* and *IRX8*), lignin biosynthesis (*4CL1* and *CCoAOMT1*), and lignin polymerisation (*LAC4*) seem to be indirect targets. CHX treatment decreased the expression of all examined genes but *IRX7*, indicating an inhibitory effect on native factors regulating gene expression either positively or in case of *IRX7* negatively. Intriguingly, it could be shown that MsSND1 is capable to activate many of the same downstream target genes as previously identified for secondary wall NACs like AtSND1, AtVND6, and AtVND7 (Ohashi-Ito et al., 2010; Zhong et al., 2010c). Although there are some discrepancies in previous studies about the direct and indirect targets of AtSND1 and AtVND7, respectively. For example, in an electrophoretic mobility shift assay (EMSA) AtSND1 was demonstrated to bind fragments of *CesA8* promoter (Taylor-Teeples et al., 2015) but *CesA8* was not found as direct target of AtSND1 (Zhong et al., 2010c). Similar, Yamaguchi et al., 2011 found that AtVND7 directly activate *LAC4* but it was absent in the global identification of direct AtVND7/AtSND1 targets (Zhong et al., 2010c), raising the possibility that some AtSND1 target are not identified yet.
The formation of secondary cell walls is a dynamic process, requiring a number of successive steps such as biosynthesis of building blocks, transport to the cell wall, assembly of polymers, to name but a few. DEX induction of mCherry-GR-MsSND1 for 4 hours strongly elevated expression of MYB46/83 and CesA4/7/8 while expression levels of 4Cl1 and CCoAOMT showed just a moderate increase. It is tempting to speculate, that after 4 hours DEX induction, SCW formation is still in an early stage and at later time points, perhaps, genes involved in lignification will move to the fore. A detailed time-course study of inducible mCherry-GR-MsSND1 *Arabidopsis* lines might solve discrepancies and could give a deeper understanding of the dynamics of SCW formation.

*Section is adapted from Golfier et al., 2017

Supplements

Figures

Figure S1: Protein sequence alignment of MsSND1 and AtSND1 (Golfier et al., 2017).

The amino acid sequences from AtSND1 and MsSND1 were aligned with Clustal Omega software (Sievers et al., 2011). The NAC transcription factor domain (DNA binding domain) is highlighted in grey. An * (asterisk), : (colon), and . (period) indicate identical, strongly similar, and weakly similar properties of amino acid residues, respectively.

```
AtMYB85       MGRQPCCDKLGVKKGPWTVEEDKKLINFILTNGHCCWRALPKLAGLRRCGKSCRLRWTNY
MsSCM3        MGRQPCCDKLGVKRGPWTAEEDRKLINFILTNGHCCWRAVPKLAGLLRCGKSCRLRWTNY
              **************:****.***:****************:****** ************

AtMYB85       LRPDLKRGLLSHDEEQLVIDLHANLGNKWSKIASRLPGRTDNEIKNHWNTHIKKKLLKMG
MsSCM3        LRPDLKRGLLTDAEEQVVIDVHAKLGNRWSKIAAKLPGRTDNEIKNHWNTHIKKKLIKMG
              **********:. ***:***:**:***:*****::**********************:***

AtMYB85       IDPMTHQPLNQEPSNIDNSKTIPSNPDDVSV-EPKTTNTKYVEISVT-----TTEEESSS
MsSCM3        IDPATHEPLDRKTTSSSPATTSQSTKFDEATKQQSPQNDDVVAMRDVPPDGCSPTESSMN
              *** **:**::: :. . :.*  *.  * :. : .  * . * :  .     :  *.* .

AtMYB85       TVTDQNSSMDNENHLIDNIYDDDELFSYLWSDETTKDEASWSDSNFGVGGTLYDHNISGA
MsSCM3        TVSTGGSSS---SSSSGSGHDQDPLVKWLMEEEPPTGDEPWLNFTGSVDVDEFSSI--AA
              **:  .**    .   .. :*:* *..:* .:*  ..:  * : . .*.   :.    .*

AtMYB85       DADFPIWSPERINDEKMFLDYCQDFGVHDFGF----------------
MsSCM3        GLELLPWDG-----ATDWLLDYQDFGLGDSATLVDGYMVNNSSNGAKF
              . ::  *.       . :*   ****: * .
```

Figure S2: Protein sequence alignment of MsSCM3 and AtMYB85. The amino acid sequences from *A. thaliana* MYB85 and *M. sinensis* SCM3 were aligned with Clustal Omega software (Sievers et al., 2011). The highly conserved R2R3 MYB-binding domain (DNA-binding domain) is highlighted in grey with crucial tryptophan residues in red.

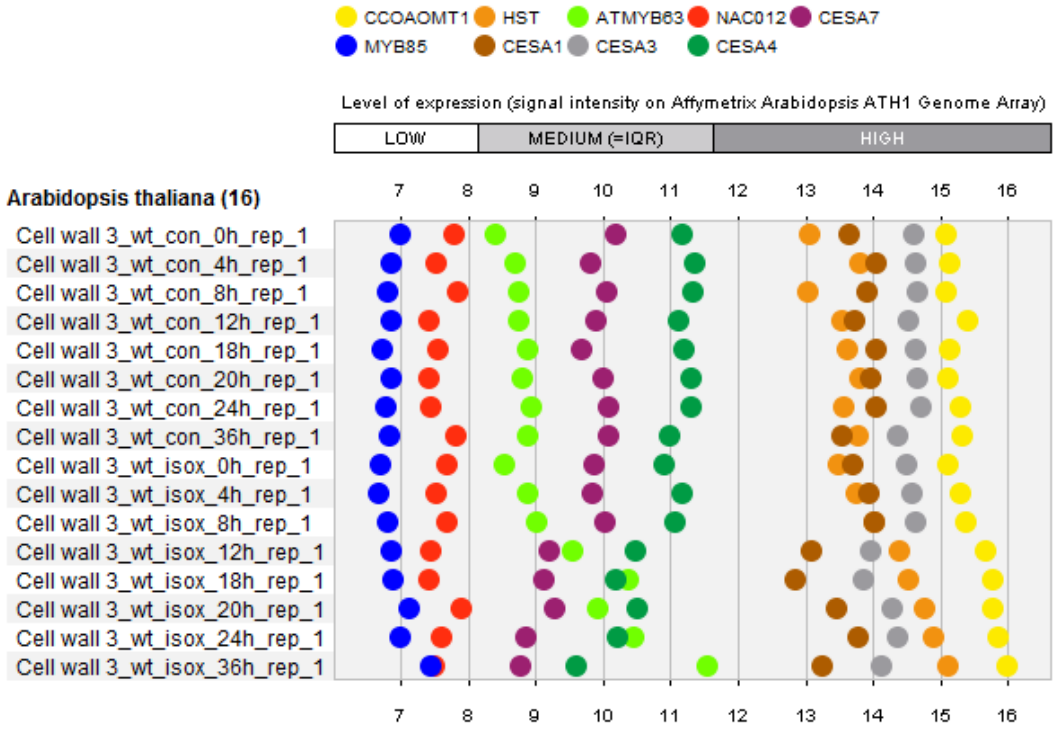

Figure S3: Time series of expression profiles of selected genes from *Arabidopsis thaliana*. 6 day old *Arabidopsis* seedlings were treated with 600 nM isoxaben for 36 hours followed by gene expression analysis via Affymetrix ATH1 (Hamann et al., 2009). The values represent normalised levels of expression plotted on a logarithmic scale. HST corresponds to HCT and NAC012 describes SND1.

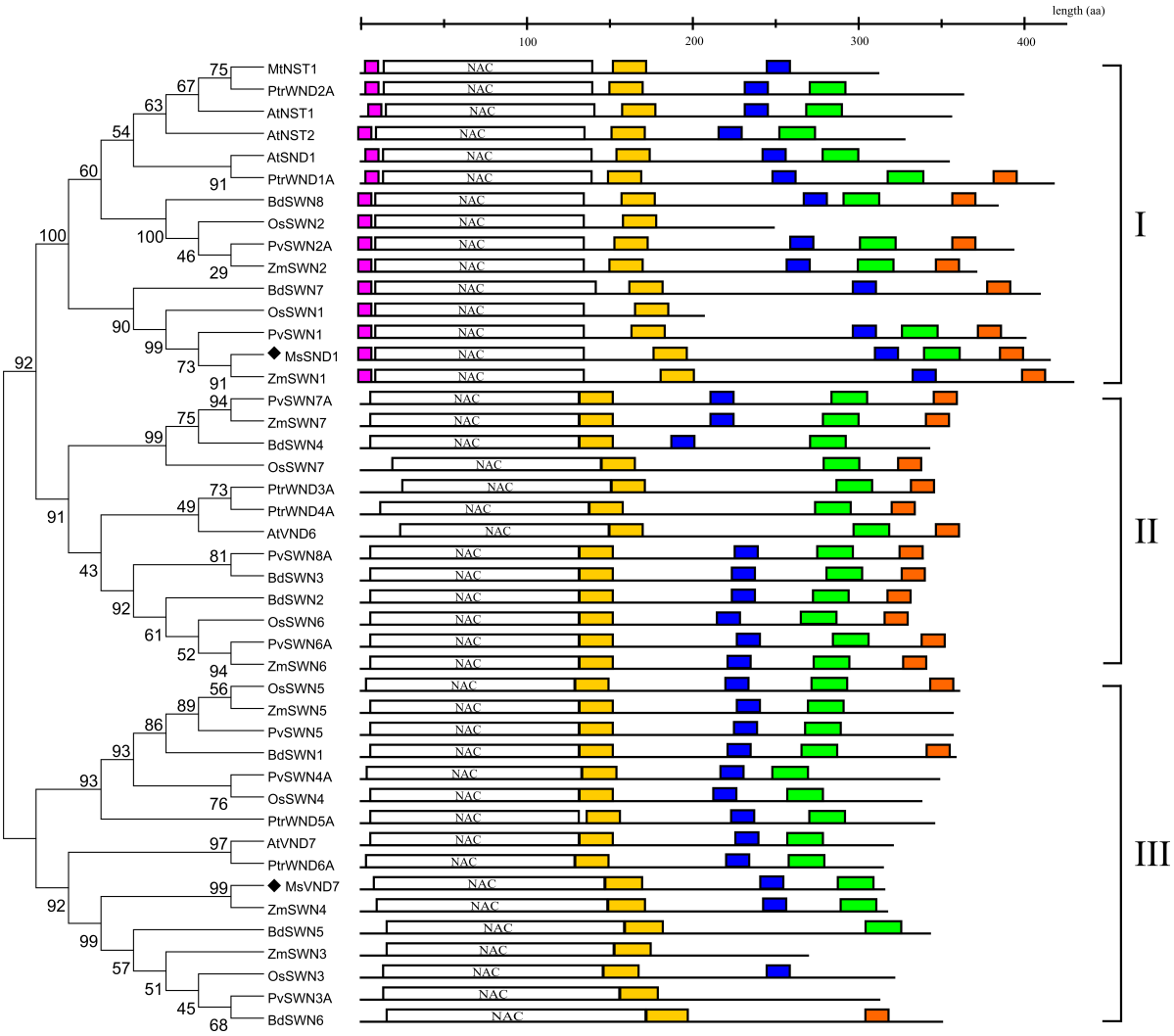

Figure S4: Phylogenetic analysis of the NAC subfamily Ic (see Figure 7) and schematic amino acid structure with motifs identified by MEME suite. A cut-off E-value of 1E-40 and a minimal amino acid width of 8 resulted in 9 motif (NAC DNA-binding domain summarises 4 motifs). E-values of each motif is depicted in Figure S5.

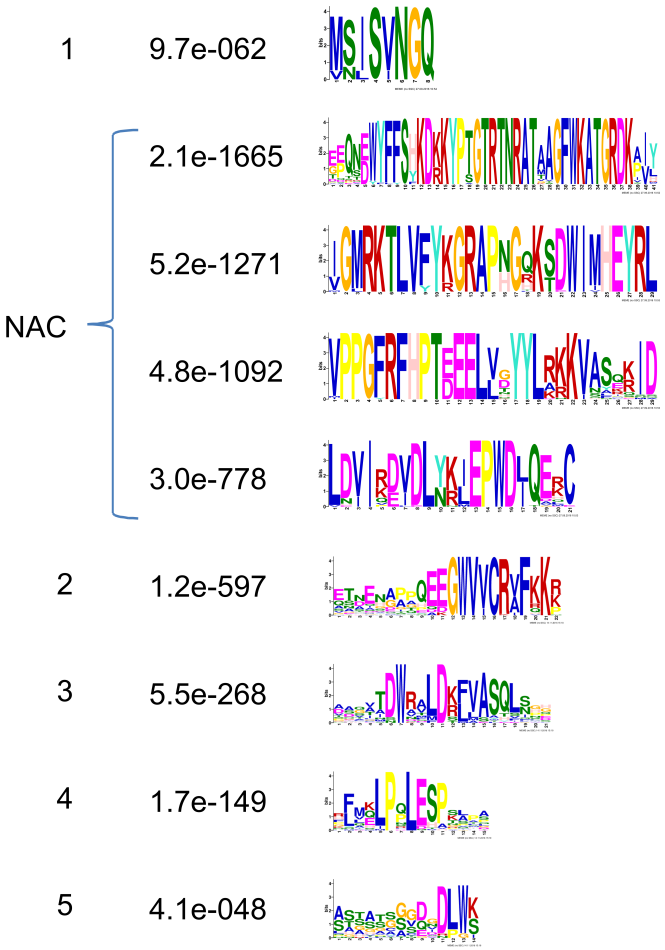

Figure S5: Consensus amino acid sequence of MEME motifs (Figure S4) with E-values. For simplicity the NAC DNA-binding domain summarises 4 motifs.

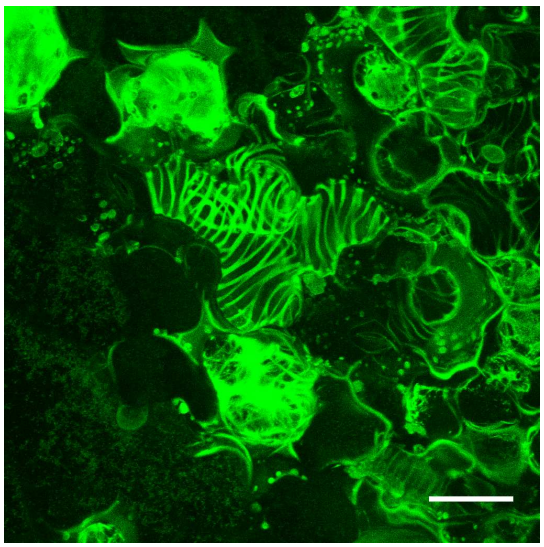

Figure S6: Ectopic expression of Ms*VND7* induces ectopic deposition of patterned lignin in a tobacco leaf after 6 days incubation. Leaf was stained with basic fuchsin for lignin. Scale bar: 40 µm.

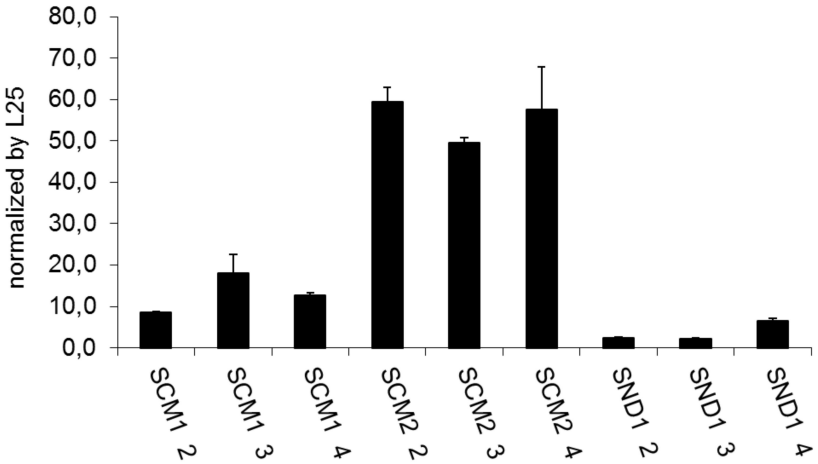

Figure S7: Relative expression of Ms*SCM1*, Ms*SCM2* and Ms*SND1* in tobacco leaves after 2, 3 and 4 days incubation. The values combine three technical replicates normalised against ribosomal protein L25.

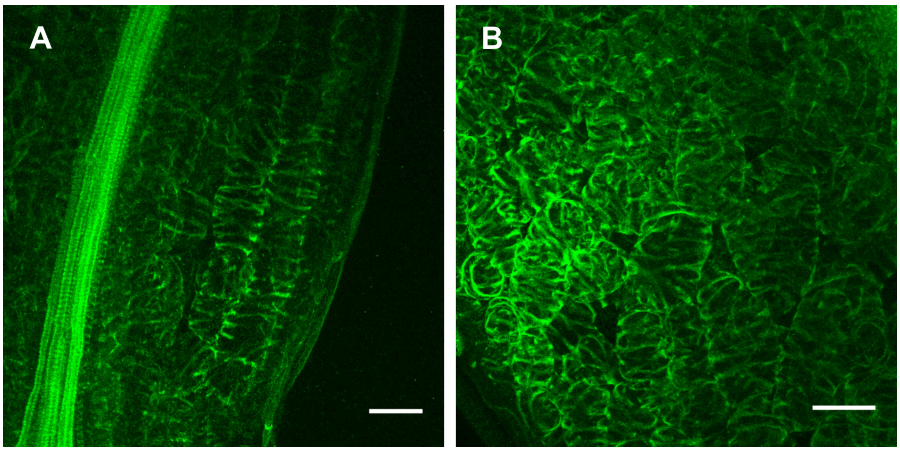

Figure S8: Induction of MsVND7 leads to secondary cell wall differentiation in *Arabidopsis*. Transgenic *Arabidopsis* mCherry-GR-MsVND7 seedlings (line 2-2) were treated with dexamethasone (DEX) for 4 days and lignin was stained with basic fuchsin. Scale bar 30 µm.

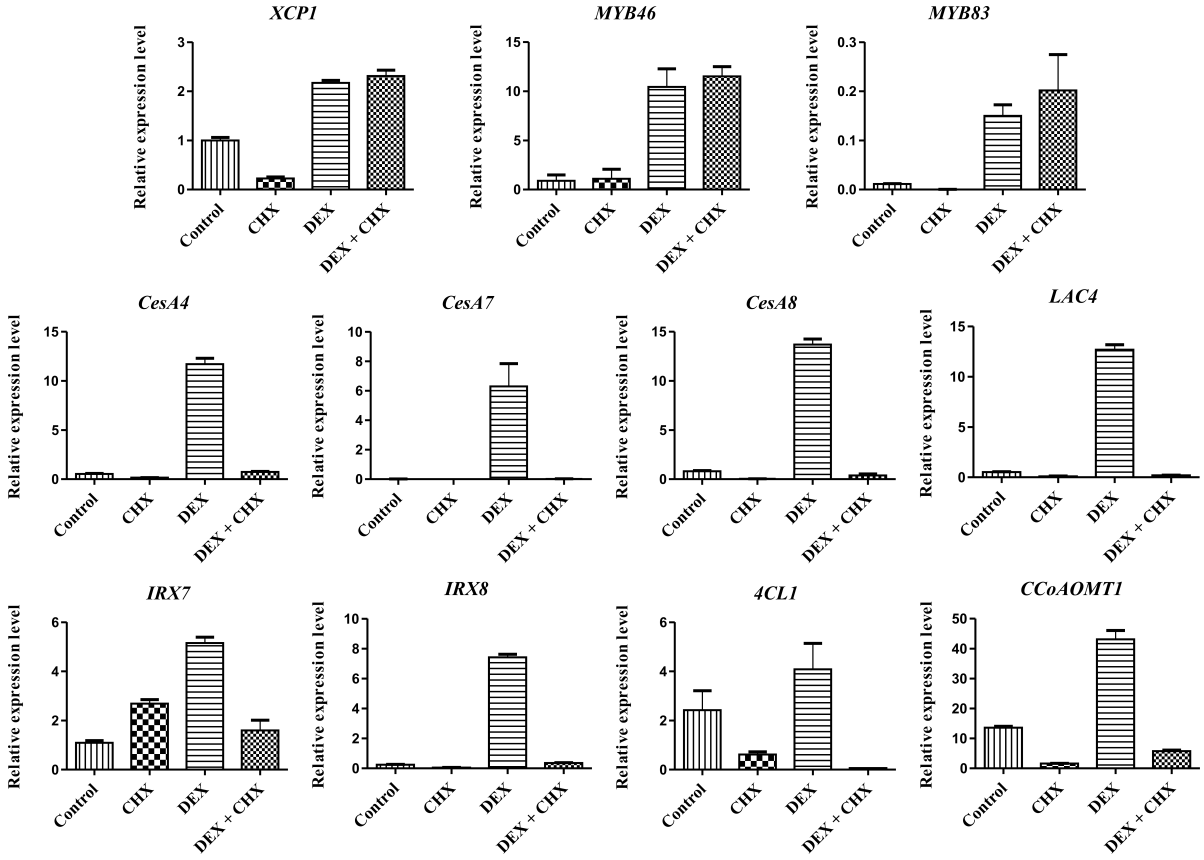

Figure S9: Induction of mCherry-GR-MsSND1 activates expression of genes involved in SCW formation. Expression analysis of candidate genes directly and indirectly targeted by MsSND1. Ten-day-old heterozygous *Arabidopsis* mCherry-GR-Ms*SND1* seedlings (line 18) were treated with cycloheximide (CHX) and/or dexamethasone (DEX). Gene expression is normalised against clathrin adaptor subunit. Bars depict means + SE from three technical replicates.

List of Abbreviations

%	percent
35S	*cauliflower mosaic virus* 35S promoter
A. thaliana	*Arabidopsis thaliana*
A. tumefaciens	*Agrobacterium tumefaciens*
Amp	ampicillin
bp	base pair
°C	degree celsius
Carb	carbenicillin
cDNA	complementary DNA
CHX	cycloheximide
C-terminus	carboxyl-terminus
cv.	cultivar
ddH_2O	double distilled water
DEX	dexamethasone
DMSO	dimethyl sulfoxide
DNA	deoxyribonucleic acid
dNTP	2'-deoxynucleosidetriphosphate
E. coli	*Escherichia coli*
EDTA	ethylenediamine tetraacetic acid
g	gravitational force
GC	Grape Cormier (medium)
GC/MS	gas chromatography-mass spectrometry
GR	ligand-binding domain of the rat glucocorticoid receptor
gDNA	genomic DNA
h	hour(s)
HPLC	high pressure liquid chromatography
Kan	kanamycin
kb	kilobase
LARII	luciferase assay reagent II
LB	Luria Bertani (medium)

M	molar concentration (mol/m^3)
mRNA	messenger RNA
MYB	myeoblastosis
MS	mass spectrometry
N. benthamiana	*Nicotiana benthamiana*
NAC	NAM, ATAF, and CUC
nst	NAC secondary wall thickening promoting factor
N-terminus	amino-terminus
OD_{600}	optical density at wavelength 600 nm
PCR	polymerase chain reaction
pH	negative decadic logarithm of hydronium ions
qRT-PCR	quantitative real-time polymerase chain reaction
RBCS	ribulose-1,5-bisphosphate carboxylase small subunit terminator
Rif	rifampicin
RT	room temperature
SCW	secondary cell wall
SDS	sodium dodecyl sulfate
S/G	ratio of syringyl to guaiacyl
snd	secondary wall-associated NAC domain
Tet	tetracycline
tDNA	transfer DNA (*Agrobacterium*)
TF	transcription factor
UBQ10	polyubiquitin 10 promoter (thale cress)
vnd	vascular-related NAC-domain
v/v	volume per volume
V. vinifera	*Vitis vinifera*
Wt	wildtype
w/v	weight per volume

Bibliography

Amougou, N., Bertrand, I., Machet, J. M. & Recous, S. (2011). Quality and decomposition in soil of rhizome, root and senescent leaf from Miscanthus x giganteus, as affected by harvest date and N fertilization. *Plant and Soil*, *338*(1), 83–97. doi:10.1007/s11104-010-0443-x

Aylott, M. J., Casella, E., Tubby, I., Street, N. R., Smith, P. & Taylor, G. (2008). Yield and spatial supply of bioenergy poplar and willow short-rotation coppice in the UK. *New Phytol. 178*(2), 358–370. doi:10.1111/j.1469-8137.2008.02396.x

Barling, A., Swaminathan, K., Mitros, T., James, B. T., Morris, J., Ngamboma, O., ... Moose, S. P. (2013). A detailed gene expression study of the Miscanthus genus reveals changes in the transcriptome associated with the rejuvenation of spring rhizomes. *BMC Genomics*, *14*, 864. doi:10.1186/1471-2164-14-864

Barrière, Y., Riboulet, C., Mechin, V., Maltese, S., Pichon, M., Cardinal, A., ... Martinant, J.-P. (2007). Genetics and genomics of lignification in grass cell walls based on maize as model species. *G3*, *1*(2), 133–156.

Barros, J., Serrani-Yarce, J. C., Chen, F., Baxter, D., Venables, B. J. & Dixon, R. A. (2016). Role of bifunctional ammonia-lyase in grass cell wall biosynthesis. *Nature Plants*, *2*(6), 16050. doi:10.1038/nplants.2016.50

Baskin, T. I. (2001). On the alignment of cellulose microfibrils by cortical microtubules: A review and a model. *Protoplasma*, *215*(1-4), 150–171. doi:10.1007/BF01280311

Baxter, X., Darvell, L., Jones, J., Barraclough, T., Yates, N. & Shield, I. (2014). Miscanthus combustion properties and variations with Miscanthus agronomy. *Fuel*, *117*, 851–869. doi:10.1016/j.fuel.2013.09.003

Bernard, P. & Couturier, M. (1992). Cell killing by the F plasmid CcdB protein involves poisoning of DNA-topoisomerase II complexes. *J. Mol. Biol. 226*(3), 735–45. doi:10.1016/0022-2836(92)90629-X

Bischoff, V., Cookson, S. J. & Wu, S. (2009). Thaxtomin A affects CESA-complex density , expression of cell wall genes , cell wall composition , and causes ectopic lignification in Arabidopsis thaliana seedlings. *60*(3), 955–965. doi:10.1093/jxb/ern344

Bomal, C., Bedon, F., Caron, S., Mansfield, S. D., Levasseur, C., Cooke, J. E. K., ... MacKay, J. (2008). Involvement of Pinus taeda MYB1 and MYB8 in phenylpropanoid

metabolism and secondary cell wall biogenesis: a comparative in planta analysis. *J. Exp. Bot. 59*(14), 3925–3939. doi:10.1093/jxb/ern234

Bonawitz, N. D. & Chapple, C. (2013). Can genetic engineering of lignin deposition be accomplished without an unacceptable yield penalty ? *Curr. Opin. Biotechnol. 24*(2), 336–343. doi:10.1016/j.copbio.2012.11.004

Bonawitz, N. D., Kim, J. I., Tobimatsu, Y., Ciesielski, P. N., Anderson, N. a., Ximenes, E., ... Chapple, C. (2014). Disruption of Mediator rescues the stunted growth of a lignin-deficient Arabidopsis mutant. *Nature*, *509*(7500), 376–380. doi:10.1038/nature13084

Brabham, C., Stork, J., Barrett, M. & DeBolt, S. (2017). Grass cell walls have a role in the inherent tolerance of grasses to the cellulose biosynthesis inhibitor isoxaben. *Pest Manag. Sci.* n/a–n/a. doi:10.1002/ps.4779

Bringmann, M., Li, E., Sampathkumar, A., Kocabek, T., Hauser, M.-T. & Persson, S. (2012). POM-POM2/CELLULOSE SYNTHASE INTERACTING1 Is Essential for the Functional Association of Cellulose Synthase and Microtubules in Arabidopsis. *Plant Cell*, *24*(1), 163–177. doi:10.1105/tpc.111.093575

Brosse, N., Dufour, A., Meng, X., Sun, Q. & Ragauskas, A. (2012). Miscanthus: a fast-growing crop for biofuels and chemicals production. *Biofuels, Bioprod. Biorefin. 6*(3), 246–256. doi:10.1002/bbb

Bullock, W. O., Fernandez, J. M. & Short, J. M. (1987). XL1-Blue: a high efficiency plasmid transforming recA Escherichia coli strain with β-galactosidase selection. *BioTechniques*, *5*, 376–79.

Caño-Delgado, A., Metzlaff, K. & Bevan, M. W. (2000). The eli1 mutation reveals a link between cell expansion and secondary cell wall formation in Arabidopsis thaliana. *Development*, *127*(15), 3395–3405. eprint: http://dev.biologists.org/content/127/15/3395.full.pdf

Caño-Delgado, A., Penfield, S., Smith, C., Catley, M. & Bevan, M. (2003). Reduced cellulose synthesis invokes lignification and defense responses in Arabidopsis thaliana. *Plant J. 34*(3), 351–362. doi:10.1046/j.1365-313X.2003.01729.x

Cartharius, K., Frech, K., Grote, K., Klocke, B., Haltmeier, M., Klingenhoff, A., ... Werner, T. (2005). MatInspector and beyond: promoter analysis based on transcription factor binding sites. *Bioinformatics*, *21*(13), 2933–2942. doi:10.1093/bioinformatics/bti473

Chapelle, A., Morreel, K., Vanholme, R., Le-Bris, P., Morin, H., Lapierre, C., ... Demont-Caulet, N. (2012). Impact of the Absence of Stem-Specific β-Glucosidases on Lignin and Monolignols. *Plant Physiol. 160*(3), 1204–1217. doi:10.1104/pp.112.203364

Chen, Y., Zhang, X., Wu, W., Chen, Z., Gu, H. & Qu, L.-J. (2006). Overexpression of the Wounding-Responsive Gene AtMYB15 Activates the Shikimate Pathway in Ar-

abidopsis. *J. Integr. Plant Biol. 48*(9), 1084–1095. doi:10.1111/j.1744-7909.2006.00311.x

Clifton-Brown, J. C., Hastings, A., Mos, M., McCalmont, J. P., Ashman, C., Awty-Carroll, D., ... Flavell, R. (2017). Progress in upscaling Miscanthus biomass production for the European bio-economy with seed-based hybrids. *GCB Bioenergy*, *9*(1), 6–17. doi:10.1111/gcbb.12357

Clifton-Brown, J. C. & Lewandowski, I. (2002). Screening Miscanthus genotypes in field trials to optimise biomass yield and quality in Southern Germany. *Eur. J. Agron. 16*(2), 97–110. doi:10.1016/S1161-0301(01)00120-4

Clough, S. J. & Bent, A. F. (1998). Floral dip: A simplified method for Agrobacterium-mediated transformation of Arabidopsis thaliana. *Plant J. 16*(6), 735–43. doi:10.1046/j.1365-313X.1998.00343.x

Cosgrove, D. J. (2016). Plant cell wall extensibility: Connecting plant cell growth with cell wall structure, mechanics, and the action of wall-modifying enzymes. *J. Exp. Bot. 67*(2), 463–476. doi:10.1093/jxb/erv511

Costa, T. H., Vega-Sánchez, M. E., Milagres, A. M., Scheller, H. V. & Ferraz, A. (2016). Tissue-specific distribution of hemicelluloses in six different sugarcane hybrids as related to cell wall recalcitrance. *Biotechnol. Biofuels*, *9*(1), 1–13. doi:10.1186/s13068-016-0513-2

Czechowski, T., Stitt, M., Altmann, T., Udvardi, M. K. & Scheible, W.-R. (2005). Genome-Wide Identification and Testing of Superior Reference Genes for Transcript Normalization in Arabidopsis. *Plant Physiol. 139*(1), 5–17. doi:10.1104/pp.105.063743

Czemmel, S., Stracke, R., Weisshaar, B., Cordon, N., Harris, N. N., Walker, A. R., ... Bogs, J. (2009). The Grapevine R2R3-MYB Transcription Factor VvMYBF1 Regulates Flavonol Synthesis in Developing Grape Berries. *Plant Physiol. 151*(3), 1513–30. doi:10.1104/pp.109.142059

da Costa, R. M. F., Lee, S. J., Allison, G. G., Hazen, S. P., Winters, A. & Bosch, M. (2014). Genotype, development and tissue-derived variation of cell-wall properties in the lignocellulosic energy crop Miscanthus. *Ann. Bot. 114*(6), 1265–1277. doi:10.1093/aob/mcu054

da Costa, R. M. F., Pattathil, S., Avci, U., Lee, S. J., Hazen, S. P., Winters, A., ... Bosch, M. (2017). A cell wall reference profile for Miscanthus bioenergy crops highlights compositional and structural variations associated with development and organ origin. *New Phytol. 213*(4), 1710–1725. doi:10.1111/nph.14306

Dalman, F. C., Scherrer, L. C., Taylor, L. P., Akil, H. & Pratt, W. B. (1991). Localization of the 90-kDa heat shock protein-binding site within the hormone-binding domain of the glucocorticoid receptor by peptide competition. *J. Biol. Chem. 266*(6), 3482–3490.

Dammer, L., Carus, M., Piotrowski, S., Puente, Á., Breitmayer, E., Liptow, C. & de Beus, N. (2017). Sustainable First and Second Generation Bioethanol for Europe: A sustainability assessment of first and second generation bioethanol in the context of the European Commission's REDII proposal. Retrieved from http://news.bio-based.eu/media/2017/09/17-09-07-PR-Bioethanol-sustainability-study.pdf

Debolt, S. & Brabham, C. (2013). Chemical genetics to examine cellulose biosynthesis. *Front. Plant Sci. 3*, 309. doi:10.3389/fpls.2012.00309

Desprez, T., Juraniec, M., Crowell, E. F., Jouy, H., Pochylova, Z., Parcy, F., ... Vernhettes, S. (2007). Organization of cellulose synthase complexes involved in primary cell wall synthesis in Arabidopsis thaliana. *PNAS*, *104*(39), 15572–15577. doi:10.1073/pnas.0706569104

Desprez, T., Vernhettes, S., Fagard, M., Refrégier, G., Desnos, T., Aletti, E., ... Höfte, H. (2002). Resistance against Herbicide Isoxaben and Cellulose Deficiency Caused by Distinct Mutations in Same Cellulose Synthase Isoform CESA6. *Plant Physiol. 128*(2), 482–490. doi:10.1104/pp.010822

Dima, O., Morreel, K., Vanholme, B., Kim, H., Ralph, J. & Boerjan, W. (2015). Small Glycosylated Lignin Oligomers Are Stored in Arabidopsis Leaf Vacuoles. *Plant Cell*, *27*(3), 695–710. doi:10.1105/tpc.114.134643

Dubos, C., Stracke, R., Grotewold, E., Weisshaar, B., Martin, C. & Lepiniec, L. (2010). MYB transcription factors in Arabidopsis. *Trends Plant Sci. 15*(10), 573–581. doi:10.1016/j.tplants.2010.06.005

Edwards, K., Johnstone, C. & Thompson, C. (1991). A simple and rapid method for the preparation of plant genomic DNA for PCR analysis. *Nucleic Acids Res. 19*(6), 1349.

Ellis, C., Karafyllidis, I., Wasternack, C. & Turner, J. G. (2002). The Arabidopsis Mutant cev1 Links Cell Wall Signaling to Jasmonate and Ethylene Responses. *Plant Cell*, *14*(7), 1557–1566. doi:10.1105/tpc.002022

Feller, A., Machemer, K., Braun, E. L. & Grotewold, E. (2011). Evolutionary and comparative analysis of MYB and bHLH plant transcription factors. *Plant J. 66*(1), 94–116. doi:10.1111/j.1365-313X.2010.04459.x

Gallego-Giraldo, L., Escamilla-Trevino, L., Jackson, L. A. & Dixon, R. A. (2011). Salicylic acid mediates the reduced growth of lignin down-regulated plants. *PNAS*, *108*(51), 20814–20819. doi:10.1073/pnas.1117873108

Goicoechea, M., Lacombe, E., Legay, S., Mihaljevic, S., Rech, P., Jauneau, A., ... Grima-Pettenati, J. (2005). EgMYB2, a new transcriptional activator from Eucalyptus xylem, regulates secondary cell wall formation and lignin biosynthesis. *Plant J. 43*(4), 553–567. doi:10.1111/j.1365-313X.2005.02480.x

Golfier, P., Volkert, C., He, F., Rausch, T. & Wolf, S. (2017). Regulation of secondary cell wall biosynthesis by a NAC transcription factor from Miscanthus. *Plant Direct*, *1*(5), e00024–n/a. doi:10.1002/pld3.24

Hafez, I. & Hassan, E. B. (2015). Rapid liquefaction of giant miscanthus feedstock in ethanol-water system for production of biofuels. *Energy Convers. Manag. 91*(2015), 219–224. doi:10.1016/j.enconman.2014.12.016

Hamann, T., Bennett, M., Mansfield, J. & Somerville, C. (2009). Identification of cell-wall stress as a hexose-dependent and osmosensitive regulator of plant responses. *Plant J. 57*(6), 1015–1026. doi:10.1111/j.1365-313X.2008.03744.x

Harris, P. J. & Trethewey, J. A. (2010). The distribution of ester-linked ferulic acid in the cell walls of angiosperms. *Phytochem. Rev. 9*(1), 19–33. doi:10.1007/s11101-009-9146-4

Heaton, E., Voigt, T. & Long, S. P. (2004). A quantitative review comparing the yields of two candidate C4 perennial biomass crops in relation to nitrogen, temperature and water. *Biomass Bioenergy*, *27*(1), 21–30. doi:10.1016/j.biombioe.2003.10.005

Heim, D. R., Bjelk, L. A., James, J., Schneegurt, M. A. & Larrinua, I. M. (1993). Mechanism of Isoxaben Tolerance in Agrostis palustris var. Penncross. *J. Exp. Bot. 44*(7), 1185–1189. doi:10.1093/jxb/44.7.1185

Heisler, M. G., Hamant, O., Krupinski, P., Uyttewaal, M., Ohno, C., Jönsson, H., ... Meyerowitz, E. M. (2010). Alignment between PIN1 polarity and microtubule orientation in the shoot apical meristem reveals a tight coupling between morphogenesis and auxin transport. *PLoS biol. 8*(10), e1000516. doi:10.1371/journal.pbio.1000516

Hellens, R. P., Edwards, E. A., Leyland, N. R., Bean, S. & Mullineaux, P. M. (2000). pGreen: a versatile and flexible binary Ti vector for Agrobacterium-mediated plant transformation. *Plant Mol. Biol. 42*(6), 819–32. doi:10.1023/A:1006496308160

Höll, J. (2014). *The R2R3 MYB Transcription Factors VvMYB14 and VvMYB15 as Regulators of the Stilbene Biosynthesis in Vitis vinifera* (Doctoral dissertation, Heidelberg University).

Hu, W.-J., Harding, S. A., Lung, J., Popko, J. L., Ralph, J., Stokke, D. D., ... Chiang, V. L. (1999). Repression of lignin biosynthesis promotes cellulose accumulation and growth in transgenic trees. *Nature biotech. 17*(8), 808–812.

Iqbal, Y. & Lewandowski, I. (2014). Inter-annual variation in biomass combustion quality traits over five years in fifteen Miscanthus genotypes in south Germany. *Fuel Process. Technol. 121*(2014), 47–55. doi:10.1016/j.fuproc.2014.01.003

Iqbal, Y. & Lewandowski, I. (2016). Biomass composition and ash melting behaviour of selected miscanthus genotypes in Southern Germany. *Fuel*, *180*, 606–612. doi:10.1016/j.fuel.2016.04.073

Jayaraman, K. & Gökalp, I. (2015). Pyrolysis, combustion and gasification characteristics of miscanthus and sewage sludge. *Energy Convers. Manag. 89*(2015), 83–91. doi:10.1016/j.enconman.2014.09.058

Jia, L., Clegg, M. T. & Jiang, T. (2004). Evolutionary Dynamics of the DNA-Binding Domains in Putative R2R3-MYB Genes Identified from Rice Subspecies indica and japonica Genomes. *Plant Physiol. 134*(2), 575–585. doi:10.1104/pp.103.027201

Jin, H., Cominelli, E., Bailey, P., Parr, A., Mehrtens, F., Jones, J., ... Martin, C. (2000). Transcriptional repression by AtMYB4 controls production of UV-protecting sunscreens in Arabidopsis. *EMBO J. 19*(22), 6150–6161.

Kadier, Y., Zu, Y.-y., Dai, Q.-m., Song, G., Lin, S.-w., Sun, Q.-p., ... Lu, M. (2017). Genome-wide identification, classification and expression analysis of NAC family of genes in sorghum [Sorghum bicolor (L.) Moench]. *Plant Growth Regul. 83*(2), 301–312. doi:10.1007/s10725-017-0295-y

Kaneda, M., Rensing, K. H., Wong, J. C., Banno, B., Mansfield, S. D. & Samuels, A. L. (2008). Tracking Monolignols during Wood Development in Lodgepole Pine. *Plant Physiol. 147*(4), 1750–1760. doi:10.1104/pp.108.121533

Kiesel, A. & Lewandowski, I. (2017). Miscanthus as biogas substrate - cutting tolerance and potential for anaerobic digestion. *GCB Bioenergy*, *9*(1), 153–167. doi:10.1111/gcbb.12330

Kim, W.-C., Kim, J.-Y., Ko, J.-H., Kang, H. & Han, K.-H. (2014). Identification of direct targets of transcription factor MYB46 provides insights into the transcriptional regulation of secondary wall biosynthesis. *Plant Mol. Biol. 85*(6), 589–599. doi:10.1007/s11103-014-0205-x

Ko, J.-H., Kim, W.-C. & Han, K.-H. (2009). Ectopic expression of MYB46 identifies transcriptional regulatory genes involved in secondary wall biosynthesis in Arabidopsis. *Plant J. 60*(4), 649–665. doi:10.1111/j.1365-313X.2009.03989.x

Kubo, M., Udagawa, M., Nishikubo, N., Horiguchi, G., Yamaguchi, M., Ito, J., ... Demura, T. (2005). Transcription switches for protoxylem and metaxylem vessel formation. *Genes Dev. 19*(16), 1855–60. doi:10.1101/gad.1331305

Kulkarni, A. R., Pattathil, S., Hahn, M. G., York, W. S. & O'Neill, M. A. (2012). Comparison of Arabinoxylan Structure in Bioenergy and Model Grasses. *Ind. Biotechnol. 8*(4), 222–229. doi:10.1089/ind.2012.0014

Lampropoulos, A., Sutikovic, Z., Wenzl, C., Maegele, I., Lohmann, J. U. & Forner, J. (2013). GreenGate - A Novel, Versatile, and Efficient Cloning System for Plant Transgenesis. *PLoS One*, *8*(12), e83043. doi:10.1371/journal.pone.0083043

Lan, W., Lu, F., Regner, M., Zhu, Y., Rencoret, J., Ralph, S. A., ... Ralph, J. (2015). Tricin, a Flavonoid Monomer in Monocot Lignification. *Plant Physiol. 167*(4), 1284–1295. doi:10.1104/pp.114.253757

Landrein, B. & Hamant, O. (2013). How mechanical stress controls microtubule behavior and morphogenesis in plants: history, experiments and revisited theories. *Plant J. 75*(2), 324–338. doi:10.1111/tpj.12188

Lanz, T., Tropf, S., Marner, F. J., Schröder, J. & Schröder, G. (1991). The role of cysteines in polyketide synthases. Site-directed mutagenesis of resveratrol and chalcone synthases, two key enzymes in different plant-specific pathways. *J. Biol. Chem. 266*(15), 9971–9976.

Le Ngoc Huyen, T., Rémond, C., Dheilly, R. M. & Chabbert, B. (2010). Effect of harvesting date on the composition and saccharification of Miscanthus x giganteus. *Bioresource Tech. 101*(21), 8224–8231. doi:10.1016/j.biortech.2010.05.087

Lewandowski, I., Clifton-Brown, J. C., Scurlock, J. & Huisman, W. (2000). Miscanthus: European Experience with a Novel Energy Crop. *Biomass Bioenergy*, *19*(2000), 209–227. doi:10.1016/S0961-9534(00)00032-5

Lewandowski, I., Clifton-Brown, J. C., Trindade, L. M., van der Linden, G. C., Schwarz, K.-U., Müller-Sämann, K., ... Kalinina, O. (2016). Progress on Optimizing Miscanthus Biomass Production for the European Bioeconomy: Results of the EU FP7 Project OPTIMISC. *Front. Plant Sci. 7*, 1–23. doi:10.3389/fpls.2016.01620

Li, E., Bhargava, A., Qiang, W., Friedmann, M. C., Forneris, N., Savidge, R. a., ... Douglas, C. J. (2012). The Class II KNOX gene KNAT7 negatively regulates secondary wall formation in Arabidopsis and is functionally conserved in Populus. *New Phytol. 194*(1), 102–15. doi:10.1111/j.1469-8137.2011.04016.x

Li, P., Ponnala, L., Gandotra, N., Wang, L., Si, Y., Tausta, S. L., ... Brutnell, T. P. (2010). The developmental dynamics of the maize leaf transcriptome. *Nat. Genet. 42*(12), 1060–1067. doi:10.1038/ng.703

Lu, F. & Ralph, J. (1997). Derivatization Followed by Reductive Cleavage (DFRC Method), a New Method for Lignin Analysis: Protocol for Analysis of DFRC Monomers. *J. Agric. Food Chem. 45*(7), 2590–2592. doi:10.1021/jf970258h

Manfield, I. W., Orfila, C., McCartney, L., Harholt, J., Bernal, A. J., Scheller, H. V., ... Willats, W. G. T. (2004). Novel cell wall architecture of isoxaben-habituated Arabidopsis suspension-cultured cells: global transcript profiling and cellular analysis. *Plant J. 40*, 260–275. doi:10.1111/j.1365-313X.2004.02208.x

Matsushita, Y., Kakehi, A., Miyawaki, S. & Yasuda, S. (2004). Formation and chemical structures of acid-soluble lignin II: reaction of aromatic nuclei model compounds with xylan in the presence of a counterpart for condensation, and behavior of lignin model compounds with guaiacyl and syringyl nuclei in 72% sulfuric. *J. Wood Sci. 50*(2), 136–141. doi:10.1007/s10086-003-0543-9

McCann, M. C., Stacey, N. J., Dahiya, P., Milioni, D., Sado, P. E. & Roberts, K. (2001). Zinnia. Everybody needs good neighbors. *Plant Physiol. 127*(4), 1380–1382. doi:10.1104/pp.010883.1380

McCarthy, R. L., Zhong, R. & Ye, Z.-H. (2009). MYB83 Is a Direct Target of SND1 and Acts Redundantly with MYB46 in the Regulation of Secondary Cell Wall Biosynthesis in Arabidopsis. *Plant Cell Physiol. 50*(11), 1950–1964. doi:10.1093/pcp/pcp139

McCartney, L., Marcus, S. E. & Knox, J. P. (2005). Monoclonal Antibodies to Plant Cell Wall Xylans and Arabinoxylans. *J. Histochem. Cytochem. 53*(4), 543–46. doi:10.1369/jhc.4B6578.2005

McCartney, L., Steele-King, C. G., Jordan, E. & Knox, J. P. (2003). Cell wall pectic (1→4)-β-D-galactan marks the acceleration of cell elongation in the Arabidopsis seedling root meristem. *Plant J. 33*(3), 447–54. doi:10.1046/j.1365-313X.2003.01640.x

McFarlane, H. E., Döring, A. & Persson, S. (2014). The Cell Biology of Cellulose Synthesis. *Annu. Rev. Plant Biol. 65*(1), 69–94. doi:10.1146/annurev-arplant-050213-040240

Mérai, Z., Kerényi, Z., Molnár, A., Barta, E., Válóczi, A., Bisztray, G., ... Silhavy, D. (2005). Aureusvirus P14 Is an Efficient RNA Silencing Suppressor That Binds Double-Stranded RNAs without Size Specificity. *J. Virol. 79*(11), 7217–26. doi:10.1128/JVI.79.11.7217-7226.2005

Miao, Y.-C. & Liu, C.-J. (2010). ATP-binding cassette-like transporters are involved in the transport of lignin precursors across plasma and vacuolar membranes. *PNAS*, *107*(52), 22728–33. doi:10.1073/pnas.1007747108

Mitsuda, N., Iwase, A., Yamamoto, H., Yoshida, M., Seki, M., Shinozaki, K. & Ohme-Takagi, M. (2007). NAC transcription factors, NST1 and NST3, are key regulators of the formation of secondary walls in woody tissues of Arabidopsis. *Plant Cell*, *19*(1), 270–80. doi:10.1105/tpc.106.047043

Mitsuda, N., Seki, M., Shinozaki, K. & Ohme-takagi, M. (2005). The NAC Transcription Factors NST1 and NST2 of Arabidopsis Regulate Secondary Wall Thickenings and Are Required for Anther Dehiscence. *Plant Cell*, *17*, 2993–3006. doi:10.1105/tpc.105.036004.1

Mottiar, Y., Vanholme, R., Boerjan, W., Ralph, J. & Mansfield, S. D. (2016). Designer lignins: Harnessing the plasticity of lignification. *Curr. Opin. Biotechnol. 37*, 190–200. doi:10.1016/j.copbio.2015.10.009

Musha, Y. & Goring, D. A. I. (1975). Distribution of syringyl and guaiacyl moieties in hardwoods as indicated by ultraviolet microscopy. *Wood Sci. Technol. 9*(1), 45–58. doi:10.1007/BF00351914

Musielak, T. J., Schenkel, L., Kolb, M., Henschen, A. & Bayer, M. (2015). A simple and versatile cell wall staining protocol to study plant reproduction. *Plant Reprod. 28*(3-4), 161–69. doi:10.1007/s00497-015-0267-1

Nairn, C. J. & Haselkorn, T. (2005). Three loblolly pine CesA genes expressed in developing xylem are orthologous to secondary cell wall CesA genes of angiosperms. *New Phytol. 166*(3), 907–915. doi:10.1111/j.1469-8137.2005.01372.x

Newman, R. H., Hill, S. J. & Harris, P. J. (2013). Wide-Angle X-Ray Scattering and Solid-State Nuclear Magnetic Resonance Data Combined to Test Models for Cellulose Microfibrils in Mung Bean Cell Walls. *Plant Physiol. 163*(4), 1558–1567. doi:10.1104/pp.113.228262

Noda, S., Koshiba, T., Hattori, T., Yamaguchi, M., Suzuki, S. & Umezawa, T. (2015). The expression of a rice secondary wall-specific cellulose synthase gene, OsCesA7, is directly regulated by a rice transcription factor, OsMYB58/63. *Planta*, *242*(3), 589–600. doi:10.1007/s00425-015-2343-z

Oda, Y. & Fukuda, H. (2013). Rho of Plant GTPase Signaling Regulates the Behavior of Arabidopsis Kinesin-13A to Establish Secondary Cell Wall Patterns. *Plant Cell*, *25*, 1–13. doi:10.1105/tpc.113.117853

Ohashi-Ito, K., Oda, Y. & Fukuda, H. (2010). Arabidopsis VASCULAR-RELATED NAC-DOMAIN6 Directly Regulates the Genes That Govern Programmed Cell Death and Secondary Wall Formation during Xylem Differentiation. *Plant Cell*, *22*(10), 3461–3473. doi:10.1105/tpc.110.075036

Öhman, D., Demedts, B., Kumar, M., Gerber, L., Gorzsás, A., Goeminne, G., ... Sundberg, B. (2013). MYB103 is required for FERULATE-5-HYDROXYLASE expression and syringyl lignin biosynthesis in Arabidopsis stems. *Plant J. 73*(1), 63–76. doi:10.1111/tpj.12018

Olsen, A. N., Ernst, H. A., Leggio, L. L. & Skriver, K. (2005). NAC transcription factors: structurally distinct, functionally diverse. *Trends Plant Sci. 10*(2), 79–87. doi:10.1016/j.tplants.2004.12.010

Paredez, A. R., Somerville, C. & Ehrhardt, D. (2006). Visualization of Cellulose Synthase with Microtubules. *Science*, *312*, 1491–1495. doi:10.1126/science.1126551

Paredez, A. R., Wright, A. & Ehrhardt, D. W. (2006). Microtubule cortical array organization and plant cell morphogenesis. *Curr. Opin. Plant Biol. 9*(6), 571–578. doi:10.1016/j.pbi.2006.09.005

Patzlaff, A., McInnis, S., Courtenay, A., Surman, C., Newman, L. J., Smith, C., ... Campbell, M. M. (2003). Characterisation of a pine MYB that regulates lignification. *Plant J. 36*(6), 743–754. doi:10.1046/j.1365-313X.2003.01916.x

Persson, S., Paredez, A. R., Carroll, A., Palsdottir, H., Doblin, M., Poindexter, P., ... Somerville, C. R. (2007). Genetic evidence for three unique components in primary cell-wall cellulose synthase complexes in Arabidopsis. *PNAS*, *104*(39), 15566–15571. doi:10.1073/pnas.0706592104

Petti, C., Shearer, A., Tateno, M., Ruwaya, M., Brutnell, T., Nokes, S. & Debolt, S. (2013). Comparative feedstock analysis in Setaria viridis L. as a model for C4 bioenergy grasses and Panicoid crop species. *Front. Plant Sci. 4*, 181. doi:10.3389/fpls.2013.00181

Pomar, F., Merino, F. & Barceló, A. R. (2002). O-4-Linked coniferyl and sinapyl aldehydes in lignifying cell walls are the main targets of the Wiesner (phloroglucinol-HCl) reaction. *Protoplasma*, *220*(1), 17–28. doi:10.1007/s00709-002-0030-y

Preston, J., Wheeler, J., Heazlewood, J., Li, S. F. & Parish, R. W. (2004). AtMYB32 is required for normal pollen development in Arabidopsis thaliana. *Plant J. 40*(6), 979–995. doi:10.1111/j.1365-313X.2004.02280.x

Ragauskas, A. J., Beckham, G. T., Biddy, M. J., Chandra, R., Chen, F., Davis, M. F., ... Wyman, C. E. (2014). Lignin valorization: Improving lignin processing in the biorefinery. *Science*, *344*(6185). doi:10.1126/science.1246843

Ralph, J., Grabber, J. H. & Hatfield, R. D. (1995). Lignin-ferulate cross-links in grasses: active incorporation of ferulate polysaccharide esters into ryegrass lignins. *Carbohydr. Res. 275*(1), 167–178. doi:10.1016/0008-6215(95)00237-N

Rennie, E. A. & Scheller, H. V. (2014). Xylan biosynthesis. *Curr. Opin. Biotechnol. 26*, 100–107. doi:10.1016/j.copbio.2013.11.013

Robinson, A. R. & Mansfield, S. D. (2009). Rapid analysis of poplar lignin monomer composition by a streamlined thioacidolysis procedure and near-infrared reflectance-based prediction modeling. *Plant J. 58*(4), 706–14. doi:10.1111/j.1365-313X.2009.03808.x

Robson, P., Jensen, E., Hawkins, S., White, S. R., Kenobi, K., Clifton-Brown, J., ... Farrar, K. (2013). Accelerating the domestication of a bioenergy crop: Identifying and modelling morphological targets for sustainable yield increase in Miscanthus. *J. Exp. Bot. 64*(14), 4143–4155. doi:10.1093/jxb/ert225

Ros Barceló, A. (2005). Xylem parenchyma cells deliver the H_2O_2 necessary for lignification in differentiating xylem vessels. *Planta*, *220*(5), 747–756. doi:10.1007/s00425-004-1394-3

Sainsbury, P. D., Hardiman, E. M., Ahmad, M., Otani, H., Seghezzi, N., Eltis, L. D. & Bugg, T. D. H. (2013). Breaking down lignin to high-value chemicals: The conversion of lignocellulose to vanillin in a gene deletion mutant of rhodococcus jostii RHA1. *ACS Chem. Biol. 8*(10), 2151–2156. doi:10.1021/cb400505a

Sakamoto, S. & Mitsuda, N. (2015). Reconstitution of a secondary cell wall in a secondary cell wall-deficient arabidopsis mutant. *Plant Cell Physiol. 56*(2), 299–310. doi:10.1093/pcp/pcu208

Sambrook, J. & Russell, D. W. (2006). The Inoue Method for Preparation and Transformation of Competent E. Coli: “Ultra-Competent” Cells. *Cold Spring Harb. Protoc. 2006*(1), pdb.prot3944. doi:10.1101/pdb.prot3944

Scheible, W.-R., Eshed, R., Richmond, T., Delmer, D. & Somerville, C. (2001). Modifications of cellulose synthase confer resistance to isoxaben and thiazolidinone herbicides in Arabidopsis Ixr1 mutants. *PNAS*, *98*(18), 10079–10084. doi:10.1073/pnas.191361598

Schneider, R., Hanak, T., Persson, S. & Voigt, C. A. (2016). Cellulose and callose synthesis and organization in focus, what’s new? *Curr. Opin. Plant Biol. 34*, 9–16. doi:10.1016/j.pbi.2016.07.007

Scully, E. D., Gries, T., Palmer, N. A., Sarath, G., Funnell-Harris, D. L., Baird, L., . . . Sattler, S. E. (2018). Overexpression of *SbMyb60* in *Sorghum bicolor* impacts both primary and secondary metabolism. *New Phytol. 217*(1), 82–104. doi:10.1111/nph.14815

Scully, E. D., Gries, T., Sarath, G., Palmer, N. A., Baird, L., Serapiglia, M. J., . . . Sattler, S. E. (2016). Overexpression of SbMyb60 impacts phenylpropanoid biosynthesis and alters secondary cell wall composition in Sorghum bicolor. *Plant J. 85*(3), 378–395. doi:10.1111/tpj.13112

Sievers, F., Wilm, A., Dineen, D., Gibson, T. J., Karplus, K., Li, W., . . . Higgins, D. G. (2011). Fast, scalable generation of high-quality protein multiple sequence alignments using Clustal Omega. *Mol. Syst. Biol. 7*(1). doi:10.1038/msb.2011.75

Slavov, G. T., Nipper, R., Robson, P., Farrar, K., Allison, G. G., Bosch, M., . . . Jensen, E. (2014). Genome-wide association studies and prediction of 17 traits related to phenology, biomass and cell wall composition in the energy grass Miscanthus sinensis. *New Phytol. 201*(4), 1227–1239.

Smith, R. A., Schuetz, M., Karlen, S. D., Bird, D. A., Tokunaga, N., Sato, Y., . . . Samuels, A. L. (2017). Defining the Diverse Cell Populations Contributing to Lignification in Arabidopsis thaliana Stems. *Plant Physiol.* pp.00434.2017. doi:10.1104/pp.17.00434

Smith, R. A., Schuetz, M., Roach, M., Mansfield, S. D., Ellis, B. & Samuels, L. (2013). Neighboring parenchyma cells contribute to Arabidopsis xylem lignification, while lignification of interfascicular fibers is cell autonomous. *Plant Cell*, *25*(10), 3988–99. doi:10.1105/tpc.113.117176

Sommersacher, P., Brunner, T. & Obernberger, I. (2012). Fuel indexes: A novel method for the evaluation of relevant combustion properties of new biomass fuels. *Energy Fuels*, *26*(1), 380–390. doi:10.1021/ef201282y

Spence, A. K., Boddu, J., Wang, D., James, B., Swaminathan, K., Moose, S. P. & Long, S. P. (2014). Transcriptional responses indicate maintenance of photosynthetic proteins as key to the exceptional chilling tolerance of C4 photosynthesis in Miscanthus x giganteus. *J. Exp. Bot. 65*(13), 3737–3747. doi:10.1093/jxb/eru209

Stewart, J. J., Akiyama, T., Chapple, C., Ralph, J. & Mansfield, S. D. (2009). The Effects on Lignin Structure of Overexpression of Ferulate 5-Hydroxylase in Hybrid Poplar1. *Plant Physiol. 150*(2), 621–635. doi:10.1104/pp.109.137059

Stracke, R., Werber, M. & Weisshaar, B. (2001). The R2R3 - MYB gene family in Arabidopsis thaliana. *Curr. Opin. Plant Biol. 4*(5), 447–456.

Tamura, K., Stecher, G., Peterson, D., Filipski, A. & Kumar, S. (2013). MEGA6: Molecular evolutionary genetics analysis version 6.0. *Mol. Biol. Evol. 30*(12), 2725–29. doi:10.1093/molbev/mst197

Taylor-Teeples, M., Lin, L., de Lucas, M., Turco, G., Toal, T. W., Gaudinier, A., ... Brady, S. M. (2015). An Arabidopsis gene regulatory network for secondary cell wall synthesis. *Nature*, *517*, 571–575. doi:10.1038/nature14099

Taylor, J. G., Owen, T. P., Koonce, L. T. & Haigler, C. H. (1992). Dispersed lignin in tracheary elements treated with cellulose synthesis inhibitors provides evidence that molecules of the secondary cell wall mediate wall patterning. *Plant J. 2*(6), 959–970. doi:10.1111/j.1365-313X.1992.00959.x

Taylor, N. G., Howells, R. M., Huttly, A. K., Vickers, K. & Turner, S. R. (2003). Interactions among three distinct CesA proteins essential for cellulose synthesis. *PNAS*, *100*(3), 1450–1455. doi:10.1073/pnas.0337628100

Tsang, D. L., Edmond, C., Harrington, J. L. & Nuhse, T. S. (2011). Cell Wall Integrity Controls Root Elongation via a General 1-Aminocyclopropane-1-Carboxylic Acid-Dependent, Ethylene-Independent Pathway. *Plant Physiol. 156*(2), 596–604. doi:10.1104/pp.111.175372

Turner, S. & Kumar, M. (2018). Cellulose synthase complex organization and cellulose microfibril structure. *Philos. Trans. Royal Soc. A. 376*(2112). doi:10.1098/rsta.2017.0048

Valdivia, E. R., Herrera, M. T., Gianzo, C., Fidalgo, J., Revilla, G., Zarra, I. & Sampedro, J. (2013). Regulation of secondary wall synthesis and cell death by NAC transcription factors in the monocot Brachypodium distachyon. *J. Exp. Bot. 64*(5), 1333–43. doi:10.1093/jxb/ers394

Vallet, C., Chabbert, B., Czaninski, Y. & Monties, B. (1996). Histochemistry of Lignin Deposition during Sclerenchyma Differentiation in Alfalfa Stems. *Ann. Bot. 78*, 625–632. doi:10.1006/anbo.1996.0170

Vanholme, R., Morreel, K., Darrah, C., Oyarce, P., Grabber, J. H., Ralph, J. & Boerjan, W. (2012). Metabolic engineering of novel lignin in biomass crops. *New Phytol. 196*(4), 978–1000. doi:10.1111/j.1469-8137.2012.04337.x

Vanholme, R., Morreel, K., Ralph, J. & Boerjan, W. (2008). Lignin engineering. *Curr. Opin. Plant Biol. 11*(3), 278–285. doi:10.1016/j.pbi.2008.03.005

Vega-Sanchez, M. E., Verhertbruggen, Y., Christensen, U., Chen, X., Sharma, V., Varanasi, P., ... Ronald, P. C. (2012). Loss of Cellulose Synthase-Like F6 Function Affects Mixed-Linkage Glucan Deposition, Cell Wall Mechanical Properties, and Defense Responses in Vegetative Tissues of Rice. *Plant Physiol. 159*(1), 56–69. doi:10.1104/pp.112.195495

Vogel, J. (2008). Unique aspects of the grass cell wall. *Curr. Opin. Plant Biol. 11*(3), 301–307. doi:10.1016/j.pbi.2008.03.002

Vogt, T. (2010). Phenylpropanoid biosynthesis. *Mol. Plant*, *3*(1), 2–20. doi:10.1093/mp/ssp106

Voxeur, A., Wang, Y. & Sibout, R. (2015). Lignification: different mechanisms for a versatile polymer. *Curr. Opin. Plant Biol. 23*, 83–90. doi:10.1016/j.pbi.2014.11.006

Vukašinović, N., Oda, Y., Pejchar, P., Synek, L., Pečenková, T., Rawat, A., ... Žárský, V. (2017). Microtubule-dependent targeting of the exocyst complex is necessary for xylem development in Arabidopsis. *New Phytol. 213*(3), 1052–1067. doi:10.1111/nph.14267

Wang, L., Czedik-Eysenberg, A., Mertz, R. A., Si, Y., Tohge, T., Nunes-Nesi, A., ... Brutnell, T. P. (2014). Comparative analyses of C_4 and C_3 photosynthesis in developing leaves of maize and rice. *Nat. Biotechnol. 32*(11), 1158–1165. doi:10.1038/nbt.3019

Wang, Y., Chantreau, M., Sibout, R. & Hawkins, S. (2013). Plant cell wall lignification and monolignol metabolism. *Front. Plant Sci. 4*, 220. doi:10.3389/fpls.2013.00220

Watanabe, Y., Meents, M. J., McDonnell, L. M., Barkwill, S., Sampathkumar, A., Cartwright, H. N., ... Mansfield, S. D. (2015). Visualization of cellulose synthases in Arabidopsis secondary cell walls. *Science*, *350*(6257), 198–203. doi:10.1126/science.aac7446

Whittaker, C., Hunt, J., Misselbrook, T. & Shield, I. (2016). How well does Miscanthus ensile for use in an anaerobic digestion plant? *Biomass Bioenergy*, *88*, 24–34. doi:10.1016/j.biombioe.2016.03.018

Wightman, R. & Turner, S. R. (2008). The roles of the cytoskeleton during cellulose deposition at the secondary cell wall. *Plant J. 54*(5), 794–805. doi:10.1111/j.1365-313X.2008.03444.x

Wilkerson, C. G., Mansfield, S. D., Lu, F., Withers, S., Park, J., Karlen, S. D., ... Ralph, J. (2014). Introduces Chemically Labile Linkages into the Lignin Backbone. *Science*, *344*(6179), 90–93. doi:10.1126/science.1250161

Wittkopp, P. J. & Kalay, G. (2012). Cis-regulatory elements: Molecular mechanisms and evolutionary processes underlying divergence. *Nature Rev. Genet. 13*(1), 59–69. doi:10.1038/nrg3095

Woodcock, D. M., Crowther, P. J., Doherty, J., Jefferson, S., DeCruz, E., Noyer-Weidner, M., ... Graham, M. W. (1989). Quantitative evaluation of Escherichia coli host strains

for tolerance to cytosine methylation in plasmid and phage recombinants. *Nucleic Acids Res. 17*(9), 3469–78. doi:10.1093/nar/17.9.3469

Yamaguchi, M., Goué, N., Igarashi, H., Ohtani, M., Nakano, Y., Mortimer, J. C., ... Demura, T. (2010). VASCULAR-RELATED NAC-DOMAIN6 and VASCULAR-RELATED NAC-DOMAIN7 Effectively Induce Transdifferentiation into Xylem Vessel Elements under Control of an Induction System. *Plant Physiol. 153*(3), 906–914. doi:10.1104/pp.110.154013

Yamaguchi, M., Mitsuda, N., Ohtani, M., Ohme-Takagi, M., Kato, K. & Demura, T. (2011). VASCULAR-RELATED NAC-DOMAIN 7 directly regulates the expression of a broad range of genes for xylem vessel formation. *Plant J. 66*(4), 579–590. doi:10.1111/j.1365-313X.2011.04514.x

Yoshida, K., Sakamoto, S., Kawai, T., Kobayashi, Y., Sato, K., Ichinose, Y., ... Mitsuda, N. (2013). Engineering the Oryza sativa cell wall with rice NAC transcription factors regulating secondary wall formation. *Front. Plant Sci. 4*, 383. doi:10.3389/fpls.2013.00383

Zhao, Q., Wang, H., Yin, Y., Xu, Y., Chen, F. & Dixon, R. A. (2010). Syringyl lignin biosynthesis is directly regulated by a secondary cell wall master switch. *PNAS*, *107*(32), 14496–14501. doi:10.1073/pnas.1009170107

Zhong, R., Demura, T. & Ye, Z.-H. (2006). SND1, a NAC domain transcription factor, is a key regulator of secondary wall synthesis in fibers of Arabidopsis. *Plant Cell*, *18*(11), 3158–70. doi:10.1105/tpc.106.047399

Zhong, R., Lee, C., McCarthy, R. L., Reeves, C. K., Jones, E. G. & Ye, Z.-H. (2011). Transcriptional Activation of Secondary Wall Biosynthesis by Rice and Maize NAC and MYB Transcription Factors. *Plant Cell Physiol. 52*(10), 1856–1871. doi:10.1093/pcp/pcr123

Zhong, R., Lee, C. & Ye, Z.-H. (2010a). Evolutionary conservation of the transcriptional network regulating secondary cell wall biosynthesis. *Trends Plant Sci. 15*(11), 625–632. doi:10.1016/j.tplants.2010.08.007

Zhong, R., Lee, C. & Ye, Z.-H. (2010b). Functional characterization of poplar wood-associated NAC domain transcription factors. *Plant Physiol. 152*(2), 1044–55. doi:10.1104/pp.109.148270

Zhong, R., Lee, C. & Ye, Z.-H. (2010c). Global analysis of direct targets of secondary wall NAC master switches in arabidopsis. *Mol. Plant*, *3*(6), 1087–1103. doi:10.1093/mp/ssq062

Zhong, R., Lee, C., Zhou, J., McCarthy, R. L. & Ye, Z.-H. (2008). A Battery of Transcription Factors Involved in the Regulation of Secondary Cell Wall Biosynthesis in Arabidopsis. *Plant Cell*, *20*(10), 2763–82. doi:10.1105/tpc.108.061325

Zhong, R., McCarthy, R. L., Haghighat, M. & Ye, Z.-H. (2013). The Poplar MYB Master Switches Bind to the SMRE Site and Activate the Secondary Wall Biosynthetic Program during Wood Formation. *PLoS ONE*, *8*(7), e69219. doi:10.1371/journal.pone.0069219

Zhong, R., McCarthy, R. L., Lee, C. & Ye, Z.-H. (2011). Dissection of the Transcriptional Program Regulating Secondary Wall Biosynthesis during Wood Formation in Poplar. *Plant Physiol. 157*(3), 1452–1468. doi:10.1104/pp.111.181354

Zhong, R., Richardson, E. A. & Ye, Z.-H. (2007a). The MYB46 transcription factor is a direct target of SND1 and regulates secondary wall biosynthesis in Arabidopsis. *Plant Cell*, *19*(9), 2776–92. doi:10.1105/tpc.107.053678

Zhong, R., Richardson, E. A. & Ye, Z.-H. (2007b). Two NAC domain transcription factors, SND1 and NST1, function redundantly in regulation of secondary wall synthesis in fibers of Arabidopsis. *Planta*, *225*(6), 1603–11. doi:10.1007/s00425-007-0498-y

Zhong, R. & Ye, Z.-H. (2012). MYB46 and MYB83 Bind to the SMRE Sites and Directly Activate a Suite of Transcription Factors and Secondary Wall Biosynthetic Genes. *Plant Cell Physiol. 53*(2), 368–380. doi:10.1093/pcp/pcr185

Zhong, R., Yuan, Y., Spiekerman, J. J., Guley, J. T., Egbosiuba, J. C. & Ye, Z.-H. (2015). Functional characterization of NAC and MYB transcription factors involved in regulation of biomass production in switchgrass (Panicum virgatum). *PLoS One*, *10*(8), 1–24. doi:10.1371/journal.pone.0134611

Zhou, J., Lee, C., Zhong, R. & Ye, Z.-H. (2009). MYB58 and MYB63 Are Transcriptional Activators of the Lignin Biosynthetic Pathway during Secondary Cell Wall Formation in Arabidopsis. *Plant Cell*, *21*(1), 248–66. doi:10.1105/tpc.108.063321

Zhou, J., Zhong, R. & Ye, Z.-H. (2014). Arabidopsis NAC domain proteins, VND1 to VND5, are transcriptional regulators of secondary wall biosynthesis in vessels. *PLoS One*, *9*(8), e105726. doi:10.1371/journal.pone.0105726

Zhu, T., Nevo, E., Sun, D. & Peng, J. (2012). PHYLOGENETIC ANALYSES UNRAVEL THE EVOLUTIONARY HISTORY OF NAC PROTEINS IN PLANTS. *Evolution*, *66*(6), 1833–1848. doi:10.1111/j.1558-5646.2011.01553.x

Danksagung

Ich möchte meinen allerherzlichsten Dank aussprechen an alle Menschen, die mich während meiner Doktorarbeit begleitet und unterstützt haben.

Allen voran, bedanke ich mich bei Prof. Dr. Thomas Rausch und Dr. Sebastian Wolf, die mir zusammen die bestmögliche Betreuung zukommen ließen: Viel Freiheit um meine eigenen Gedanken zu entwickeln, umzusetzen und Interessen zu verfolgen aber immer mit Rat zur Stelle, wenn er gebraucht wurde.

Den größten Dank gebührt meinen Kollegen der Arbeitsgruppen Rausch und Wolf, ohne die die Zeit in Heidelberg nicht so schön gewesen wäre.

Nicht zu vergessen sind meine Familie und Freunde, ohne deren starken Rückhalt ich niemals so weit gekommen wäre.

Ich hätte mir keine bessere Promotion vorstellen können.

Vielen Dank für die tolle Zeit !